The Journal of Experimental Biology 200, 2597–2608 (1997)
Printed in Great Britain © The Company of Biologists Limited 1997
JEB1052

SEXUAL SIGNALLING IN BLADDER GRASSHOPPERS: TACTICAL DESIGN FOR MAXIMIZING CALLING RANGE

MOIRA J. VAN STAADEN* AND HEINER RÖMER
Institute for Zoology, Karl-Franzens-University, Universitätsplatz 2, Graz A-8010, Austria

Accepted 29 July 1997

Summary

Pair formation in the bladder grasshopper (*Bullacris membracioides*) is by duetting and male phonotaxis. Low-frequency stridulatory signals are emitted by an abdominal resonator in the male and are answered by females using a species-specific time delay. Acoustic transmission in the natural environment was studied using playback of sexual signals over distances of 450 m under two atmospheric conditions (day and night). Upward-refracting sound conditions and a sound shadow zone beyond approximately 50 m prevailed during the day. Acoustic enhancement was demonstrated at night when downward-refracting temperature inversions created a tunnel effect with sound caught between the ground and zones of different temperatures. Transmission conditions are almost ideal at night when the species actually calls; calling distances of 150 m for the male signal in the afternoon increased to 1.5–1.9 km at night, arguably the largest calling distance yet reported for insects. In contrast, female calls transmit over a maximum of 50 m, signifying a marked discrepancy in the active space of sex-specific signals. Transmission distance may, however, be profoundly affected by levels of masking noise. Adaptations to increase the signal range may variously be found in the signal itself, in behaviour patterns or in the sensory system. Here we demonstrate aspects of the first two types of adaptation in the sexual signalling system of a grasshopper in which maximizing the calling range appears to be the major selection pressure, with lesser effects imposed by inter- and intraspecific pressures and by the transmission channel.

Key words: *Bullacris membracioides*, grasshopper, acoustic signalling, transmission distance, meteorology.

Introduction

Recent attention has focused on the characteristics of natural transmission channels and the effects of physical factors on acoustic signals, and has generated considerable debate over whether the maximum range of detection is in fact the primary selection pressure on animal vocalizations (Michelsen, 1978; Richards and Wiley, 1980; Römer, 1997; Wiley and Richards, 1978, 1982). Constraints imposed by acoustic characteristics of the habitat are important in that they provide the framework within which other selection pressures must operate. Yet the generality of any ‘rule’ is questionable owing to the multiplicity of local factors affecting sound propagation, our relative ignorance of strategic design in many taxa, and the fact that the signal itself is not an evolutionarily independent trait. Signal, sensory systems and behaviour are functionally related (Endler, 1992), and adaptations to increase signal range may be found in any, or all, of these areas.

In the context of intraspecific communication, natural selection to maximize broadcast range favours characteristics that maximize the received signal relative to background noise and that minimize signal degradation. Female preference for the more intense of two or more competing signals found in empirical studies on a variety of insect taxa indicates a strong selection to maximize calling range (Bailey and Yeoh, 1988; Bailey *et al.* 1990; Forrest, 1983; Forrest and Green, 1991; Latimer and Sippel, 1987; Partridge *et al.* 1987; Shuvalov and Popov, 1973; Thorson *et al.* 1982). Moreover, selection to increase sound output has favoured the development of a variety of behavioural mechanisms including the use of amplifying burrows (Bennet-Clark, 1987), baffles (Prozesky-Schulze *et al.* 1975), resonators (Young and Hill, 1977), temporal sound windows (Gogala and Riede, 1995; Moore *et al.* 1989; Narins, 1995) and preferred signalling sites (Arak and Eiriksson, 1992; Paul and Walker, 1979). The use of spatial sound windows and atmospheric controls on long-distance animal vocalizations has rarely been considered, however, particularly with respect to insects. Enhanced transmission of signals between 1.6 and 2.5 kHz indicated a ground-level sound window for this frequency range in forest habitat (Morton, 1975). Waser and Waser (1977) suggested that canopy monkeys in tropical forests give their long-distance vocalizations primarily in the few hours after sunrise when the advantageous temperature gradient for sound transmission is likely to be best developed above the canopy. Similarly, the early evening peak in elephant social activity and infrasound

*e-mail: m.van-staaden@kfunigraz.ac.at

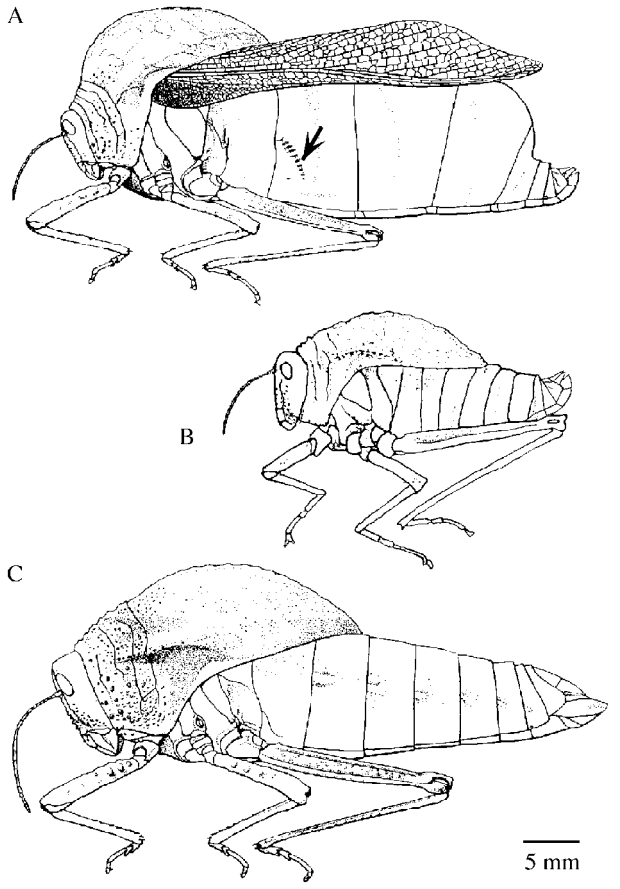

Fig. 1. Trimorphism in *Bullacris membracioides*. (A) Adult male with strongly inflated abdomen; stridulatory file arrowed. (B) Apterous 'alternative' male which lacks the anatomy for sexual stridulation. (C) Typically acridid-shaped micropterous adult female. All morphs have a pair of hearing organs attached laterally in the first abdominal segment, but frank tympana are absent. A and C are taken from Dirsh (1965) with permission; copyright Natural Resources Institute, UK.

vocalization corresponds with optimal sound transmission conditions created by the formation of a thermal inversion 1–2 h after sunset (Garstang *et al.* 1995).

This study focuses on the tactical design (Guilford and Dawkins, 1991) of long-distance acoustic signals in bladder grasshoppers (Orthoptera, Pneumoridae), a taxon for which spectacular auditory signalling is a defining characteristic, but for which our knowledge of natural history in general, and the communication system in particular, is meagre (Alexander, 1992; Lewis, 1891; Péringuey, 1916; Thunberg, 1775; van Son, 1958). The family is endemic to southern Africa, where it occurs in a patchy distribution primarily within the coastal belt. The conspicuous nocturnal calls of males are audible to humans over several kilometres, but in all other respects the taxon is cryptic (Dirsh, 1965). Females are micropterous and typically acridid-shaped; however, males can function as a flighted, stridulating adult with a strongly inflated abdomen or may mate as an apterous 'alternative' morph (Fig. 1) without the anatomy or behaviour for sexual stridulation (Alexander and van Staaden, 1989).

Here we examine properties of acoustic signals and signalling behaviour that maximize calling range in *Bullacris membracioides* (Walker). We characterize the sexual signals and the mechanisms by which they are produced, measure acoustic transmission distances directly in the natural habitat under two different atmospheric conditions, and assess the behavioural strategies by which adult males minimize or eliminate factors producing sound attenuation in excess of that due to geometrical spreading.

Materials and methods

Study site

Field experiments were performed in February of 1994–1996 in undisturbed habitat at Inchanga (KwaZulu-Natal, 29.74346° S, 30.67759° E), 814 m above sea level and approximately in the centre of the species' range. The area is characterized by steep-sided valleys, high humidity levels and vegetation that is essentially tropical in affinity, comprising a mixed mosaic of bush and grassland. The latter is C4 grassland with *Themeda*, *Tristachya*, *Trachypogon* and *Aristida* spp. the most prominent components. Average grass height is 50 cm, with approximately 60 % ground cover. An anemometer (type 260 P/D; Kroneis) was positioned 2 m above ground in open grassland, and electronic temperature sensors (type NTC; Kroneis) encased in open-ended aluminium sleeves were mounted at heights of 1, 5 and 10 m. Wind speed and temperature measurements were registered every 5 s and averaged over 5 min periods on a datalogger, providing a continuous weather profile. Humidity readings were taken at a height of 1.5 m using a stick hygrometer (Hanna Instruments, Hi 8565) at the start of each transmission experiment.

Sound recording, signalling mechanisms and laser vibrometry

Bullacris membracioides were hand-caught, and nymphs were raised to adulthood in groups of 5–10 individuals in the laboratory. The natural calling songs of adult males and females were recorded dorsally at a distance of 1 m in wire-mesh cages, using a sound level meter (Bruel & Kjaer, model 2009, 1/2 inch condenser microphone, type 2540 Larson & Davis; A weighting; RMS fast). Songs were digitized at a sampling rate of 44 kHz on an Apple Macintosh Powerbook 520 computer *via* the built-in 16-bit A/D sound board, edited (Macromedia, SoundEdit 16) and stored digitally. Measurement of female response time to playback calls of males was performed in wire-mesh cages using the same experimental set-up as for sound transmission (see below). Playback intensity at the position of the female was 85 dB SPL. Mechanisms of sound production were determined in the laboratory using a combination of laser vibrometry and scanning electron microscopy with standard preparative techniques.

Vibration of the air-filled abdomen of males was measured

with a laser vibrometer (Polytech OFV-3000, with measurement head OFV 501), which enables sound-induced vibrations of cuticular structures to be measured without contact (reviewed in Lewin *et al.* 1990). The animal was attached to a holder by its ventral thorax using dental wax, with the air-filled abdominal cavity left free to vibrate. Since the quality of the laser measurement depends strongly on the amount of light reflected from the cuticular vibrating surface, signal-to-noise-ratio was considerably enhanced by attaching up to five small retro-reflecting glass spheres (approximately 0.2 μg each, Scotchlite no. 7610, OM company) to the pleura of the third abdominal segment, where all measurements were made. The preparation was placed in the centre of an anechoic chamber such that echoes at the position of the preparation were more than 40 dB less intense than the signal. Pure tone stimuli were broadcast through a wide-band amplifier (Realistic 80W) and speaker (TW8 special) mounted on a holder at a distance of 45 cm. Sound pulses with different pure tone carriers between 800 Hz and 12 kHz (duration 1 s; repetition rate 0.5 s^{-1}) were generated to study the vibration velocity of the cuticle.

Sound transmission

The transmission distances of sexual signals were measured along a 450 m straight-line transect in essentially flat, open grassland, with markers at 5, 10 or 50 m intervals to aid placement of the microphone and sound level meter. The majority of experiments were conducted during the normal calling time of 22:00–24:00 h, under environmental conditions in which temperature varied from 18.5 to 24 °C and relative humidity from 74 to 100 % between experiments. For comparative purposes, transmission distances for the male call were also measured between 10:00 and 17:00 h. To obtain transmission data unconfounded by variable wind conditions, night measurements were performed only when there was essentially no wind, and in no case did wind speed during the day exceed 1 m s^{-1}. In the windless conditions under which measurements were performed, the background noise level excluding other calling insects was usually below the sensitivity of the microphone at night (27 dB SPL) and varied from 32 to 46 dB SPL during the day. In the latter case, most of the background noise was at frequencies below 500 Hz as a result of traffic on a highway at a distance of approximately 1 km.

Playback stimuli for sound transmission measurements were typical male and female calls (see Fig. 2), amplified by a custom-made wide-band amplifier driven by a car battery and broadcast at a rate of 0.5 s^{-1} through a speaker (Siemens RL 101 G4). The mean height of the song post and receiver was 2 m (M. J. van Staaden and H. Römer, personal observation); hence, the speaker was placed on a pole at a height of 2 m and calls were broadcast at typical sound intensities of 98 dB SPL for male calls and at 60 dB SPL (at 1 m) for female calls. Sound pressure levels (SPLs) were determined at 5 or 10 m intervals using a portable sound level meter (Bruel & Kjaer, model 2009; 1/2 inch condenser microphone, type 2540 Larson & Davis; A weighting; RMS fast reading). The microphone was separated from the sound level meter by a 3 m extension cord fixed on a pole at a height of 2 m and directed towards the loudspeaker. SPLs are expressed in dB re 2×10^{-5} Pa. Because of the variability of SPL observed with RMS-fast readings, we recorded levels for three consecutive sounds at each test distance and then calculated the mean, after converting SPL into pressure units. The transmitted male call was simultaneously recorded using an Aiwa JS215 cassette recorder for later spectral analysis of sounds recorded on the transect.

Results

Sexual signalling behaviour

Pair formation of *B. membracioides* females and primary males is achieved by duetting and male phonotaxis. Under calm conditions, males broadcast a high-intensity calling song (Fig. 2A) from approximately 22:00 h until shortly before daylight. Calling is at irregular intervals from a stationary position high up in the vegetation, usually taking advantage of high bushes and trees, and males may move distances of up to 500 m between successive calls in the absence of a female response. Receptive females, including virgins, respond with a low-intensity call (Fig. 2A) within 860 ms of the end of the male call (range 720–860 ms; mean ± S.D. 788.5±44.9 ms; *N*=13) when the SPL of the male call at the position of the female was kept constant at 86 dB. Auditory response induces the development of a duet and male phonotaxis, such that he makes a short flight and moves up to a high point on the vegetation before calling again, reorienting and repeating the procedure until the female is contacted. As the male approaches the responding female, his calls become softer and less resonant. Orientation is extremely direct and accurate (an estimated 30 cm vertically and horizontally) once the male is within hearing range of a female's response or an acoustic model in the field, suggesting a high degree of directionality of hearing in an open-loop situation which merits further examination. No courtship song or complex premating behaviour have been noted.

Pair formation calls are simple and highly stereotyped in this species. The male call is relatively invariant in form, comprising five short, 'noisy' syllables and a sixth long, resonant syllable centred around 1.7 kHz (range 1.58–2.05 kHz; mean ± S.D. 1.73±0.12 kHz; *N*=22; Fig. 2A). First and second harmonics occur at approximately 3.4 and 5.1 kHz (see Fig. 7A), attenuated by approximately 20 dB at 3.4 kHz and by approximately 30 dB at 5.1 kHz relative to the carrier frequency. An additional 'noisy' syllable occurs prior to 16 % (*N*=446) of calls. The SPL of the short introductory syllables is attenuated by 20–25 dB relative to the final syllable.

The female call has a narrow frequency spectrum (3–11 kHz) with maximum energy between 5 and 7 kHz, a short duration (range 130–175 ms; mean ± S.D. 155±13.6 ms; *N*=15) and is produced in a series of 1–8 syllables (Fig. 2A,C). The male response to a crude model of the female call, in which

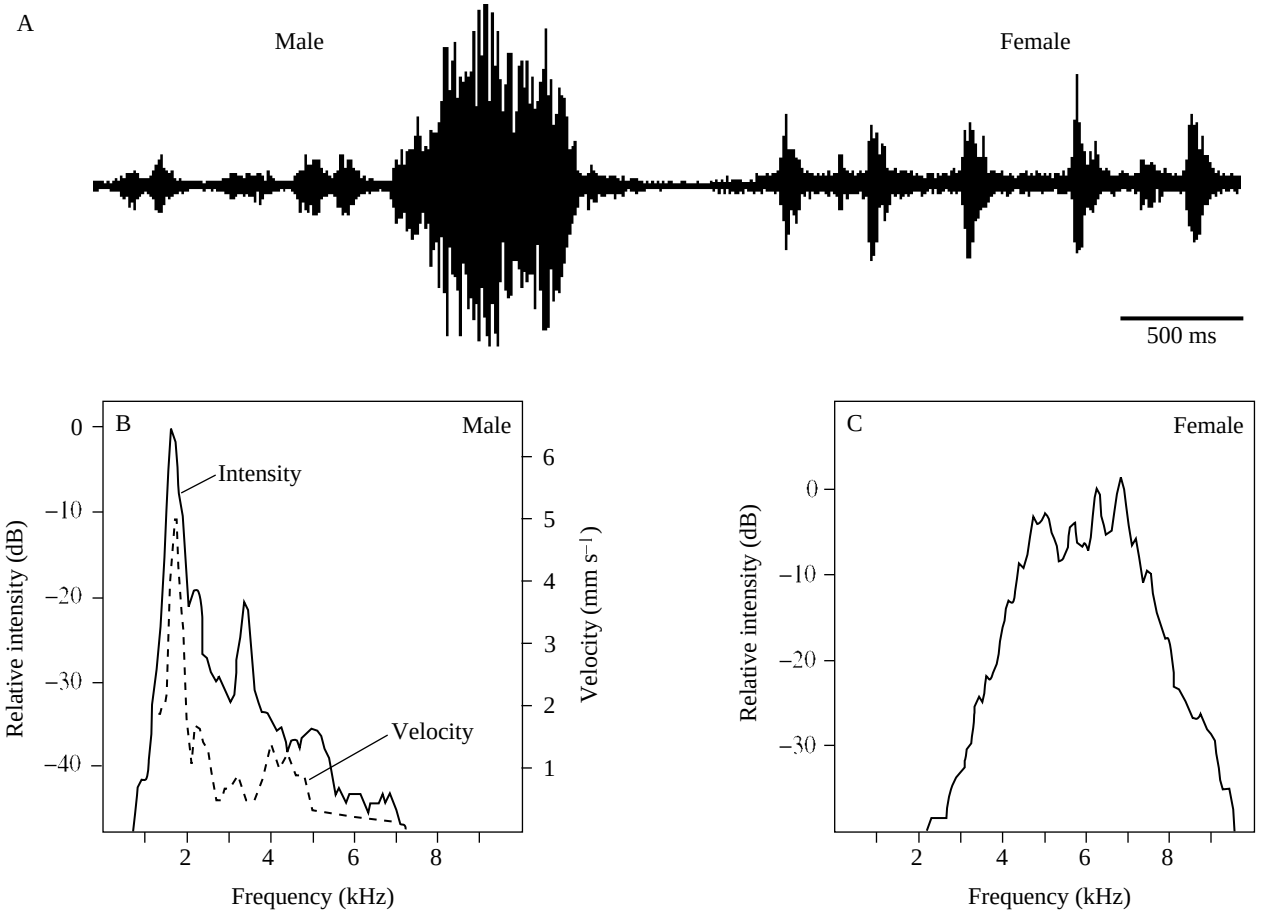

Fig. 2. Oscillograms (above) and power spectra (below) of adult *Bullacris membracioides* pair formation calls recorded in captivity at a distance of 3 m. (A) Call form is a stereotyped six syllables in males, but variable from 1 to 8 syllables in females. The mean latency of the female response is 788.5±44.9 ms (mean ± S.D.; *N*=13) after the end of the male call. (B) Male power spectrum and laser-Doppler vibrometry for vibration velocity of the inflated abdomen in response to acoustic stimulation with pure tones at an SPL of 86 dB, recorded laterally on the third abdominal segment. The maximal vibration velocity at 1.7 kHz (range 1.6–2.1 kHz) corresponds with the carrier frequency of male calls (range 1.58–1.96 kHz). (C) Female power spectrum.

the frequency range was not well reproduced but which was faithful to the temporal pattern and to the latency relative to the males' last syllable, indicates that a broad-band sound alone is sufficient for pair formation and that the frequency characteristics of the female call are relatively unimportant.

Sound production mechanisms

Sexual signals are produced by abdominal–femoral stridulation in males and abdominal–wing stridulation in females. In males, a short scraper consisting of a high carina with a small row of strong, transverse ridges (range 18–25; mean ± S.D. 21±2.4; *N*=20) on the proximal side of the hind femur (Fig. 3B), is moved along a file of nine (range 8–9; mean ± S.D. 8.9±0.3; *N*=20) strongly sclerotized ridges on the second abdominal tergite (Fig. 3A). Both elements are highly symmetrical. At the final larval instar, the abdomen expands dramatically, forming a permanently inflated bladder. Laser vibrometry indicates that maximal vibration velocity occurs at frequencies of approximately 1.7 kHz (range 1.6–2.1 kHz; Fig. 2B). The impact of file and scraper is spread across the large surface of the resonating abdomen, producing a sound output of 98 dB SPL at 1 m for the last syllable.

The female response, which averages 60 dB SPL at 1 m (*N*=13), is produced by rubbing teeth-bearing veins on the ventral margins of the wings (Fig. 3D) across raised pegs in a differentiated region of the tergum beneath the resting wing (Fig. 3C). Ablation experiments confirm that the elytra play no part in the production of the female sexual signal.

Sound transmission in the field

Meteorological measurements revealed that super-adiabatic conditions, in which temperature drops rapidly with height above the hot ground surface, prevail from mid-morning to mid-afternoon (Fig. 4A; values for 5 m were between those for 1 and 10 m). This gradient (between 1.5 and 4.5 °C at a depth of 9 m) results in moderately turbulent mixing and the development of significant surface wind (wind speed greater than 7 m s^{-1}) as the ground warms (Fig. 4B). In contrast,

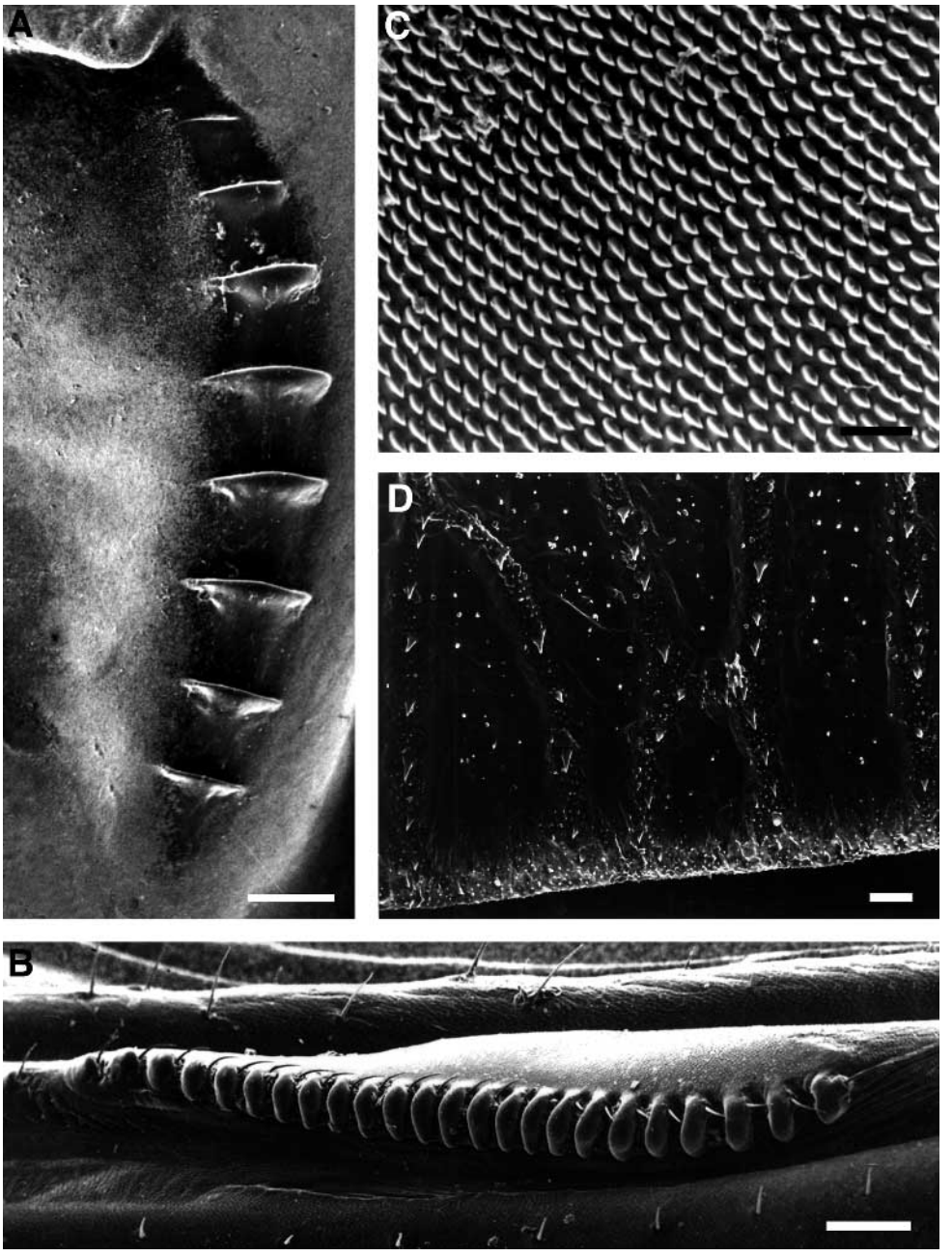

Fig. 3. Scanning electron micrographs of adult stridulatory mechanisms. (A) Sclerotised file on pleura of male second abdominal segment. Scale bar, 400 µm. (B) Scraper on proximal surface of male hind femur. Scale bar, 100 µm. (C) Stridulatory pegs in differentiated region of female abdominal tergite. Scale bar, 25 µm. (D) Ventral surface of female wing showing stridulatory teeth on veins. Scale bar, 200 µm.

temperature increases with height from the ground at night. The strong temperature inversions that form at the surface shortly after sunset (1.2 °C over 9 m) and decay with sunrise are accompanied by calm wind conditions (less than 2 m s^{-1}) during early to late evening.

Measurements of SPL for male calls played back during the day showed substantial variability (Fig. 5A; open circles) which increased with distance from the sound source. Almost all values fell below the theoretical ideal (6 dB per doubling of distance; solid line) beyond 50 m and were below the masking noise beyond 100 m. In contrast, at night when *B. membracioides* actually communicates acoustically, the male call suffers little excess attenuation (Fig. 5A; filled circles). Under a wide variety of environmental conditions (Fig. 5A), the variability in SPL of played-back calls is lower compared with daytime conditions, and attenuation approaches values according to geometrical spreading of sound for distances up to 450 m. Variability increases little with distance, but over the entire 450 m for which sound pressure levels were directly measured, the range does not deviate from the theoretical ideal.

Broadcast area is defined as the area within which the SPL of a call exceeds the auditory threshold of a receiver (Brenowitz, 1982). Neurophysiological recordings from the afferent nerve carrying the axons of fibres of the hearing organ in abdominal segment A1 indicated that the hearing threshold of females to conspecific male calls averages 33.3±3.6 dB SPL (mean ± S.D.; *N*=18; Römer and van Staaden, 1996). Extrapolating the male call transmission trajectory until the

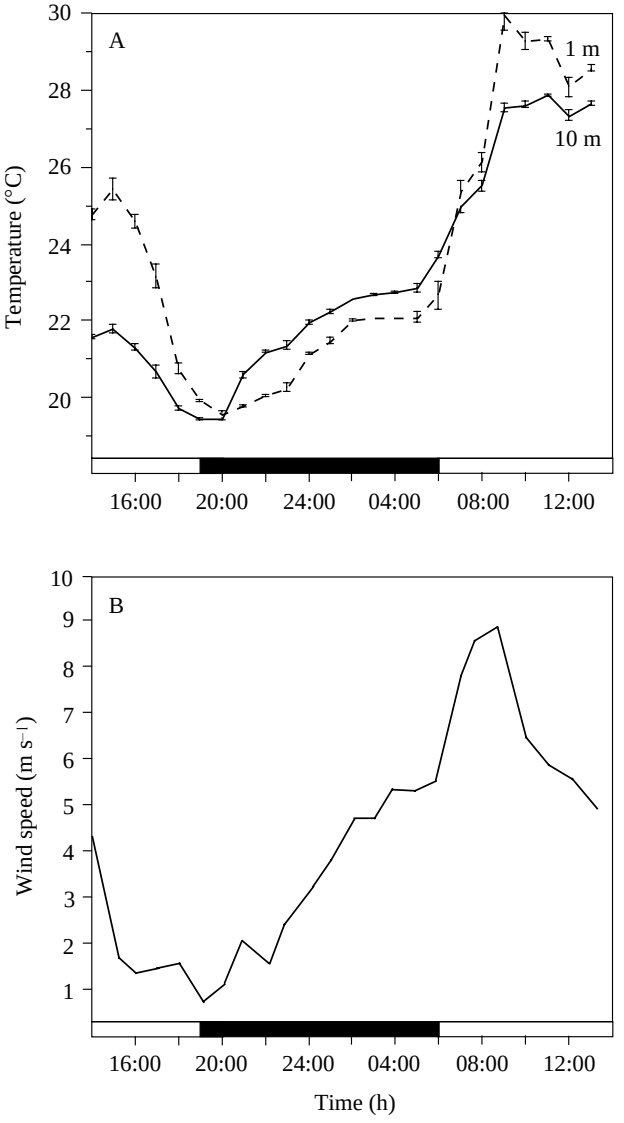

Fig. 4. Weather profile recorded over 24 h in open grassland at Inchanga (elevation 814 m) on 12–13 February 1996. Time is in Local Solar Time with sunrise at approximately 06:00 h and sunset at approximately 19:00 h. (A) Thermal profiles for sensors at 1 m (broken line) and 10 m (solid line) height above ground. Values are shown at 30 min intervals and are the mean of 60 measurements over a 5 min period. Error bars show S.D. (B) Wind speed (anemometer height above ground 2 m). Velocity and temperature measurements were registered every 5 s and averaged over 5 min periods. The profile shown is typical of the summer weather pattern in this area, although the absolute values of thermal gradients are usually higher than occurred in 1996.

SPL of the transmitted call intersects the hearing threshold (Fig. 5C) gives a potential transmission distance for the male call to conspecific females ranging between 1500 and 1900 m. If we assume a male *B. membracioides* is an omnidirectional sound source and that homogeneous transmission occurs in all directions, the corresponding area over which a female would be able to detect the call would vary between 7.1 and 11.3 km^2. Under a comparable range of environmental conditions, the female call also suffers little or no excess attenuation (Fig. 5B). However, the broadcast SPL of the female call is considerably lower at 60 dB (at 1 m), which results in an estimated effective detection distance by the male of only 50 m, given the male hearing threshold of 29.1±4.9 dB SPL (mean ± S.D.; *N*=13; H. Römer and M. J. van Staaden, in preparation) to the female response. The corresponding broadcast area would be limited to 0.078 km^2. Thus, there is a more than 100-fold difference in the maximum broadcast areas of male and female calls.

Estimation of the maximum transmission distances for male and female calls (Fig. 5) assumes the absence of masking noise in the field that might otherwise interfere with the detection of conspecific calls. Potential masking sounds for acoustic communication between male and female *B. membracioides* are primarily produced by a variety of nocturnal crickets with call power spectra ranging from 2 to 6 kHz (Fig. 6) and song duty cycles of 15–90 % depending on the species. These calls could interfere with the detection of *B. membracioides* signals since the sensitivity of the hearing organ of the latter is centred at 4 kHz (Römer and van Staaden, 1996). We therefore analyzed the level and frequency spectrum of background noise for night-time transmission conditions. The distribution of heterospecific cricket males on the transect was patchy in time and space, with most crickets calling in the early to late evening. As a result, the background noise level was neither uniform in time nor uniform over the whole area of the transect. Fig. 7 shows a series of spectra analysed from night-time recordings of a male call on the transect, at distances ranging from 100 to 400 m. The sensitivity of the hearing organ in abdominal segment A1 of a typical young female is superimposed on the spectra to demonstrate the effect of sound transmission and background noise on the detection of the male call. At a distance of 100 m (Fig. 7A), the SPL of the recorded male call was 60 dB, and both the carrier frequency of the call at 1.9 kHz and the frequency components including the first harmonic at approximately 3.8 kHz contribute to detection at this distance. At 250 m, the SPL was 54 dB, but there was also some background noise close to 5 kHz from a distant cricket, which potentially interferes with the hearing sensitivity of a female at this position, despite the energy of the cricket call being 20 dB lower than that of *B. membracioides* (Fig. 7B). A much better detection situation was found at a distance of 400 m and an SPL of 52 dB, although there was a cricket calling at approximately 6 kHz (arrows in Fig. 7B,C). This is, however, outside the hearing sensitivity of *B. membracioides* females.

Discussion

Long-distance acoustic signalling in bladder grasshoppers involves a complex of anatomical and behavioural adaptations that together result in the longest effective transmission distance yet recorded among insects. While the abdomino-femoral stridulatory mechanisms and a concentration of air spaces in the thorax and abdomen are not unique to pneumorids

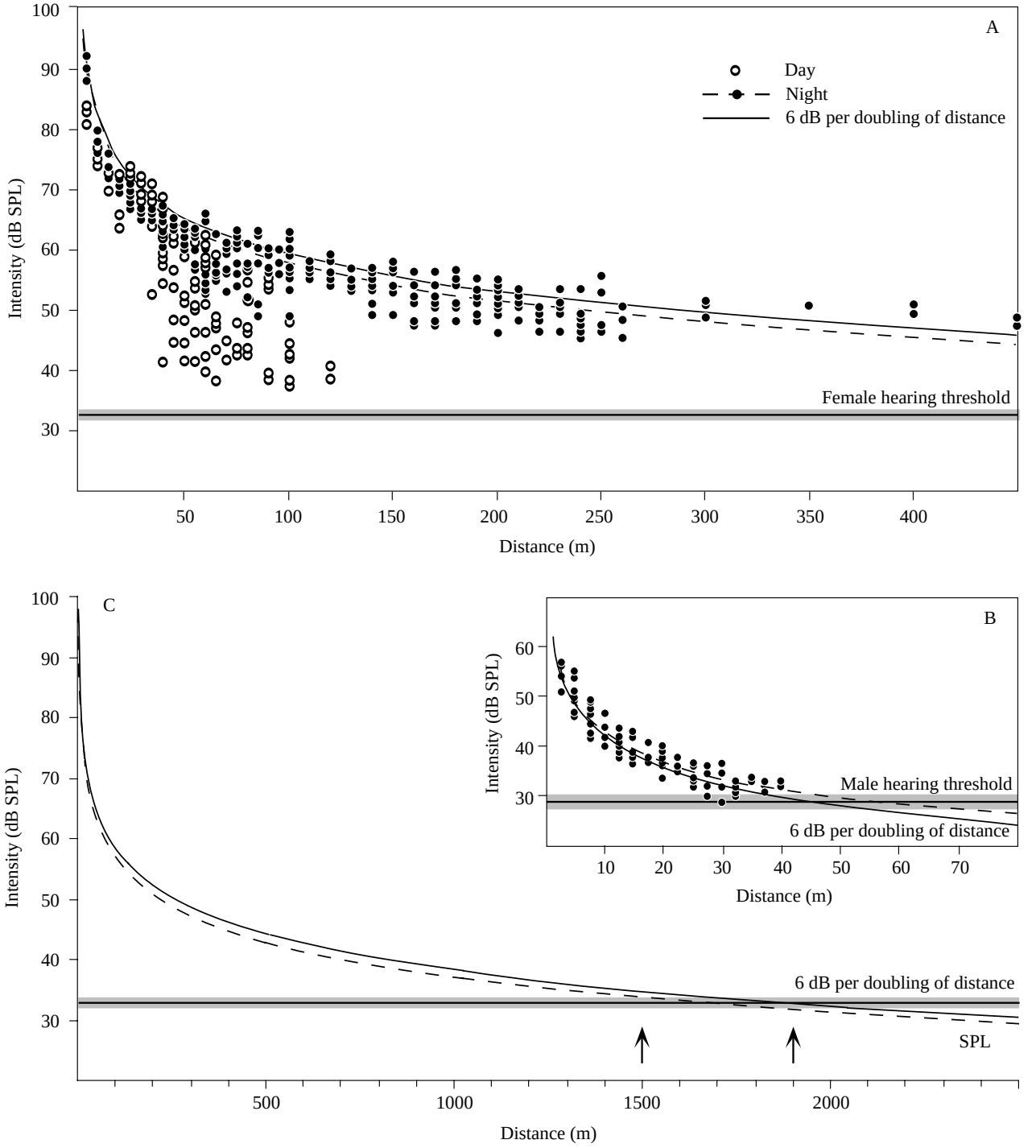

Fig. 5. Transmission of (A) male and (B) female sexual signals in natural habitat at increasing distance from a speaker broadcasting at a constant SPL (males 98 dB; females 60 dB SPL; height of speaker above ground 2 m). Sound pressure levels were measured at a height of 2 m during the day (open circles) and night (filled circles) in February 1994–1996. Each data point represents a mean for three consecutive sounds at each test distance; for A yielding 320 data points at distances less than 100 m, 108 points for distances between 100 and 200 m, and 51 points for distances greater than 200 m. A logarithmic curve was fitted to the night-time data (broken line, y=96.2746–19.7915log$x$; r^2=0.902). For comparison, the theoretical transmission with attenuation due only to geometrical spreading (6 dB per doubling of distance) is shown (solid line). The shaded areas indicate the hearing sensitivity of insects of the opposite sex receiving the signal (mean ± S.D.). (C) Proposed transmission distance (between arrows) of the male call based on field measurements over a distance of up to 450 m and the mean sensitivity of female hearing to this signal.

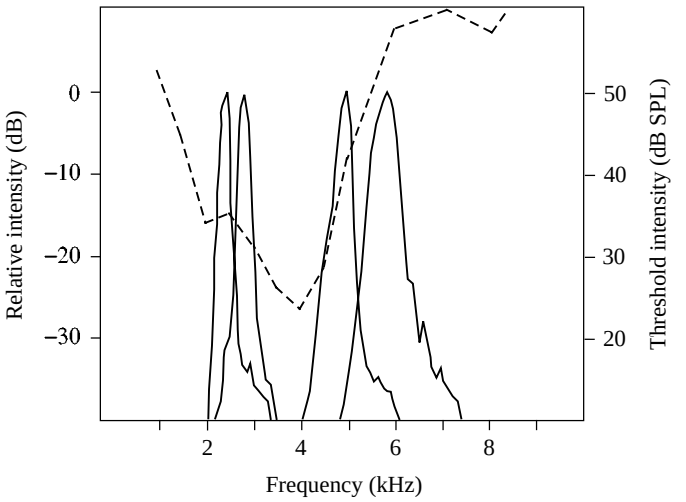

Fig. 6. Power spectra of four species of cricket recorded at or near the transect where the transmission of *Bullacris membracioide*s calls was examined. The carrier frequencies of the calls range from 2.3 and 2.5 kHz for the two *Oecanthus* species (left) to 5.0 and 5.9 kHz for two other unidentified cricket species. The potential masking effect of these signals is demonstrated by superimposing on the spectra the averaged female tuning curve (*N*=9) for the hearing organ in abdominal segment A1 (broken line).

(Bennet-Clark, 1994; Field, 1978), the trend reaches its highest point of specialization in the inflated bodies and sound output levels of this taxon. Our data suggest that the efficiency of male pneumorid signal transmission may be a function of both increased sound output and exploitation of weather conditions. This is the first such demonstration for insect auditory signalling and is consistent with results of empirical studies of sound propagation outdoors (Canard-Coruna *et al.* 1990; Piercy *et al.* 1977) and on calculations of atmospheric effects on low-frequency communication in African elephants (Garstang *et al.* 1995).

Atmospheric control on transmission distance

Our results suggest that the distance over which pneumorid males transmit their calls increases more than tenfold at night. Optimum conditions occur 1–2 h after sunset on warm, misty and calm nights, and at these times ranges in excess of 1.5 km are likely. Sound waves are refracted when they meet a change in the acoustic impedance of the medium, e.g. volumes of air differing in temperature, humidity or wind velocity (for reviews, see Embleton, 1996; Larom *et al.* 1997). Vertical gradients in temperature occur regularly in natural habitats. Lapse conditions during the day, in which atmospheric temperature decreases with height from the ground, reduce the speed of sound with height and cause sound waves to bend upwards. Reduced sound levels near the surface thus create shadow zones beyond a certain distance from the source where no direct sound can penetrate. Indeed, our measurements during the day (Fig. 5A) indicate a sudden drop in SPL of the broadcast male call starting at distances of approximately 40 m,

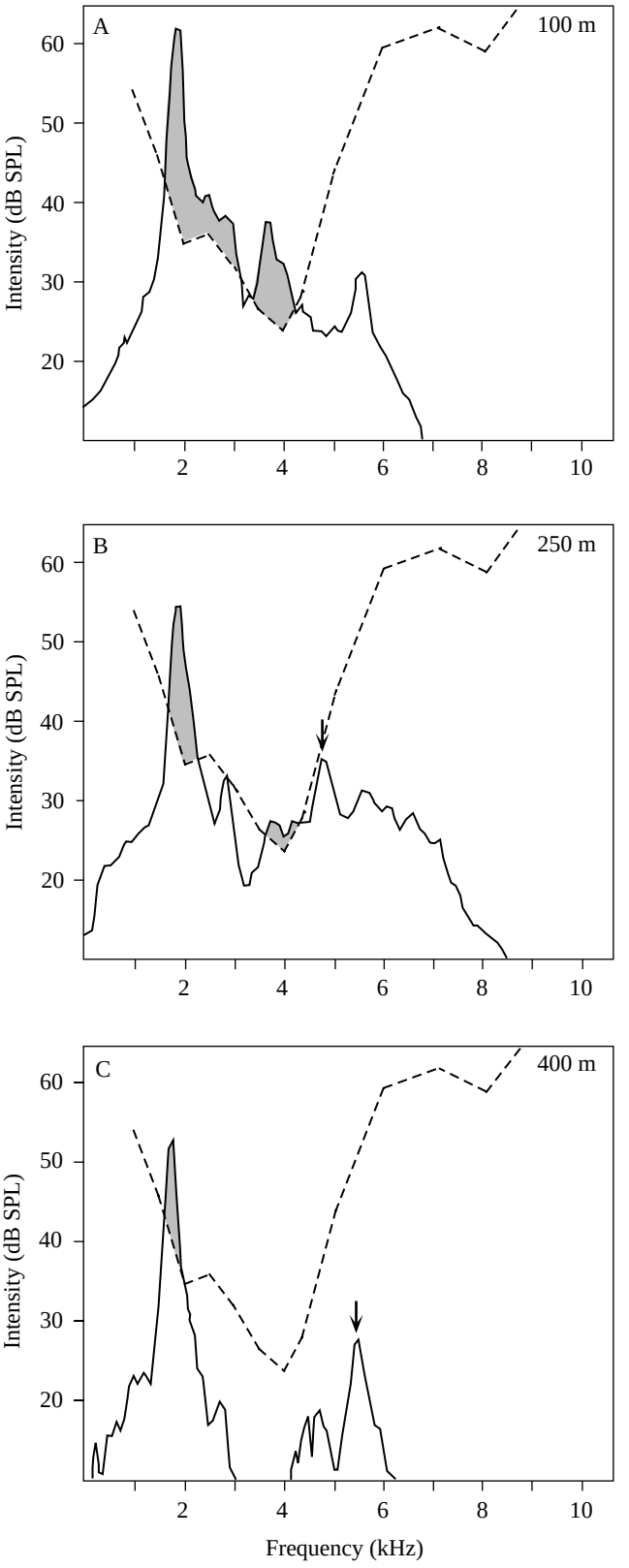

Fig. 7. Power spectra of night recordings of *Bullacris membracioides* male calls on the transect over various distances. Superimposed on the spectra is the averaged female tuning curve (*N*=9) for the hearing organ in abdominal segment A1 (broken line). For further explanation, see the text.

which is consistent with the existence of a shadow zone. Thus, ignoring masking background noise levels (see below), a male calling in the afternoon would at best reach a potential female at distances of only 100–150 m.

Night-time cooling creates temperature inversions, such that temperatures increase with height. Consequently, air is stratified, resulting in calm conditions with reduced wind noise near the ground and downward-reflecting sound waves. The latter give rise to an acoustic enhancement (the opposite of excess attenuation) and, thus, an increase in the SPL at some distance from the source relative to the 6 dB per doubling of distance relationship. These so-called ground-level inversions contrast with elevated inversions, where temperature gradients develop at some height above the ground (tens or hundreds of metres) and therefore do not have the same enhancing effect for sound signals broadcast near the ground (Larom *et al.* 1997). Calculations based on tethered balloon measurements of temperature inversions over African savanna predict an enhancement of 12–15 dB, given a 5 °C inversion strength, for the infrasound frequencies of 15–30 Hz used in elephant communication (Garstang *et al.* 1995). Our experimental data for night-time transmission show only a small amount of evidence for a direct enhancement of the call (see values over 300 m; Fig. 5A). However, the measured SPL at each distance is the additive effect of all enhancing and attenuating conditions experienced by the sound wave, and excess attenuation due to high grass vegetation on the transect is most likely to have negated the enhancing effect of temperature inversions. Moreover, compared with the infrasound frequencies on which the calculations of Garstang *et al.* (1995) and Larom *et al.* (1997) are based, enhancement effects should be reduced at the higher frequencies of *B. membracioides* calls. In this context, it is singularly interesting that a sound window in the same frequency range has been found in forest environments (Morton, 1975).

Although the data illustrated in Fig. 4 demonstrate the temperature inversion occurring at the experimental site, they are not representative of the most common situation for sound transmission in this species. More extreme thermal inversions would normally prevail than are indicated by recordings in the unusually cool and wet 1996 field season. This is true for both the strength of the inversion (the difference in temperature at 10 m relative to ground level) and more particularly for wind speed conditions. In 1995, when the majority of sound transmission experiments were performed, windless conditions for several hours after sunset were the rule rather than the exception. In 1996, in contrast, wind speed at the transmission site was rarely below $1\,m\,s^{-1}$. Hence, thermal gradients and temperature inversions during the 1995 measurements were stronger than those shown in Fig. 4, and our measurements of transmission area are thus conservative. For example, an increase in inversion strength from 0.5 to 2 °C was calculated to result in a tenfold increase in broadcast area from 30 km^2 to approximately 300 km^2 (Larom *et al.* 1997).

Topography and wind conditions are other important variables for sound transmission and are clearly more important at greater distances (km) than at shorter distances (Embleton, 1996). However, at present, we know very little about the effect of topography on the formation of shadow zones in the pneumorid frequency range. In general, wind moving up or down a ridge results in up-slope enhancement and down-slope degradation, respectively, and a numerical study demonstrated strong acoustic shadows behind ridges which were downwind of a source (Robertson *et al.* 1989). In KwaZulu-Natal, prevailing nocturnal winds are predominantly down-valley (Preston-Whyte and Tyson, 1988) so that the effects of ground topography on the transmission distance of mating calls are expected to be reflected in the overall patterns of population genetic structure.

The above consideration has neglected the effects of masking noise for the detection of male calls, which potentially limits communication distance. Levels of masking noise are known to be relatively high in certain habitats and may result in temporal or spatial segregation, call inhibition and other behavioural responses (Gogala and Riede, 1995; Greenfield, 1988; Narins, 1995; Römer *et al.* 1989). A particular problem with respect to masking in the pneumorid communication system is the fact that male and female hearing is mismatched to the male call; the ear is approximately 15 dB less sensitive at the male carrier frequency of 1.7 kHz than at its best frequency of 4 kHz (see female tuning curves in Fig. 7). Thus, any heterospecific sounds at frequencies near 4 kHz would have a strong masking effect on the detection of the male call. Recorded calls of crickets on the transect (Fig. 7) have carrier frequencies ranging from 2.3 kHz to approximately 5.9 kHz and could potentially interfere with detection of the signal (Fig. 6). However, the distribution of calling crickets was found to be patchy in time and space at the usual signalling times of *B. membracioides*, so that it very much depends on the location of the receiver (microphone or female) relative to the masking source whether interference takes place. For instance, there was no relevant masking noise at a distance of 400 m, since the low-intensity cricket song at 6 kHz was outside the average hearing sensitivity of a female, whereas at 250 m the SPL of the cricket call (Fig. 7B, arrowed) was just subthreshold at a signal-to-noise ratio of 20 dB. The same masking noise level at a distance of 1.4 km would equal the signal level at that distance and probably render the detection of the male call impossible. The same limitation would occur at a distance of only 400 m, however, if the SPL of the cricket were 20 dB higher. It is evident, then, that female detection of the male call can be strongly influenced by any cricket calling nearby (since the female is largely immobile), resulting in a large variation of transmission distances from an ideal of approximately 2 km to only 100 or a few hundred metres. Males, in contrast, could potentially avoid nearby masking sounds simply by flying to another receiver position.

This study determined pneumorid communication distances by extrapolating from transmission measured directly to 450 m, until the SPL curve intersected the hearing threshold (as determined by neurophysiological techniques). While extrapolating beyond measured data points is not ideal, in this

The Journal of Experimental Biology 200, 2609–2616 (1997)
Printed in Great Britain © The Company of Biologists Limited 1997
JEB0920

SULFIDE ACQUISITION BY THE VENT WORM *RIFTIA PACHYPTILA* APPEARS TO BE *VIA* UPTAKE OF HS^-, RATHER THAN H_2S

SHANA K. GOFFREDI*, JAMES J. CHILDRESS, NICOLE T. DESAULNIERS AND FRANCOIS H. LALLIER†
Marine Science Institute and Department of Ecology, Evolution, and Marine Biology, University of California, Santa Barbara, CA 93106, USA

Accepted 23 July 1997

Summary

Deep-sea hydrothermal vents are home to a variety of invertebrate species, many of which host chemosynthetic bacteria in unusual symbiotic arrangements. The vent tubeworm *Riftia pachyptila* (Vestimentifera) relies upon internal chemolithoautotrophic bacterial symbionts to support its large size and high growth rates. Because of this, *R. pachyptila* must supply sulfide to the bacteria, which are far removed from the external medium. Internal ΣH_2S ($[H_2S+HS^-+S^{2-}]$) can reach very high levels in *R. pachyptila* (2–12 mmol l^{-1} in the vascular blood), most of which is bound to extracellular hemoglobins. The animal can potentially take up sulfide from the environment *via* H_2S diffusion or *via* mediated uptake of HS^-, or both. It was expected that H_2S diffusion would be the primary sulfide acquisition mechanism, paralleling the previously demonstrated preferential uptake of CO_2. Our data show, however, that the uptake of HS^- is the primary mechanism used by *R. pachyptila* to obtain sulfide and that H_2S diffusion into the worm apparently proceeds at a much slower rate than expected. This unusual mechanism may have evolved because HS^- is less toxic than H_2S and because HS^- uptake decouples sulfide and inorganic carbon acquisition. The latter occurs *via* the diffusion of CO_2 at very high rates due to the maintenance of an alkaline extracellular fluid pH. ΣH_2S accumulation is limited, however, to sulfide that can be bound by the hemoglobins, protecting the animal from sulfide toxicity and the symbionts from sulfide inhibition of carbon fixation.

Key words: tubeworm, *Riftia pachyptila*, sulfide, symbiosis, hydrothermal vent, diffusion, mediated transport, vestimentiferan.

Introduction

The hydrothermal vent tubeworm *Riftia pachyptila* was first found to be symbiotic with intracellular carbon-fixing sulfide-oxidizing bacteria in 1981 (Cavanaugh *et al.* 1981; Felbeck *et al.* 1981). Because *R. pachyptila* relies upon these internal bacterial symbionts for its nutrition, it must supply them with carbon dioxide, oxygen, hydrogen sulfide and other nutrients (Fisher, 1990; Childress and Fisher, 1992). These compounds are taken up from the environment across the plume and transported, *via* a well-developed vascular system, to the bacteria, found in a highly vascularized organ known as the trophosome (Jones, 1981; Arp *et al.* 1985; Childress and Fisher, 1992). This organ is located within the trunk of the worm, surrounded by non-circulating coelomic fluid, which is apparently in equilibrium with the circulating vascular blood for smaller molecules such as CO_2, H^+ and H_2S (Childress *et al.* 1984, 1991).

These worms have two extracellular hemoglobins in the vascular blood and another in the coelomic fluid that bind and transport both oxygen and hydrogen sulfide to the symbiont (Arp *et al.* 1985, 1987; Childress *et al.* 1991; Zal *et al.* 1996*a*,*b*). Vascular blood has a higher capacity for sulfide and contains more total sulfide (ΣH_2S) than coelomic fluid because the larger of the two vascular hemoglobins has a higher capacity (approximately threefold higher) for sulfide binding and overall hemoglobin concentration in the vascular blood is higher (Arp *et al.* 1987; Childress *et al.* 1991). *R. pachyptila* body fluids can reach extremely high concentrations of ΣH_2S (including H_2S, HS^- and S^{2-}), up to 6 mmol l^{-1} in the coelomic fluid and 12 mmol l^{-1} in the vascular blood (Childress *et al.* 1991). Other than the binding of sulfide by the hemoglobins, however, the mechanism of sulfide uptake has not been studied.

Goffredi *et al.* (1997) proposed that the mechanism for inorganic carbon acquisition in these worms is diffusion of the undissociated CO_2 species, which is supported by effective control of body fluid pH by proton-equivalent export, rather than mediated uptake of HCO_3^-. Both carbon dioxide and hydrogen sulfide demonstrate strong pH-dependent dissociation. The pK values, or dissociation constants (i.e. the pH values at which the ratios CO_2:HCO_3^- and H_2S:HS^- are 1:1), for CO_2 and H_2S are 6.1 and 6.6, respectively (Dickson

*e-mail: goffredi@lifesci.ucsb.edu
†Present address: Laboratoire d'Ecophysiologie, Station Biologique, CNRS, BP 74, 29682 Roscoff Cedex, France.

and Millero, 1987; Millero *et al.* 1988), at 10 °C and 101.3 kPa. Thus, H_2S, like CO_2, is the dominant chemical species *in situ* owing to the acidic pH (near 6.0) around the worms. H_2S diffusion into the worms would be a function of the external and internal (intra- and extracellular) concentrations of free H_2S, which are functions of ΣH_2S, pH and sulfide binding by the hemoglobins in the blood. Hypothetically, if sulfide were acquired *via* H_2S diffusion, sulfide would be concentrated in the blood, as is the case for inorganic carbon because, at the physiological pH of 7.1–7.5 of *R. pachyptila*, H_2S dissociates into HS^- and H^+ and the protons would normally be eliminated (Childress *et al.* 1984, 1991; Goffredi *et al.* 1997). One would predict in this case that, all else being unchanged, a lower external pH would increase the rate of sulfide uptake while a lower internal (extracellular) pH would decrease uptake.

In contrast, if the mechanism for sulfide acquisition in *R. pachyptila* were HS^- uptake, the pH-dependence of this mechanism would be expected to differ from that of CO_2 and H_2S uptake. HS^- uptake would probably be mediated by the negative charge of the ion. If it were to occur *via* facilitated diffusion, uptake of HS^- might increase with decreases in extracellular pH, because of effects on the equilibrium in the body fluids. It is possible, however, that the uptake of HS^- may not be affected much by changes in internal hydrogen ion concentration.

The purpose of the present study was to determine the mechanism used by *R. pachyptila* to acquire sulfide from the environment. This involved the measurement of internal sulfide concentrations from freshly captured worms and the execution of live animal experiments in pressure systems on board ship. To differentiate between H_2S diffusion and mediated uptake of HS^-, we measured coelomic fluid and vascular blood ΣH_2S of worms in two types of experiments: in one, we varied external H_2S and HS^- levels around the worms; in the other, we forced a decrease in the extracellular pH of the worms by exposing them either to hypoxic water or to a non-specific inhibitor of H^+-ATPases, *N*-ethylmaleimide.

Materials and methods

Collections

Riftia pachyptila Jones were collected at a mean depth of 2600 m by submersible (D.S.R.V. *Alvin* and *Nautile*) during research expeditions to 9°N (9°50′N, 104°18′W) and 13°N (12°48′N, 103°57′W) along the East Pacific Rise in 1994 and 1996. In 1994, hot venting water and warm water samples around the tubeworms were collected using titanium samplers from the *Alvin*. Animals were brought to the surface in a temperature-insulated container and transferred to cold sea water (5 °C) in a refrigerated van on board ship. Worms were then sorted to be used either for experiments on living animals or for immediate measurements of physiological parameters. Live animal experiments were initiated within 2 h of surfacing.

Pressure aquaria

All experiments were conducted inside a refrigerated van. Sea water was chilled by moving the water through polypropylene tubing past a refrigeration unit, after which it was pumped by high-pressure, Teflon diaphragm, metering pumps through stainless-steel vessels at flow rates ranging from 4 to 12 l h^{-1}, at a pressure of approximately 21.5 MPa. Pressure gauges and sample ports were placed in-line immediately after flow through the vessels to allow monitoring of pressure and water conditions. All worms were kept in these pressurized flowing-water aquaria, in which we were able to re-create many aspects of the vent environment, such as temperature, pressure and a variety of chemical conditions, including pH, ΣCO_2, ΣH_2S, O_2 and N_2 concentrations (Quetin and Childress, 1980; Goffredi *et al.* 1997). Water ΣCO_2, O_2 and N_2 levels and P_{CO_2} were varied by bubbling CO_2, O_2 and N_2 gas directly into a gas equilibration column, which supplied water to the high pressure pumps (see diagram in Kochevar *et al.* 1992). Sulfide concentrations were controlled by continuously pumping anaerobic solutions of sodium sulfide (30–50 mmol l^{-1}) into the gas equilibration column at rates dependent upon the desired final concentrations of sulfide. At the end of each experiment, the animals were quickly removed from the pressure vessel and dissected.

Experiments

In one type of experiment (‘sulfide series’), worms were placed in experimental vessels immediately upon collection from the sea floor. Thirty worms were kept at 8 °C and exposed to 4.0±0.5 mmol l^{-1} ΣCO_2 (mean ± S.E.M. for all values given) and 191±18 μmol l^{-1} O_2 for 17–20.5 h. To stabilize the pH, 10 mmol l^{-1} Mops or Mes buffer was added to the sulfide solutions. In some cases, depending on the desired final pH value, it was necessary to alter the pH of the buffered solutions by titration with hydrochloric acid. In this particular experiment, we achieved external [H_2S] values between 0 and 362 μmol l^{-1} and [HS^-] values between 0 and 265 μmol l^{-1} by controlling the external pH between 5.59 and 7.21 and ΣH_2S values between 63 and 511 μmol l^{-1}.

In another experiment (‘hypoxia’ experiments), we exposed twelve worms to hypoxic conditions (at 15 °C) with external oxygen levels no greater than 42 μmol l^{-1} O_2 for 13 h, while control worms were kept at oxygen levels of 316±23 μmol l^{-1}. *In situ* concentrations of O_2 around the worms fluctuate due to the mixing of vent waters (0 μmol l^{-1}) with ambient water (110 μmol l^{-1}). Data on the metabolism of the worms and the distribution of O_2 around them, however, show that they take up O_2 primarily from concentrations approaching 100 μmol l^{-1} (Johnson *et al.* 1988; Childress *et al.* 1991). In our experience, O_2 concentrations between 100 and 400 μmol l^{-1} do not appear to affect the symbioses (P. Girguis, personal communication). All worms in these experiments were kept in the aquaria described above and exposed to typical vent water concentrations of ΣCO_2 (4.4±0.2 mmol l^{-1}), ΣH_2S (156±21 μmol l^{-1}) and pH (6.23±0.05).

In additional experiments (‘inhibitor’ experiments), we initially kept worms in flowing-water maintenance aquaria, also at 8 °C and 21.5 MPa, supplied with surface sea water

(ΣCO_2 levels of 2.1 mmol l^{-1}, pH 8.2, and no sulfide). This experiment, in which we needed a uniform starting point for all of the worms, was directed at measuring the rates of uptake of CO_2 and sulfide over time; thus, we needed these worms to have low internal levels of ΣCO_2 and ΣH_2S, which resulted from maintenance in surface sea water. In order to observe uptake rates over time, the animals were then transferred to experimental vessels (for 0–20 h), and water conditions (ΣCO_2 4.8±0.1 mmol l^{-1}, O_2 230±9 μmol l^{-1}, ΣH_2S 311±39 μmol l^{-1} and pH 5.96±0.05) were controlled in the same manner as described for the sulfide series and hypoxia experiments. 15 worms were used as controls and 9 worms were exposed to *N*-ethylmaleimide (NEM), a non-specific inhibitor of H^+-ATPases, at concentrations between 1.1 and 1.6 mmol l^{-1} for 1–2 h (Marver, 1984; Stone *et al.* 1984).

It is important to note that during the 1–12 h of these inhibitor experiments, it is likely that the worms were not in autotrophic balance. It has been suggested that it takes at least 14 h in the presence of sulfide for these worms to become autotrophic (net uptake of CO_2; Childress *et al.* 1991). Another study has shown that, at 12 h, and under conditions similar to ours, there is some assimilation of both $^{13}CO_2$ and $^{15}NO_3^-$ by *R. pachyptila*, indicating that the symbionts are functioning (Lee and Childress, 1994). Regardless, time points before 12 h are meaningful in terms of the functioning of the animal, and for our studies it was more important to isolate the physiology of the worms from that of the symbionts.

Analytical techniques

All worm dissection techniques were similar to those described in Childress *et al.* (1991) and Goffredi *et al.* (1997). ΣCO_2 and ΣH_2S of coelomic fluid, vascular blood and water samples were measured on 0.5 ml samples using a Hewlett Packard 5880A series gas chromatograph (Childress *et al.* 1984). 'ΣH_2S', as measured by the gas chromatograph, represents the sum of H_2S, HS^-, S^{2-} concentrations and the amount of sulfide bound to the hemoglobins. 'ΣCO_2', as measured by the gas chromatograph, represents the sum of CO_2, HCO_3^- and CO_3^{2-} concentrations. Body fluid and water pH were measured using a thermostatted Radiometer BMS-2 blood pH analyzer equipped with a G299A capillary pH electrode and connected to a PHM73 pH meter. Additional water pH measurements were made using a double-junction combination electrode (Broadley-James) connected to a PHM93 pH meter (Radiometer).

Statistics

The Kendall rank correlation was used to test for correlations. The Mann–Whitney *U*-test was used to test for differences in distribution between data sets. Simple regressions were used to show linear relationships, and multiple regressions were used to compare influences of various parameters. The analysis of covariance (ANCOVA) was used to compare slopes and magnitudes of different data sets.

Results

Both freshly collected and experimental worms showed an increase in internal sulfide levels as the surrounding water pH increased. For freshly collected worms, the ΣH_2S values in both coelomic fluid and vascular blood increased as the surrounding water pH increased (P=0.0025 and P=0.0151, respectively, Kendall rank correlation). For 'sulfide series' worms, the coelomic fluid and vascular blood ΣH_2S levels also increased as we increased the surrounding water pH (P=0.0007 and P=0.0013, respectively, Kendall rank correlation). In addition, the internal ΣH_2S levels of these worms were positively correlated with the extracellular pH (y=3.451x–23.676, P=0.0006, and y=6.661x–43.014, P<0.0001 for the regressions of coelomic fluid and vascular blood of 'sulfide series' worms, respectively, where y is ΣH_2S and x is extracellular pH).

Worms collected from the sea floor and placed immediately into 'sulfide series' experiments had initial internal ΣH_2S levels of 0.18±0.12 mmol l^{-1} and 0.43±0.17 mmol l^{-1} for coelomic fluid and vascular blood, respectively. In order to determine which external species of sulfide influenced internal ΣH_2S levels, we controlled the free H_2S and HS^- concentrations in the surrounding water for 17–20.5 h. It should be noted that there was no correlation between water H_2S and HS^- levels during these experiments (P=0.55, Kendall rank correlation). In order to determine whether this 3.5 h variation among experiments played an important role in the values measured, we plotted internal sulfide concentration *versus* the incubation time of these experiments. Both graphs (data not shown) showed no dependence of internal sulfide levels on incubation time over the limited range of times used in our experiments (P=0.95 and P=0.74 for the regressions of vascular blood and coelomic fluid, respectively). This time, however, far exceeds the time necessary to reach sulfide equilibrium with the surrounding water, as considered below.

Fig. 1 shows that both coelomic fluid and vascular blood ΣH_2S levels correlated well with external HS^- (P<0.0001), but not with H_2S (P=1). A multiple regression was used to determine whether H_2S or HS^- level in the external medium had a greater influence on internal ΣH_2S values. It was apparent from this test that HS^- plays a greater role (P=0.0001) in predicting coelomic fluid ΣH_2S than does H_2S (P=0.0901) and also in predicting vascular blood ΣH_2S values (P=0.001 for HS^- and P=0.81 and H_2S). Both the coelomic fluid and vascular blood pH increased as water HS^- increased (y=1.875x+7.287, P=0.0058, and y=2.411x+7.182; P=0.0018, respectively, for the regression equations, where y is pH and x is water [HS^-]). A multiple regression analysis was used to determine whether H_2S or HS^- level in the external medium had a greater influence on extracellular pH. Again, HS^- plays a greater role in predicting coelomic fluid and vascular blood pH (P=0.0124 and P=0.0052, respectively) than does H_2S (P=0.39 and P=0.21, respectively).

To test the effect of body fluid pH upon sulfide uptake, we conducted two types of whole-animal experiments in which we forced a decrease in the extracellular pH of the worms. In the

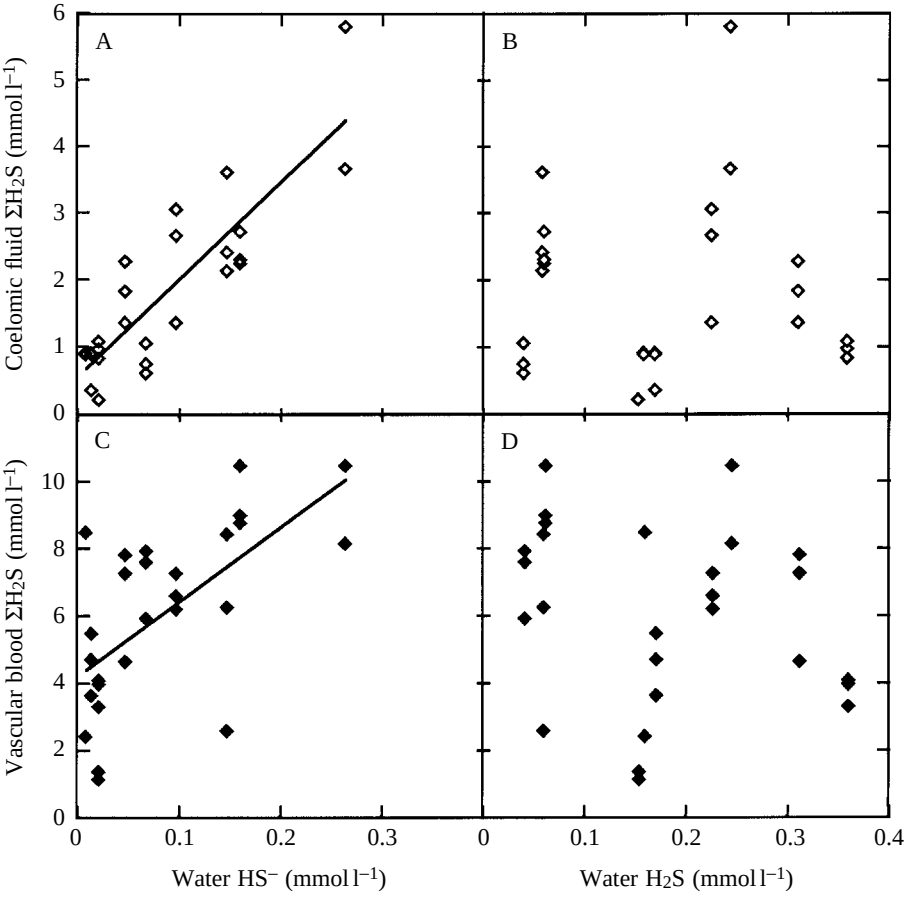

Fig. 1. Relationship between total inorganic sulfide concentration, ΣH_2S, in coelomic fluid and vascular blood from the tubeworm *Riftia pachyptila* and the HS^- (A,C) and H_2S (B,D) levels of the surrounding water during 12 shipboard experiments. Experimental vessel conditions were controlled at fixed combinations of pH and ΣH_2S. ΣH_2S values between 63 and 511 μmol l^{-1}, and pH values between 5.6 and 7.2 were achieved (N=30). (A) y=0.515+14.585x, r=0.86, P<0.0001; (B) y=1.789+0.030x, r=0.003, P=1, not significant; (C) y=4.164+22.177x, r=0.63, P=0.0004; and (D) y=7.049+5.617x, r=0.23, P=1, not significant.

first experiment, twelve worms were exposed to hypoxic conditions with external oxygen levels no greater than 42 μmol l^{-1} O_2. Exposure to these low oxygen levels resulted in significantly decreased extracellular pH (Table 1), probably because of the build up of end-products of anaerobic metabolism. However, this decrease in extracellular pH failed to significantly affect internal ΣH_2S levels in these worms (Table 1). The situation for internal ΣCO_2 was reversed in that the decrease in extracellular pH caused a significant decrease in body fluid ΣCO_2 levels (Table 1). This was expected for ΣCO_2 because inorganic carbon is concentrated into the worms as a result of the pH difference maintained between the internal and external fluids (Goffredi *et al.* 1997). More importantly, the mechanism for sulfide acquisition appears to have a different pH-dependence from that for inorganic carbon acquisition.

In the second experiment, in which 9 worms were exposed to *N*-ethylmaleimide and 15 were used as controls, we followed the accumulation of sulfide and inorganic carbon in the worms over time. After 2–4 days in water with a low P_{CO_2} and no sulfide, coelomic fluid ΣCO_2 levels were 3.8±0.7 mmol l^{-1} and ΣH_2S levels were 0.002±0.001 mmol l^{-1}

Table 1. *Body fluid pH, ΣH_2S and ΣCO_2 of control and hypoxic* Riftia pachyptila

Group	Coelomic fluid pH	Coelomic fluid ΣH_2S (mmol l^{-1})	Coelomic fluid ΣCO_2 (mmol l^{-1})	Vascular blood pH	Vascular blood ΣH_2S (mmol l^{-1})	Vascular blood ΣCO_2 (mmol l^{-1})
Control worms	7.14±0.05	1.10±0.23	17.81±1.98	7.09±0.04	5.76±0.89	16.16±1.71
Hypoxic worms	6.64±0.03	0.99±0.22	6.34±0.72	6.79±0.06	4.98±1.69	5.56±0.89
P	0.0012	0.9326	0.0004	0.0253	0.9035	0.0036

Mean (± S.E.M.) extracellular pH, ΣH_2S and ΣCO_2 for control (N=14) and hypoxic (N=12) tubeworms kept in high-pressure flowing water aquaria at 15 °C, 21.5 MPa, and exposed to external ΣH_2S concentrations of 156±21 μmol l^{-1}, ΣCO_2 values of 4.4±0.2 mmol l^{-1}, and pH values of 6.23±0.05 for 13 h.

Hypoxic worms were kept at oxygen levels below 42 μmol l^{-1} and control worms were kept at oxygen levels of 316±23 μmol l^{-1}.

P values are for the Mann–Whitney U-test for differences in internal parameters between the control and hypoxic worms.

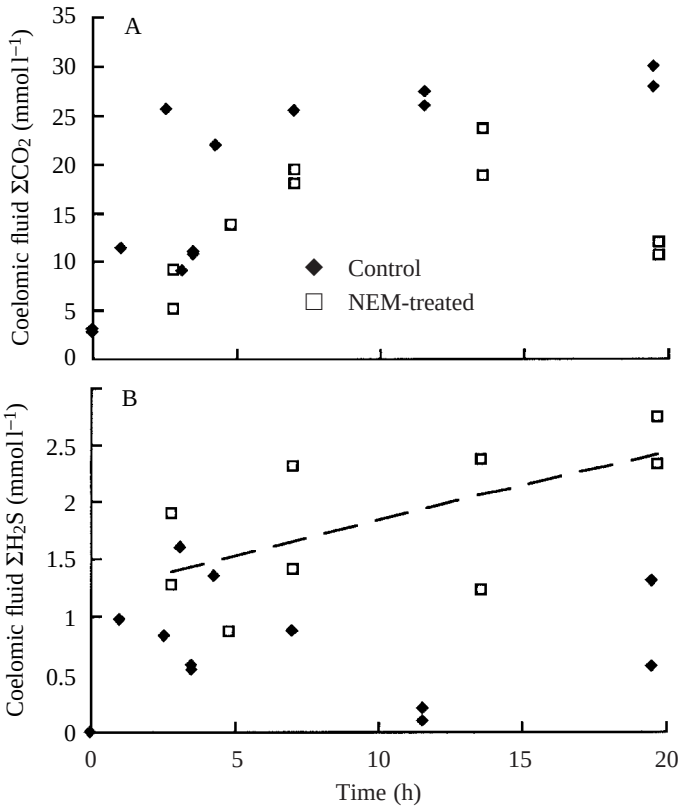

Fig. 2. Coelomic fluid ΣCO_2 (A) and ΣH_2S (B) values over time for both control (filled symbols, *N*=15) and NEM-treated (open symbols, *N*=9) *Riftia pachyptila* kept in high-pressure flowing-water aquaria and exposed to external ΣCO_2 concentrations between 4.6 and 5.5 mmol l^{-1}, a P_{CO_2} of 6.2 kPa, pH between 5.9 and 6.2, and ΣH_2S between 0.1 and 0.6 mmol l^{-1}. NEM-treated worms were exposed to *N*-ethylmaleimide at concentrations between 1.1 and 1.6 mmol l^{-1} for approximately 1–2 h. In B, the regression line for NEM-treated worms is y=1.223+0.061x, r=0.63, P=0.0211. The regression for control worms (y=0.485+0.019x, r=0.24, P=0.5339) was not significant.

(worms at time zero). When subsequently exposed to flowing water at typical vent conditions (4.8±0.1 mmol l^{-1} ΣCO_2 and 0.31±0.04 mmol l^{-1} ΣH_2S), these worms demonstrated increases in total extracellular fluid inorganic carbon and sulfide. Between 0 and 7 h, the rate of increase in coelomic fluid ΣCO_2 in control worms was 3.22 mmol l^{-1} h^{-1}, with the rate leveling off after 7 h at a mean ΣCO_2 concentration of 27.8 mmol l^{-1} (Fig. 2A) (see also Goffredi *et al.* 1997). NEM-treated worms, however, did not accumulate inorganic carbon in the blood as rapidly (2.2 mmol l^{-1} h^{-1}) and ΣCO_2 did not plateau at the same level (17.1 mmol l^{-1}; Fig. 2A). In addition, the control worms demonstrated a sulfide uptake rate of 0.97 mmol l^{-1} h^{-1} within the first hour (Fig. 2B). There appeared to be no further increase in the internal ΣH_2S of control worms (mean 0.81±0.14 mmol l^{-1}) after 1 h. There was, however, a slight increase (from 1.59 to 2.55 mmol l^{-1} at a rate of 57 μmol l^{-1} h^{-1}) in the internal ΣH_2S of NEM-treated worms over time (P=0.0211; Fig. 2B). The mean external sulfide concentrations for the two groups were not significantly different (Mann-Whitney test, 0.27±0.05 mmol l^{-1} for control and 0.37±0.07 mmol l^{-1} for NEM-treated worms); however, internal ΣH_2S and external ΣH_2S for both groups of worms are not correlated over the limited range in this data set (P=0.28, Kendall rank correlation). Thus, the difference in external ΣH_2S levels cannot explain the difference in internal ΣH_2S levels measured between the two groups. After 4 h, the increase in coelomic fluid ΣH_2S in the NEM-treated worms was not significantly different from that in the control worms (ANCOVA, P=0.1650); however, they were significantly different in overall magnitude (ANCOVA, P=0.0013).

It has been proposed that regulation of extracellular pH in *R. pachyptila* occurs primarily through proton-equivalent ion transport *via* an ATP-requiring process, specifically *via* H^+-ATPases (Goffredi *et al.* 1997). The apparent inhibition of proton-equivalent ion transport by NEM resulted in significant decreases of approximately 0.4 pH units in both coelomic fluid and vascular blood pH (Table 2). This decrease in extracellular pH, however, did not result in a decrease in internal ΣH_2S levels, as expected in the case of H_2S diffusion, but rather a significant increase in internal sulfide levels (Table 2). Again, this result is contrary to that seen for internal ΣCO_2, in which a lower extracellular pH caused a reduction in the diffusion gradient for CO_2, resulting in significant decreases in internal ΣCO_2 (Table 2). These contrasting results support different modes of acquisition for inorganic carbon and sulfide.

Table 2. *Body fluid pH, ΣH_2S and ΣCO_2 of control and NEM-treated* Riftia pachyptila

Group	Coelomic fluid pH	Coelomic fluid ΣH_2S (mmol l^{-1})	Coelomic fluid ΣCO_2 (mmol l^{-1})	Vascular blood pH	Vascular blood ΣH_2S (mmol l^{-1})	Vascular blood ΣCO_2 (mmol l^{-1})
Control worms	7.26±0.05	0.81±0.14	27.83±0.74	7.15±0.05	4.63±0.38	25.65±1.08
Hypoxic worms	6.84±0.08	1.72±0.22	17.13±1.82	6.81±0.06	8.67±0.52	15.58±1.44
P	0.0022	0.0075	0.0105	0.0007	0.0002	0.0105

Mean (± S.E.M.) extracellular pH, ΣH_2S and ΣCO_2 for control (*N*=15) and inhibited (*N*=9) tubeworms kept in high-pressure flowing water aquaria at 8 °C, 21.5 MPa, and exposed to external ΣH_2S concentrations of 311±39 μmol l^{-1}, ΣCO_2 values of 4.8±0.1 mmol l^{-1}, and pH values of 5.96±0.05 for at least 4 h.

Inhibited worms were exposed to *N*-ethylmaleimide (NEM), at concentrations between 1.1 and 1.6 mmol l^{-1} for 1–2 h.

P values are for the Mann–Whitney *U*-test for differences in internal parameters between the control and the NEM-treated worms.

Discussion

On the basis of our studies, we propose a model for sulfide uptake in *R. pachyptila* in which sulfide acquisition from the environment is primarily *via* HS^- uptake facilitated by transporter or channel proteins. Once across the outer epithelium of the plume, HS^- must enter the vascular blood compartment, where it is bound by the sulfide-binding hemoglobins present in the blood and transported to the bacterial symbionts. H_2S movement into these worms, however, appears to be severely limited.

Both freshly collected and experimental worms had higher internal ΣH_2S levels as the surrounding water pH increased. This suggests that external HS^- is the most important factor affecting internal ΣH_2S values because HS^- is more abundant than H_2S at higher pH. In addition, at higher extracellular pH in experimental worms, the internal ΣH_2S levels were also higher, suggesting that the species of sulfide being accumulated increases the internal pH. Both multiple regressions indicate that internal ΣH_2S levels and extracellular pH are influenced more by external [HS^-] than by external [H_2S]. This suggests that external HS^- levels play a greater role in the uptake of sulfide in these animals than do H_2S levels.

Our experiments involving depressed extracellular pH also support the contention that HS^- is the primary species of sulfide moving into the worms. We observed a different pH-dependence for sulfide acquisition from that expected for H_2S diffusion and measured for CO_2 diffusion (Goffredi *et al.* 1997). As the extracellular pH in these animals was depressed (by exposure to hypoxic conditions or *N*-ethylmaleimide), no decrease in internal sulfide levels was observed. NEM inhibits enzymes by forming covalent bonds with sulfhydryl groups (SH^-), causing deleterious conformational changes in these enzymes (Stone *et al.* 1984; Lin and Randall, 1993). Thus, it is possible for NEM to react with a variety of enzymes and proteins possessing reactive sulfhydryl groups, including *R. pachyptila* hemoglobins, which have been shown to contain free cysteine residues (Zal *et al.* 1997). Experiments were conducted to determine whether NEM adversely affects sulfide binding by *R. pachyptila* hemoglobin (Zal *et al.* 1997). In summary, when *R. pachyptila* hemoglobin was pre-treated with NEM, prior to any exposure to sulfide, a 30 % decrease in sulfide binding resulted. However, if the hemoglobin was first exposed to sulfide, as in the case of our experiments, there was no effect of NEM on sulfide binding (Zal *et al.* 1997). The worms were given NEM and sulfide simultaneously; therefore, they were not pretreated with the inhibitor as sulfide would be expected to move into the worms faster than NEM. In addition, we feel that because there was no decrease in internal sulfide levels, adverse effects on other proteins did not create artifacts.

Our results also show that there is discrimination against H_2S movement into the extracellular fluids of these animals. In general, organisms are believed to be unable to block the diffusion of H_2S across membranes while still retaining permeability to other gases, such as CO_2 and O_2, both of which diffuse into *R. pachyptila* (Somero *et al.* 1989; Bagarinao, 1992; Völkel, 1995; Goffredi *et al.* 1997). For example, it has been shown that the shrimp *Crangon crangon*, which inhabits shallow sandy areas, is only permeable to H_2S and that there is no uptake of HS^- (Vismann, 1996). Researchers have also shown that sulfide penetration into the alga *Valonia macrophysa* increased as external pH decreased, indicating that for this alga H_2S is the more permeable of the two sulfide species (Jacques, 1936). Although *Urechis caupo*, the fat innkeeper worm, shows a higher H_2S permeability, HS^- permeability across the body wall has been demonstrated to be 37 % of the H_2S permeability (Julian and Arp, 1992). In contrast, it appears that H_2S movement into *R. pachyptila* is much lower than expected, limited by some currently unknown mechanism.

The specific mechanism for HS^- uptake is also unknown at this time; however, we propose that HS^- enters *via* facilitated diffusion due to its charge and because of the strong correlation between internal ΣH_2S and external [HS^-]. Although [HS^-] is relatively low in the vent environment (50 $\mu mol\,l^{-1}$ at pH 6.0 and 300 $\mu mol\,l^{-1}$ ΣH_2S), a gradient for HS^- movement into the worms is created and maintained by the high concentrations of sulfide-binding hemoglobins present in the body fluids (Arp and Childress, 1983; Arp *et al.* 1987; Fisher *et al.* 1988). Sulfide binding by the hemoglobins has been shown to be maximal at pH 7.5, which suggests that the actual species of sulfide bound by the hemoglobins is HS^- (Childress *et al.* 1984).

For two reasons, we believe that HS^- uptake, as the mechanism for sulfide acquisition in *R. pachyptila*, acts as a protection against sulfide poisoning. The first is the fact that perhaps the two species of sulfide ([S^{2-}] is negligible, with a pK of 12–13) are not equally toxic to the animal (Bagarinao and Vetter, 1990). It has been suggested that H_2S is more toxic than HS^-, and that H_2S is actually the species of sulfide that binds to the cytochrome *c* oxidase complex (Smith *et al.* 1977; Powell and Somero, 1986; Bagarinao and Vetter, 1990; Oeschger and Vismann, 1994). Specifically, Powell and Somero (1986) have shown that cytochrome *c* oxidase activity in *R. pachyptila* plume tissue, in the presence of sulfide, decreases markedly with decreasing extracellular pH (from 7.0 to 6.0), suggesting that H_2S is the more inhibitory form of sulfide. In a similar experiment, it was shown that there was no HS^- inhibition of mitochondrial respiration of the killifish *Fundulus parvipinnis* and, again, that H_2S was the toxic form of sulfide (Bagarinao and Vetter, 1990). If this were the case for *R. pachyptila*, it would be advantageous for these worms to exclude H_2S while importing HS^-.

The second possibility is that if inorganic carbon and sulfide were acquired *via* the same mechanism, i.e. diffusion of the undissociated form (CO_2 and H_2S), *R. pachyptila* could not control sulfide uptake independently. Thus, the second way in which HS^- uptake could protect *R. pachyptila* from sulfide poisoning would be to decouple sulfide acquisition from inorganic carbon acquisition. Although *R. pachyptila* must maintain an alkaline extracellular pH in order to concentrate inorganic carbon internally, if sulfide were accumulated in the same way, *via* H_2S diffusion, free sulfide, like ΣCO_2, would

reach very high concentrations in the blood. This unlimited accumulation of sulfide internally could potentially poison the worm and its symbionts. However, with the proposed mechanism, sulfide uptake is expected to be largely limited by the binding capacity of the hemoglobins.

In contrast, the vesicomyid clam *Calyptogena elongata*, which also contains chemoautotrophic symbionts that it must supply with sulfide, does not maintain its extracellular pH constant in the face of changing external and internal ΣH_2S levels (Childress *et al.* 1993*a*). Specifically, when exposed to increasing amounts of internal ΣH_2S, the extracellular pH of *C. elongata* decreases (Childress *et al.* 1993*a*). *C. elongata* can potentially accumulate sulfide *via* H_2S diffusion because increasing levels of internal ΣH_2S cause the extracellular pH to decrease, which dissipates the sulfide gradient into the animal, acting as a self-limiting sulfide acquisition mechanism for the clam.

R. pachyptila, however, does not rely on the same self-limiting mechanism and has apparently evolved an alternative mode of sulfide acquisition, mediated transport of HS^-, as well as reduced permeability to, or some discrimination against, H_2S, apparently as a protection against sulfide poisoning. In this way, *R. pachyptila* is able to control sulfide movement, while keeping the extracellular pH stable and alkaline. Restricting the internal ΣH_2S level to that which can be bound by the hemoglobins ensures that, even at high external ΣH_2S levels, internal sulfide levels in *R. pachyptila* are not toxic to either partner but are still sufficient for the symbionts. This mechanism appears to be a further specialization of *R. pachyptila* for successfully supporting autotrophic endosymbionts and thriving in such a hostile environment.

Funding for this project was provided by NSF grants OCE-9301374 (J.J.C.) and OCE-9632861 (J.J.C.) and by Ifremer URM 7 (F.H.L.). The authors thank the captains and crew of the R.V. *New Horizon*, R.V. *Atlantis II*, R.V. *Nadir*, R.V. *Wecoma*, D.S.R.V. *Alvin* and D.S.R.V. *Nautile*. We also thank R. Lee, P. Girguis, S. Powell, J. Freytag and J. Smith for technical support at sea. Finally, we would like to thank L. Mullineaux and F. Gaill, chief scientists on the HERO 94 and HOT 96 expeditions, respectively.

References

ARP, A. J. AND CHILDRESS, J. J. (1983). Sulfide binding by the blood of the hydrothermal vent tube worm *Riftia pachyptila*. *Science* **219**, 295–297.

ARP, A. J., CHILDRESS, J. J. AND FISHER, C. R., JR (1985). Blood gas transport in *Riftia pachyptila*. *Bull. biol. Soc. Wash.* **6**, 289–300.

ARP, A. J., CHILDRESS, J. J. AND VETTER, R. D. (1987). The sulphide-binding protein in the blood of the vestimentiferan tube-worm, *Riftia pachyptila*, is the extracellular haemoglobin. *J. exp. Biol.* **128**, 139–158.

BAGARINAO, T. (1992). Sulfide as an environmental factor and toxicant: tolerance and adaptations in aquatic organisms. *Aquat. Toxicol.* **24**, 21–62.

BAGARINAO, T. AND VETTER, R. D. (1990). Oxidative detoxification of sulfide by mitochondria of the California killifish *Fundulus parvipinnis* and the speckled sanddab *Citharichthys stigmaeus*. *J. comp. Physiol.* B **160**, 519–527.

CAVANAUGH, C. M., GARDINER, S. L., JONES, M. L., JANNASCH, H. W. AND WATERBURY, J. B. (1981). Prokaryotic cells in the hydrothermal vent tube worm *Riftia pachyptila*: Possible chemoautotrophic symbionts. *Science* **213**, 340–342.

CHILDRESS, J. J., ARP, A. J. AND FISHER, C. R., JR (1984). Metabolic and blood characteristics of the hydrothermal vent tube worm *Riftia pachyptila*. *Mar. Biol.* **83**, 109–124.

CHILDRESS, J. J. AND FISHER, C. R. (1992). The biology of hydrothermal vent animals: physiology, biochemistry and autotrophic symbioses. *Oceanogr. mar. Biol. A. Rev.* **30**, 337–441.

CHILDRESS, J. J., FISHER, C. R., FAVUZZI, J. A., ARP, A. J. AND OROS, D. R. (1993*a*). The role of a zinc-based, serum-borne sulphide-binding component in the uptake and transport of dissolved sulphide by the chemoautotrophic symbiont containing clam *Calyptogena elongata*. *J. exp. Biol.* **179**, 131–158.

CHILDRESS, J. J., FISHER, C. R., FAVUZZI, J. A., KOCHEVAR, R., SANDERS, N. K. AND ALAYSE, A. M. (1991). Sulfide-driven autotrophic balance in the bacterial symbiont-containing hydrothermal vent tubeworm, *Riftia pachyptila*, Jones. *Biol. Bull. mar. biol. Lab., Woods Hole* **180**, 135–153.

CHILDRESS, J. J., LEE, R., SANDERS, N. K., FELBECK, H., OROS, D., TOULMOND, A., DESBRUYERES, D.. KENNICUT II, M. C. AND BROOKS, J. (1993*b*). Inorganic carbon uptake in hydrothermal vent tubeworms facilitated by high environmental p_{CO_2}. *Nature* **362**, 147–149.

DICKSON, A. G. AND MILLERO, F. J. (1987). A comparison of the equilibrium constants for the dissociation of carbonic acid in seawater media. *Deep-Sea Res.* **34**, 1733–1743.

FELBECK, H., SOMERO, G. N. AND CHILDRESS, J. J. (1981). Calvin–Benson cycle and sulphide oxidation enzymes in animals from sulphide-rich habitats. *Nature* **293**, 291–293.

FISHER, C. R. (1990). Chemoautotrophic and methanotrophic symbioses in marine invertebrates. *Crit. Rev. aquat. Sci.* **2**, 399–436.

FISHER, C. R., CHILDRESS, J. J. AND SANDERS, N. K. (1988). The role of vestimentiferan hemoglobin in providing an environment suitable for chemoautotrophic sulfide-oxidizing endosymbionts. *Symbiosis* **5**, 229–246.

GOFFREDI, S. K., CHILDRESS, J. J., DESAULNIERS, N. T., LEE, R. W., LALLIER, F. H. AND HAMMOND, D. (1997). Inorganic carbon acquisition by the hydrothermal vent tubeworm *Riftia pachyptila* depends upon high external P_{CO_2} and upon proton elimination by the worm. *J. exp. Biol.* **200**, 883–896.

JACQUES, A. G. (1936). The kinetics of penetration. XII. Hydrogen sulfide. *J. gen. Physiol.* **19**, 397–418.

JOHNSON, K. S., CHILDRESS, J. J., HESSLER, R. R., SAKAMOTO-ARNOLD, C. M. AND BEEHLER, C. L. (1988). Chemical and biological interactions in the Rose Garden hydrothermal vent field. *Deep-Sea Res.* **35**, 1723–1744.

JONES, M. L. (1981). *Riftia pachyptila*, new genus, new species, the vestimentiferan tubeworm from the Galapagos Rift geothermal vents. *Proc. biol. Soc. Wash.* **93**, 1295–1313.

JULIAN, D. AND ARP, A. J. (1992). Sulfide permeability in the marine invertebrate *Urechis caupo*. *J. comp. Physiol.* B **162**, 59–67.

KOCHEVAR, R., CHILDRESS, J. J., FISHER, C. R. AND MINNICH, L. (1992). The methane mussel: roles of symbiont and host in the metabolic utilization of methane. *Mar. Biol.* **112**, 389–401.

LEE, R. W. AND CHILDRESS, J. J. (1994). Assimilation of inorganic

nitrogen by marine invertebrates and their chemoautotrophic methanotrophic symbionts. *Appl. env. Microbiol.* **60**, 1852–1858.

LIN, H. AND RANDALL, D. J. (1993). H^+-ATPase activity in crude homogenates of fish gill tissue: inhibitor sensitivity and environmental and hormonal regulation. *J. exp. Biol.* **180**, 163–174.

MARVER, D. (1984). A biochemical evaluation of rabbit renal DCCD-sensitive ATPase activities. In *Hydrogen Ion Transport in Epithelia* (ed. J. G. Forte, D. G. Warnock and F. C. Rector, Jr), pp. 253–259. New York: John Wiley & Sons, Inc.

MILLERO, F. J., PLESE, T. AND FERNANDEZ, M. (1988). The dissociation of hydrogen sulfide in seawater. *Limnol. Oceanograph.* **33**, 269–274.

OESCHGER, R. AND VISMANN, B. (1994). Sulphide tolerance in *Heteromastus filiformis* (Polychaeta): Mitochondrial adaptations. *Ophelia* **40**, 147–158.

POWELL, M. A. AND SOMERO, G. N. (1986). Adaptations to sulfide by hydrothermal vent animals: sites and mechanisms of detoxification and metabolism. *Biol. Bull. mar. biol. Lab., Woods Hole* **171**, 274–290.

QUETIN, L. B. AND CHILDRESS, J. J. (1980). Observations on the swimming activity of two bathypelagic mysid species maintained at high hydrostatic pressures. *Deep-Sea Res.* **27**, 383–391.

SMITH, L., KRUSZYNA, H. AND SMITH, R. P. (1977). The effect of methemoglobin on the inhibition of cytochrome c oxidase by cyanide, sulfide, or azide. *Biochem. Pharmac.* **26**, 2247–2250.

SOMERO, G. N., CHILDRESS, J. J. AND ANDERSON, A. E. (1989). Transport, metabolism and detoxification of hydrogen sulfide in animals from sulfide rich marine environments. *Crit. Rev. aquat. Sci.* **1**, 591–614.

STONE, D. K., XIE, X.-S., WU, L.-T. AND RACKER, E. (1984). Proton translocating ATPases of clathrin-coated vesicles, renal medulla and Ehrlich ascites tumor cells. In *Hydrogen Ion Transport in Epithelia* (ed. J. G. Forte, D. G. Warnock and F. C. Rector, Jr), pp. 219–230. New York: John Wiley & Sons, Inc.

VISMANN, B. (1996). Sulfide species and total sulfide toxicity in the shrimp *Crangon crangon*. *J. exp. mar. Biol. Ecol.* **204**, 141–154.

VÖLKEL, S. (1995). Sulfide tolerance and detoxification in *Arenicola marina* and *Sipunculus nudus*. *Am. Zool.* **35**, 145–153.

ZAL, F., LALLIER, F. H., GREEN, B. N., VINOGRADOV, S. N. AND TOULMOND, A. (1996*a*). The multi-hemoglobin system of the hydrothermal vent tube worm *Riftia pachyptila*: Complete polypeptide chain composition investigated by maximum entropy analysis of mass spectra. *J. biol. Chem.* **271**, 8875–8881.

ZAL, F., LALLIER, F. H., WALL, J. S., VINOGRADOV, S. N. AND TOULMOND, A. (1996*b*). The multi-hemoglobin system of the hydrothermal vent tube worm *Riftia pachyptila*: Reexamination of the number and masses of its constituents. *J. biol. Chem.* **271**, 8869–8874.

ZAL, F., SUZUKI, T., KAWASAKI, Y., CHILDRESS, J. J., LALLIER, F. H. AND TOULMOND, S. (1997). The primary structure of the common polypeptide chain b from the multi-haemoglobin system of the hydrothermal vent tubeworm *Riftia pachyptila*: an insight on the sulphide binding-site. *Proteins* (in press).

instance it does provide a reliable and conservative means for estimating a very large sound field. Locally unstable temperature lapses and wind fluctuations generally preclude sufficiently steady readings for accurate, direct measurement of sound fields at large distances outdoors (Embleton, 1996).

Signal design and the importance of context

Design features of the pneumorid communication system are concordant with all expectations of natural selection to maximize broadcast range while avoiding predation and intraspecific competition (Endler, 1992). The received male signal is maximized relative to background noise by repetition of a highly stereotyped signal, increased broadcast amplitude resulting from the abdominal resonator, increased transmitted amplitude using optimal meteorological conditions, and (for an insect) extremely sensitive hearing (H. Römer and M. J. van Staaden, in preparation). In addition to the effect of maximizing broadcast range, the temporal segregation in which calling is restricted to calm, misty conditions may also contribute to avoidance of nocturnal vertebrate predators such as the microchiropteran *Nycteris thebaica* (P. Taylor, personal communication). High-frequency echolocating calls of bats suffer strong absorption at high humidity ($>3\,dB\,m^{-1}$ for sounds above 100 kHz at 25 °C and 50 % humidity; Lawrence and Simmons, 1982), whereas the absorption coefficient for pneumorid signals is minimal, estimated to be approximately 0.2 dB per 100 m (1.7 kHz at 20 °C and 90 % humidity; Harris, 1966).

Sexual selection and differences in active space

Pneumorids exhibit striking sexual differences in transmission distance of mate location signals, such that females may detect calling males ideally at a distance of 1–2 km, but males detect responding females from a maximum of only 50 m. This discrepancy in transmission distance results largely from differences in absolute signal intensity, since there is little difference in overall attenuation rates of male and female calls (Fig. 5). If active space is defined as the area in which a signal is above the threshold to elicit a *behavioural* response, however, then maximum transmission distance may not translate into effective communication distance. Moreover, any asymmetry in behavioural response threshold would profoundly affect (counteract or magnify) the observed asymmetry in transmission distance.

Sexual differences in signalling strategies are frequently attributed to differences in relative parental investment (Thornhill, 1979). The energetic and endangerment costs of calling and phonotaxis in *B. membracioides* are, however, completely unknown. Conceivably, the excessive costs for male calling are more apparent than real. Slender cursorial hindlegs and the abdominal resonator may minimize the energy expenditure of calling, and the risks of male flight may be no more than those of females exposed on top of the bush producing a locatable sound. The existence of alternative mating strategies (Alexander and van Staaden, 1989) does, however, imply a substantial fitness differential between winner and loser males, and highlights the potential importance of sexual selection.

The sex ratio of nymphal *B. membracioides* is approximately equal, but food-plant specificity, male dimorphism and differential mortality produce a low-density, patchy distribution, and behavioural observations indicate substantial opportunity for females to exercise choice (M. J. van Staaden, unpublished observations). Evolution through sexual selection may thus have forced males to produce an increasingly intense signal. Since the decrease in SPL of the male calling song is rather flat at large distances, a small increase in effective transmission results in a relatively large increase in broadcast range. Larger active calling ranges reach more females, and selection is therefore expected to act on males to produce increasingly loud signals until the benefit of increased loudness is balanced by (energetic or predation) costs. Certainly in species with more vagile females, differential attraction to louder male calling songs is quite common (for a review, see Ryan and Keddy-Hector, 1992), and field studies of mole crickets have demonstrated that males calling 2 dB below the loudest male attracted fewer females than the average male (Forrest and Green, 1991). It is also conceivable that loud calling in *B. membracioides* acts as a sensitizer for the female response.

At present, we cannot exclude intrasexual selection and a possible second function for the complex male call. Loud calling may space out males, allowing each to broadcast their signal within a zone free from competing conspecifics. The use of sound to maintain range separation and to minimize competition for resources is relatively common and has been shown to increase the ability of males to attract females (bushcrickets, Arak *et al.* 1990). Although it is often difficult to make a clear distinction between inter- and intrasexual selection, spatial genetic analyses may provide a means of distinguishing the adaptive value of sexual differences in transmission distance (M. J. van Staaden and H. Römer, in preparation).

Despite so-called phylogenetic and environmental constraints, the maximum range of detection does appear to be a primary selection pressure on at least some animal vocalizations. Evolutionary explanations for exaggerated signals are generally in terms of runaway sexual selection and honesty in signalling good genes, but the problem may also be recast as one of signal detection and female preference; part of the ‘psychological landscape’ of the receiver (Guilford and Dawkins, 1991). For a signaller, the situation is exactly the same whether receivers fail to respond to signals because of environmental attenuation or because of ‘neural attenuation’ resulting from high thresholds or narrow filters for response (Wiley, 1994). Whereas male pneumorids produce spectacular acoustic signals with high inherent detectability and minimal environmental attenuation, females do not. The question of neural attenuation is the subject of a subsequent paper.

We are indebted to the late Professor A. Alexander and her family for access to the field site and their generous hospitality.

The Journal of Experimental Biology 200, 2617–2627 (1997)
Printed in Great Britain © The Company of Biologists Limited 1997
JEB1070

WHY DO TUNA MAINTAIN ELEVATED SLOW MUSCLE TEMPERATURES? POWER OUTPUT OF MUSCLE ISOLATED FROM ENDOTHERMIC AND ECTOTHERMIC FISH

JOHN D. ALTRINGHAM[1,*] AND BARBARA A. BLOCK[2]

[1]*Department of Biology, University of Leeds, Leeds, LS2 9JT, UK* and [2]*Hopkins Marine Station, Stanford University, Pacific Grove, CA 93950, USA*

Accepted 30 July 1997

Summary

It has been hypothesised that regional endothermy has evolved in the muscle of some tunas to enhance the locomotory performance of the fish by increasing muscle power output. Using the work loop technique, we have determined the relationship between cycle frequency and power output, over a range of temperatures, in isolated bundles of slow muscle fibres from the endothermic yellowfin tuna (*Thunnus albacares*) and its ectothermic relative the bonito (*Sarda chiliensis*). Power output in all preparations was highly temperature-dependent. A counter-current heat exchanger which could maintain a 10 °C temperature differential would typically double maximum muscle power output and the frequency at which maximum power is generated (f_{opt}). The deep slow muscle of the tuna was able to operate at higher temperatures than slow muscle from the bonito, but was more sensitive to temperature change than more superficially located slow fibres from both tuna and bonito. This suggests that it has undergone some evolutionary specialisation for operation at higher, but relatively stable, temperatures. f_{opt} of slow muscle was higher than the tailbeat frequency of undisturbed cruising tuna and, together with the high intrinsic power output of the slow muscle mass, suggests that cruising fish have a substantial slow muscle power reserve. This reserve should be sufficient to power significantly higher sustainable swimming speeds, presumably at lower energetic cost than if intrinsically less efficient fast fibres were recruited.

Key words: endothermy, fish, muscle, power output, swimming, work loops, yellowfin tuna, *Thunnus albacares*, bonito, *Sarda chiliensis*.

Introduction

Tunas (Scombridae, Thunnini) are unique among teleosts because of their ability to elevate the temperature of their locomotor muscle, viscera, brain and eye tissues above that of the water temperature (Carey and Teal, 1966; Carey *et al.* 1971; Graham, 1975; Carey, 1981). Endothermy in tunas is compartmentalised in regions of high metabolic output and coupled with circulatory specialisations to reduce heat loss. Tunas have a high standard metabolic rate and numerous specialisations associated with increased oxygen delivery to the tissues and high metabolic demands (Brill, 1987, 1996). Elevation of slow-twitch (red) muscle temperatures is facilitated by the more axial positioning of the aerobic muscle mass and the presence of counter-current heat exchangers (the rete mirabilia) in the circulatory system, which reduce conductive and convective heat loss at the gills and body surfaces. Many tunas also have a higher proportion of slow-twitch, relative to fast-twitch, myotomal muscle than other teleosts (e.g. Graham *et al.* 1983). The heat generated by muscle contraction and metabolism can thus be conserved, and in these pelagic, continuously swimming fish, the temperature of the more axial slow muscle may be maintained up to 21 °C above ambient water temperature (bluefin tuna, *Thunnus thynnus*, Carey and Lawson, 1973). In *Katsuwonus pelamis*, slow-twitch muscle temperatures can be as much as 12 °C above ambient, and in other *Thunnus* species the steady-state muscle temperature elevation is 6 °C or less (Dizon and Brill, 1979; Graham and Dickson, 1981; Holland *et al.* 1992). Mechanisms for heat retention in aerobic muscle are widespread in large pelagic fish, and telemetry and anatomical studies have shown that heat conservation strategies are present in tunas, lamnid sharks (Carey *et al.* 1971), alopiid sharks (Carey, 1981; Bone and Chubb, 1983), blue sharks (Carey and Scharold, 1991) and swordfish (Carey, 1990). The convergence of similar mechanisms among sharks and fishes suggests that strong selective pressures exist for warming of the locomotor muscles. In tunas and lamnid sharks, it has been suggested by Carey and Teal (1966) and many subsequent authors that this system of regional endothermy has evolved to enhance the

*e-mail: J.D.Altringham@Leeds.ac.uk

locomotory performance of the fish by increasing muscle power output. However, this hypothesis has never been tested directly in any endothermic fish.

In addition to their endothermic adaptations, tunas have a suite of morphological characters which appear to be adaptations for efficient, and relatively rapid, sustained swimming. They have a body thickness to length ratio close to the optimum for minimum drag (Hertel, 1966) and a fusiform body which also increases swimming efficiency (Weihs, 1989). The corselet, a zone of modified skin at the deepest point of the body, may introduce microturbulence to prevent breakaway of the boundary layer which would increase drag. A narrow caudal peduncle minimises energy losses due to movement of water, and lateral keels on the peduncle reduce drag and possibly direct water over the middle part of the fin (Walters, 1962; Aleyev, 1977). Dorsal and ventral finlets, in series along the midline of the tapering edges of the body, may limit cross flow between the two sides of the body, reducing drag. Some of the fins fit into slots in the body surface when not in use, and larger fins are often placed behind the deepest part of the body (greatest dorsal to ventral height). The tails of tunas are typically lunate and have a high aspect ratio, both features increasing the efficiency of thrust generation. Kinematically, swimming in tuna is characterised by minimal lateral movement of all but the caudal region of the fish, with virtually all of the thrust coming from the caudal fin. Oxygen consumption measurements confirm the increased swimming efficiency predicted from these adaptations (Dewar and Graham, 1994*a*).

The closest living ectothermic relatives of the tunas are bonitos (tribe Sardini) (Collette, 1978). Few studies are available on vertebrate endothermic and ectothermic species in which physiological performance between taxa with close phylogenetic histories can be directly compared. The presence of extant warm and cold fishes in the scombrid lineage, along with information about their relationships, provides a valuable tool for studies on the evolution of endothermy. The ability to examine the muscle characteristics of both groups in a phylogenetic context is critical for discerning what evolutionary specialisations, if any, have occurred in the endothermic lineage (Block and Finnerty, 1994). Using the work loop technique (Josephson, 1985), we have determined the temperature-dependence of cycle frequency *versus* power output relationships in isolated bundles of slow-twitch muscle fibres from the endothermic yellowfin tuna (*Thunnus albacares*) and its ectothermic relative the bonito (*Sarda chiliensis*).

Materials and methods

Fish

Thunnus albacares (Bonaterre) and *Sarda chiliensis* (Cuvier) were caught using lift poles with barbless hooks off the coast of California in September 1995 and held in fish wells on board ship, before being transferred to holding facilities in San Diego, California, within 2–3 h of capture. Fish were then transferred *via* a specialised transport tank placed on board a flatbed truck to the Tuna Research and Conservation Center at Pacific Grove, California, a joint facility of Hopkins Marine Station (Stanford University) and the Monterey Bay Aquarium. Tuna were maintained in three tanks. The largest tank (T1) was 13 m in diameter and 3.3 m deep, and two smaller tanks (T2 and T3) were 10 m in diameter and 2 m deep. Tuna were held from October 1995 to May 1996 (the start of experiments) in T1 at 20± 0.5 °C and in T2 for the same period at 18±0.5 °C and in T3 at 24±0.5 °C. Recirculated, filtered and aerated sea water from Monterey Bay passed through all three tanks. Tuna in tanks T1 and T2 were fed three times per week on a mixed diet of fish and squid at a constant level 115 kJ kg^{-1} day^{-1}. To compensate for a higher metabolic rate in the warmer T3 tank, these fish were fed 165 kJ kg^{-1} day^{-1}. Bonito were maintained at 20 °C in a tank 6 m in diameter and 1.5 m deep. Their diet consisted of chopped fish and squid. All experiments were carried out during May and June 1996.

Muscle mechanics

Fish were captured using nets (tuna) or barbless hooks (bonito), and killed by decapitation and pithing. Blocks of slow muscle 3–5 myotomes long were rapidly dissected from the chosen region of the fish (see below) and immersed in a large volume of Ringer's solution (composition, in mmol l^{-1}: NaCl, 175.7; KCl, 7; $CaCl_2$, 1.9; $MgCl_2$, 1.1; sodium pyruvate, 10; Hepes, 10; pH 7.8 at 25 °C), bubbled with oxygen, at 20 °C. The Ringer's solution was changed frequently during the initial dissection, which was carried out with the aid of a stereomicroscope. The aim was to rapidly remove a bundle of fibres from the central myotome of the block, approximately 1–3 mm in diameter, and place it in a large volume of fresh oxygenated Ringer. The preparation was reduced in diameter to 0.5–1.5 mm by removing fibres from the outside of the bundle. A piece of myoseptum was retained at both ends, and this was trimmed to shape and mounted in a small aluminium foil clip (Altringham and Johnston, 1990*a*,*b*).

Preparations were transferred to a chamber through which Ringer's solution flowed at 20±0.1 °C. One end of the preparation was attached to an isometric force transducer (AE801, SensoNor, Horten, Norway), the other to a servo motor. The preparation was lengthened to remove slack and left for a minimum of 30 min before experimentation. Stimulation amplitude was altered to maximise twitch force, using 2 ms duration stimuli, and the length of the muscle was adjusted to place the preparation on the plateau of the length–force relationship, defined as l_0. Twitch parameters were then determined for each preparation: time from stimulus to peak force (twitch rise time, t_a), and time from peak force to half-maximum force (half-relaxation time, $t_{r0.5}$). 1 s tetani were used to determine the stimulation frequency for maximum tetanic force, and this frequency was used in all subsequent experiments on that preparation.

Maximum power output was then determined at a range of cycle frequencies using the work loop technique (Josephson, 1985; Altringham and Johnston, 1990*a*,*b*). Briefly,

preparations were subjected to sinusoidal strains symmetrical about l_0 and stimulated during part of each strain cycle. A plot of muscle length against force yields a hysteresis loop for each cycle, the area of which is the net work performed during the cycle. Previous experiments on fish muscle (Altringham and Johnston, 1990*b*) have established that, over the range of cycle frequencies yielding close to absolute maximum power output, the strain yielding maximum power output is approximately ±5 % l_0 (10 % peak to peak). Kinematic studies of swimming fish (e.g. Hess and Videler, 1984; van Leeuwen *et al.* 1990; Rome *et al.* 1993) have shown that *in vivo* strains range from ±3 to ±6 % l_0 over that part of the body believed to generate most of the power for swimming. A strain of ±5 % l_0 was used in all experiments in the present study. The number of stimuli and the phase shift between the onset of stimulation and the strain cycle were manipulated to maximise power at each frequency. Stimulation phase shift typically increased from 20 ° to 60 ° between 15 °C and 30 °C. Phase shift is defined from the strain cycle: 0/360 ° is muscle at l_0 and lengthening, one complete cycle is 360 °. In each experimental run, a preparation performed eight work loops and was then allowed to recover for 6 min before the next run. The power output was calculated from the seventh loop of each run: power typically rose by 5–20 % (depending upon cycle frequency) over the first 4–6 loops of a run, before stabilising.

A complete power *versus* frequency relationship was determined at 20, 25, 15 and 30 °C for each preparation, in the order given. To monitor any change in performance during the course of the experiment, which could take up to 10 h, regular controls were taken. At a given temperature, every third or fourth run was a repeat of a standard set of parameters: those giving maximum or near-maximum power. Runs with the same control parameters were made at 20 °C as the temperature was lowered from 25 to 15 °C, and at 20 and 25 °C as the temperature was raised to 30 °C. After experiments at 30 °C, controls were again made at 20 °C. Corrections for changes in performance over time were made, where necessary (usually only at the highest temperatures, see Results), by multiplying power by (power of initial control experiment/power of control run closest to the experimental run). At the end of each experiment, the preparation was removed from the apparatus and weighed, after removal of the clips and myosepta.

Fibres were studied from two locations along the length of the body of tuna, 0.40 and 0.65 body lengths (*BL*, snout to fork) from the snout (Fig. 1A). At both locations, fibres were taken from the centre of the broadest region of the more axially distributed slow muscle (‘deep’) (Fig. 1B). At 0.65 *BL*, fibres were additionally taken from within the superficial slow muscle zone (‘superficial’), delineated by the septa of the ‘lateral line triangle’, and from the deepest region of the slow muscle (‘very deep’), close to the vertebral column (Fig. 1B). The ‘superficial’ fibres studied were more axial to a distinct layer of mixed red fibres and were histochemically homogeneous (E. Freund, unpublished observations). Because of the nested cone arrangement of the myotomes, sites sampled at increasing depth were taken from different myotomes. We were unable to determine exactly which myotome each preparation was from, but no more than 3–4 myotomes separated the most anterior and most posterior preparations. Bonito slow muscle fibres were taken from 0.65 *BL*, at a depth of 8–10 mm, beyond at least half the total depth of the slow muscle.

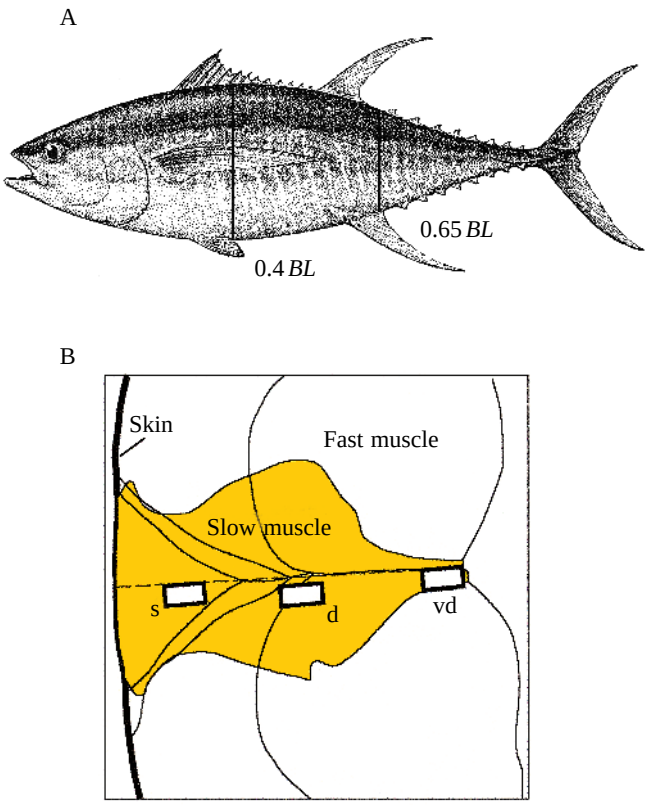

Fig. 1. (A) Location of sampling sites on the yellowfin tuna. (B) Sampling sites within the slow muscle of tuna in relation to the organisation of the slow muscle. s, superficial slow muscle; d, deep slow muscle; vd, very deep slow muscle. *BL*, body length.

Swimming kinematics

Swimming kinematics of the 18 °C- and 24 °C-acclimated tuna and the 20 °C-acclimated bonito were studied in undisturbed fish on a day on which they were not routinely fed, and during feeding. Fish, of the same size range as those used in mechanical experiments, were recorded using a Canon EX2Hi, Hi8 video camcorder, which was mounted directly above the tanks. The field of view was typically four by five fish lengths. Tracings were made from video sequences of the paths of the snout of the fish and the caudal puduncle, where the presence of the lateral keels enabled the same point to be followed with some precision from frame to frame. Twenty randomly chosen sequences were analysed for each group/condition and, from each, mean tailbeat frequency and swimming speed were determined from straight swimming sequences of 3–5 tailbeats. Analysis of alternate frames of the 50 Hz video sequences gave a resolution of 40 ms, or 2 % or better, for tailbeat frequency. Speed is expressed in

Table 1. *Body sizes of fish used in the study*

	Number	Length (m) Range Mean ± S.E.M.	Mass (kg) Range Mean ± S.E.M.
Yellowfin tuna (*Thunnus albacares*)	13	0.585–0.81 0.667±0.022	3.45–8.9 5.05±0.54
Bonito (*Sarda chiliensis*)	4	0.42–0.47 0.44±0.122	1.02–1.45 1.14±0.12

body lengths s^{-1} (*BL* s^{-1}) because the exact lengths of most fish were not known and could not be determined from the video sequences, as their vertical position in the 2 m deep water column was not known.

Results

Fish

The body sizes of the fish used in the study are summarised in Table 1.

Isometric mechanical properties

No trends were found in twitch kinetics data from differently sized yellowfin tuna: analysis of variance (ANOVA) and correlation analysis revealed no significant (P<0.05) size-related changes. In addition, no significant differences or consistent trends were observed in twitch kinetics from fish maintained at 18 °C (four fish), 20 °C (four fish) and 24 °C (five fish). Although the number of replicates was often small, variation was low: all standard errors were less than 10 % of the mean value. Data from all yellowfin tuna were therefore pooled where appropriate. Fig. 2 summarises the isometric twitch kinetics of all preparations from both fish species at 20 °C. The location of the muscle fibres in the body had a significant (P<0.05) effect on twitch kinetics in the yellowfin tuna, and the results of one-way ANOVAs are summarised in Fig. 2. The small data set meant that activation time results failed normality tests, even after transformation, and a less sensitive ANOVA on ranks was performed. Both activation and half-relaxation times of deep fibres were greater at 0.65 *BL* than at 0.4 *BL*, although only the latter was statistically significant (P<0.05). The small data set suggests caution in interpreting the results. At 0.65 *BL*, there was a tendency for twitch kinetics to become more rapid with increasing depth. Twitch parameters for bonito muscle are shown in Fig. 2C.

The effects of temperature on twitch kinetics are summarised in Fig. 3, for 0.40 *BL* muscle from the tuna and 0.65 *BL* muscle for the bonito: locations with the largest data

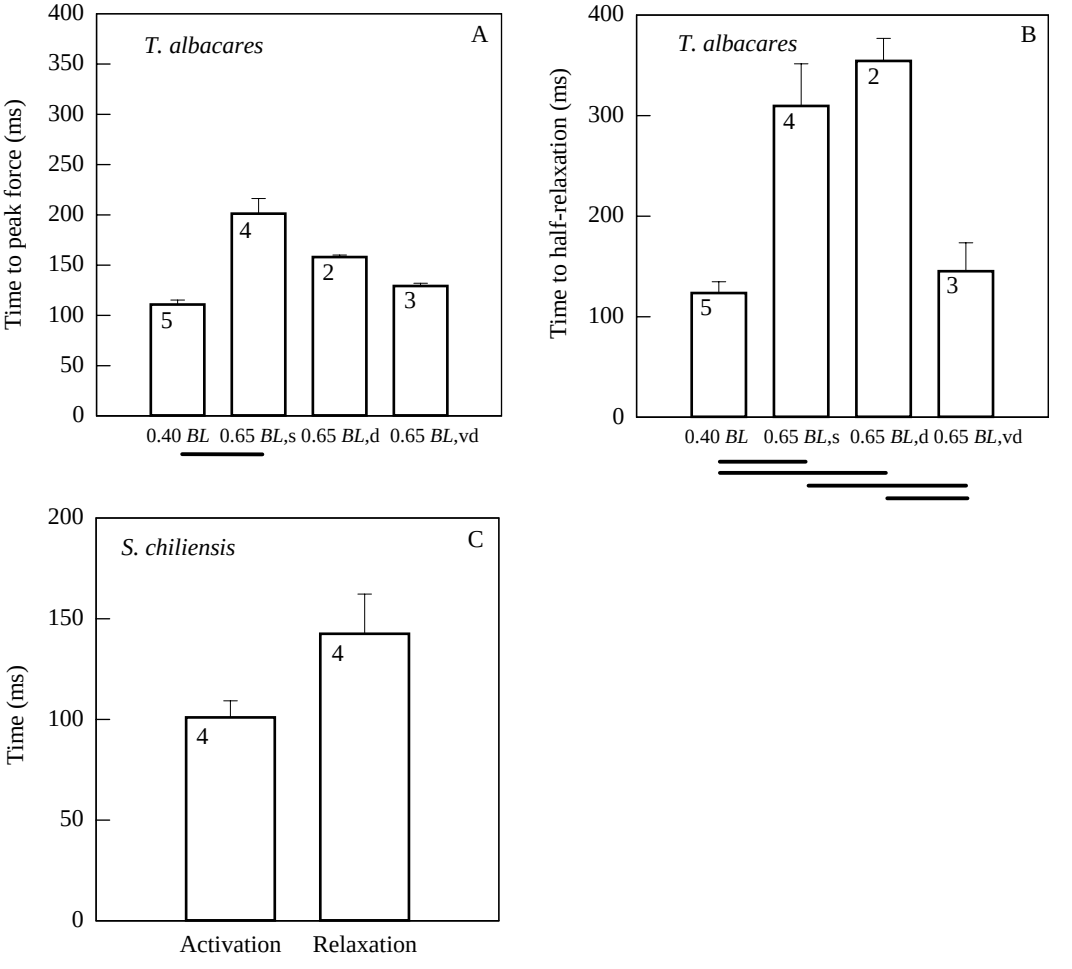

Fig. 2. Time to peak twitch force (A) and half-relaxation time (B) for yellowfin tuna preparations at different locations in the body: 0.4 *BL*=0.4 body lengths from snout. s, superficial slow muscle; d, deep slow muscle; vd, very deep slow muscle. See Fig. 1B for a full description of the locations. (C) Time to peak force (activation) and half-relaxation time for bonito muscle preparations. All data are presented as means + S.E.M.; the number of fish is given within the columns, at 20 °C. The solid lines below the figures connect columns that are significantly different from each other (ANOVA, P<0.05).

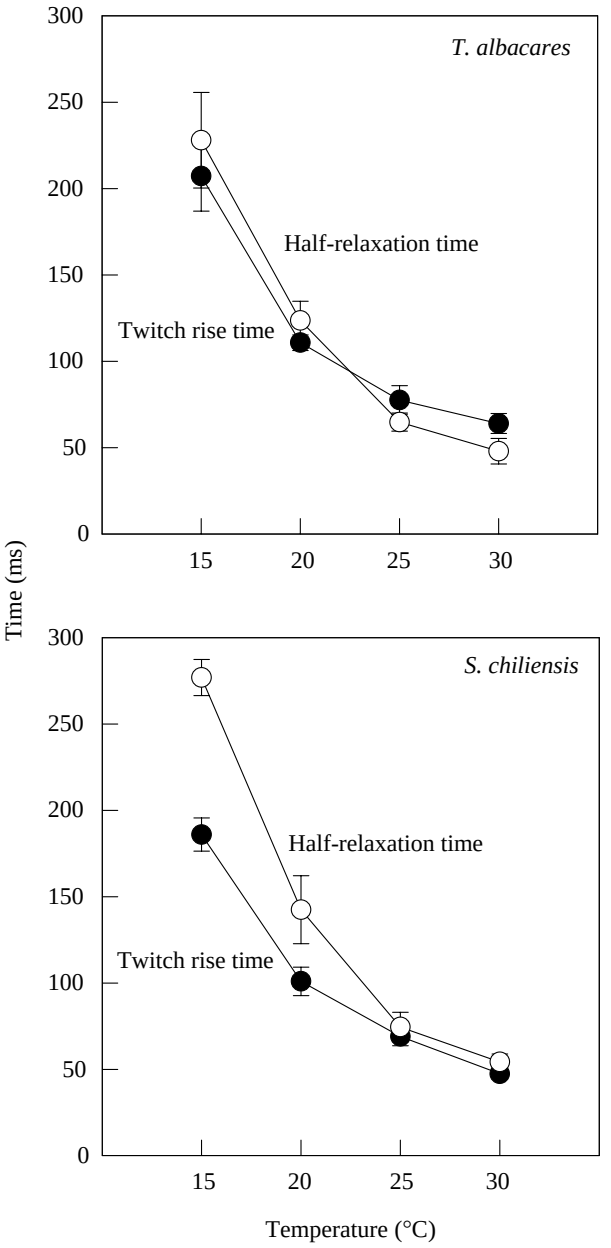

Fig. 3. Temperature-dependence of twitch rise time and half-relaxation time in yellowfin tuna *Thunnus albacares* (at 0.4 *BL*) and bonito *Sarda chiliensis* (at 0.65 *BL*) muscle. Data are presented as means ± S.E.M., N=5 tuna and N=4 bonito.

sets. Similar results were obtained from other locations on the tuna. Both twitch rise time (t_a) and half-relaxation time ($t_{r0.5}$) decreased markedly with increasing temperature. The rate of change of both parameters over 5 °C temperature increments decreased with increasing temperature (rates are expressed as a coefficient: time at x °C/time at x+5 °C; e.g. activation time at 20 °C/activation time at 25 °C). However, despite this consistent change, ANOVA showed that only the change in activation time coefficients in the tuna was significant (P<0.05). Activation times and half-relaxation times had very similar temperature coefficients, and coefficients were very similar for the two species: these results are summarised in Table 2.

Power output

Power output under optimal stimulation conditions was 12.0±1.7 W kg^{-1} (N=13) at 25 °C for tuna muscle and 13.8±1.9 W kg^{-1} (N=4) at 25 °C for bonito muscle. No significant differences were found in power output measured for tuna muscle from different body locations, so the above value is the mean of all results. Maximum power decreased with decreasing temperature in all preparations, but some notable differences were seen in temperature-dependence. Temperature coefficients (power at x °C/power at x–5 °C) are summarised in Table 3. In 'deep' and 'very deep' tuna muscle fibres, the temperature-dependence of power was greatest at lower temperatures. This trend was observed in *all* individual preparations. ANOVA showed that temperature sensitivity at 15–20 °C for tuna fibres from 0.40 *BL* was significantly greater than at 20–25 °C and 25–30 °C (ANOVA P<0.001; Student–Newman–Keuls *post-hoc* tests P<0.05). There were insufficient data at other locations for meaningful comparisons). Furthermore, although the data are sparse for some locations and temperatures, there was a clear trend towards increased sensitivity with increasing depth into the tuna. Finally, power output in 'superficial' fibres from both tuna and bonito had a low thermal dependence, which did not increase with decreasing temperature. At 15–20 °C, significant differences were found between deep tuna fibres at 0.4 *BL* and superficial tuna fibres and bonito fibres (overall ANOVA P<0.001; *post-hoc* tests P<0.05). The temperature sensitivities of deep fibres at 0.40 and 0.65 *BL* were not significantly different. A similar comparison at 20–25 °C revealed no significant differences, but the small data set means that the results should be interpreted with caution.

Power–frequency relationships

Very similar power–frequency curves were obtained from all preparations, and representative curves for tuna and bonito are shown in Fig. 4. Fig. 5 summarises all the data, normalised to maximum power at 25 °C. The greater temperature-dependence of the deep slow fibres of the tuna, relative to the superficial fibres from tuna and bonito, is clearly evident. In the physiological temperature range (20–30 °C), a 10 °C increase in temperature increased maximum power, and the frequency at which it was produced, by 50–100 % in both tuna and bonito. The frequency which produces maximum power output (f_{opt}) was in the range 2–9 Hz, depending upon muscle type and temperature. Attempts to determine the power–frequency curve for bonito preparations at 30 °C were largely unsuccessful (Fig. 5C). All bonito preparations began to deteriorate (revealed by a decline in power output) within 15 min of raising the temperature to 30 °C, and the construction of all curves relied on correcting for this fall in power output after the initial points had been collected. The 30 °C data shown in Fig. 5C are therefore unreliable and serve primarily to indicate the instability of the preparation. After 30 min at

Table 2. *Temperature coefficients of twitch kinetics for yellowfin tuna* Thunnus albacares *and bonito* Sarda chiliensis *muscle preparations*

	Temperature coefficients (time at x °C/time at x+5 °C)					
	For activation time t_a			For half-relaxation time $t_{r0.5}$		
	15–20 °C	20–25 °C	25–30 °C	15–20 °C	20–25 °C	25–30 °C
Yellowfin tuna *Thunnus albacares* 0.40 *BL* (*N*=5)	1.87±0.19	1.48±0.13	1.30±0.03	1.87±0.21	1.98±0.32	1.44±0.16
Bonito *Sarda chiliensis* 0.65 *BL* (*N*=4)	1.88±0.22	1.47±0.12	1.45±0.11	2.08±0.38	1.91±0.20	1.38±0.12

Values are means ± S.E.M.
BL, body length.

30 °C, power output declined by up to 50 %, but recovery was half complete within 30 min of reducing the temperature to 20 °C. In contrast, the deep (Fig. 5A) and very deep (not shown) slow fibres of the tuna were stable at 30 °C, but deteriorated at 35 °C. Unfortunately, no experiments were performed at 30 °C on superficial fibres from tuna. Tuna preparations were very stable at 30 °C or below for many hours: controls under given conditions were typically within 1–3 % of initial values, even after 8 h or more of experimentation. Bonito preparations were similarly stable at or below 25 °C.

Swimming kinematics

Undisturbed tuna and bonito swam primarily in schools, around the perimeter of the tanks, occasionally reversing direction or breaking formation to swim more randomly. When feeding, the schools broke up and fish swam singly, often bursting rapidly to take food. Swimming speeds and tailbeat frequencies are summarised in Table 4.

Undisturbed, 'cruising' tuna swam at a mean speed of approximately 1 $BL\,s^{-1}$, with a tailbeat frequency of approximately 1.6 Hz, much lower than the frequency which produced maximum power output in isolated slow fibres (f_{opt}). In rapid bursts during feeding, tailbeat frequency (8–12 Hz) was much greater than f_{opt}, and fast fibres were presumably recruited. The limited time resolution of the video recording, and the water turbulence created by feeding tuna, meant that burst tailbeat frequency could only be estimated roughly. The bonito had a similar cruising tailbeat frequency to the yellowfin

Table 3. *Temperature coefficients of muscle power output for yellowfin tuna* Thunnus albacares *and bonito* Sarda chiliensis *muscle preparations*

	Temperature coefficients for power (power at x °C/power at x–5 °C)		
	15–20 °C	20–25 °C	25–30 °C
Yellowfin tuna *Thunnus albacares*			
Very deep fibres, 0.65 *BL*	2.00 (1)	1.52±0.08 (2)	1.27 (1)
Deep fibres, 0.40 *BL*	1.84±0.09 (5)	1.40±0.04 (5)	1.31±0.05 (5)
Deep fibres, 0.65 *BL*	1.55±0.21 (2)	1.35±0.03 (2)	1.09 (1)
Superficial fibres, 0.65 *BL*	1.20±0.08 (4)	1.22±0.07 (4)	
Bonito *Sarda chiliensis* 0.65 *BL*	1.31±0.04 (4)	1.37±0.05 (4)	

Values are means ± S.E.M. (*N*).
BL, body length.

Table 4. *Swimming performance in yellowfin tuna* Thunnus albacares *and bonito* Sarda chiliensis

	Swimming speed ($BL\,s^{-1}$)	Tailbeat frequency (Hz)	Stride length
Yellowfin tuna (*Thunnus albacares*)			
18 °C-acclimated			
Undisturbed (*N*=20)	1.01±0.03	1.52±0.04	0.67±0.03
Feeding bursts		8–12	
24 °C-acclimated			
Undisturbed (*N*=20)	0.93±0.03	1.66±0.05	0.56±0.02
Feeding bursts		8–12	
Bonito (*Sarda chiliensis*)			
20 °C-acclimated			
Undisturbed (*N*=15)	1.21±0.02	1.55±0.04	0.79±0.02
Feeding bursts		>12	

Tailbeat frequency was significantly (P<0.05) higher in 18 °C-acclimated tuna than in 24 °C-acclimated fish.

Estimated ranges are given for tailbeat frequency during feeding bursts.

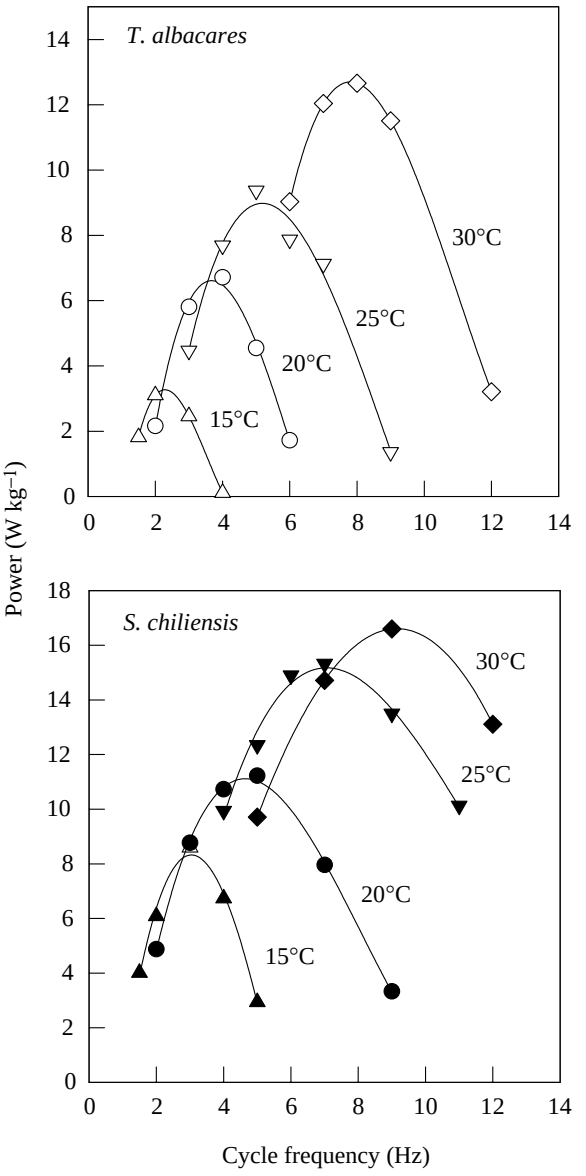

Fig. 4. Representative power *versus* frequency curves for yellowfin tuna *Thunnus albacares* and bonito *Sarda chiliensis*. Lines were fitted by third-order regressions. The bonito preparation was the only one of four to show an increase in power when the temperature was raised to 30 °C but, as with other preparations, power declined rapidly when the high temperature was maintained.

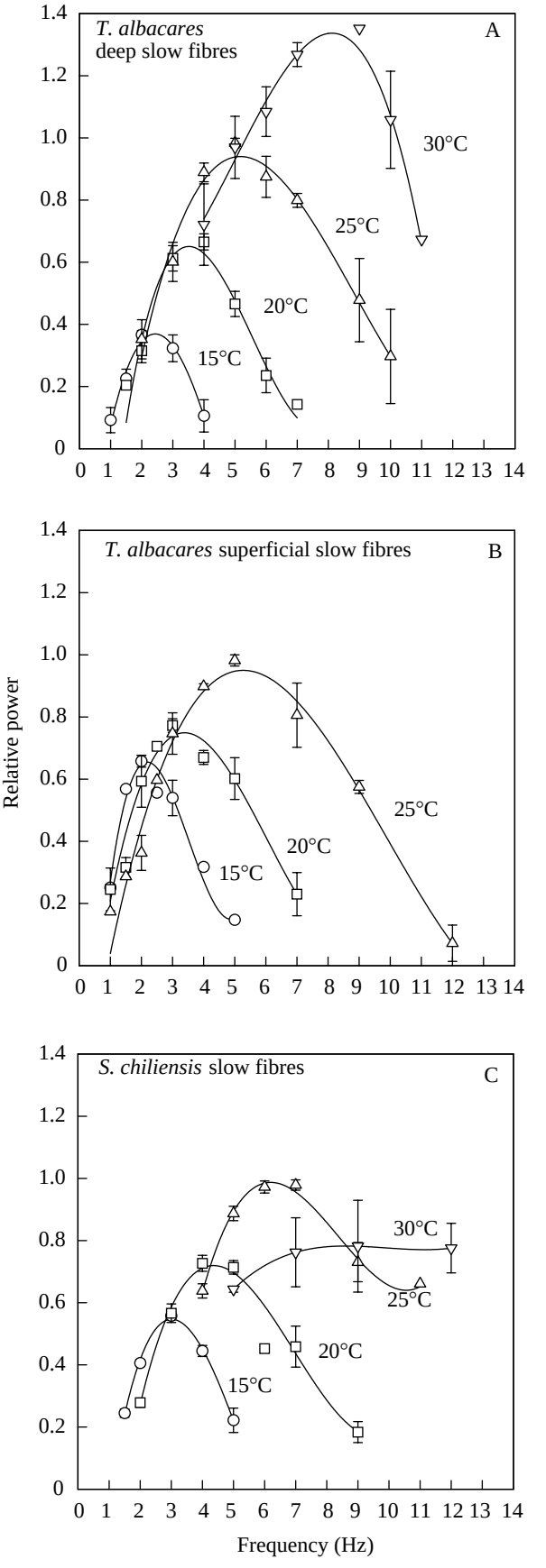

Fig. 5. Relative power *versus* frequency curves for (A) deep (N=5) and (B) superficial slow fibres (N=4) from the yellowfin tuna *Thunnus albacares* and slow fibres (C) from the bonito *Sarda chiliensis* (N=4). Data are presented as means ± S.E.M. Power is normalized to maximum power at 25 °C.

tuna, and a similar f_{opt} was found for the two species. However, the bonito had a significantly higher length-specific swimming speed (and stride length), suggesting that there may be differences in their kinematics. During feeding bursts, the tailbeat frequency of bonito exceeded 12 Hz. No evidence was found in this simple analysis for a substantial acclimation response: there was a small but significant difference in tailbeat frequency (and hence stride length, $P<0.05$, *t*-test) but not in swimming speed between 18 °C- and 24 °C-acclimated tuna.

Discussion

Twitch kinetics

Change in kinetics with muscle position along the body

A number of other studies have shown that muscle contraction kinetics slow from anterior to posterior along the length of many fish. Wardle *et al.* (1995) and L. Hammond, J. D. Altringham and C. S. Wardle (in preparation) have discussed possible reasons for this trend.

Change in twitch kinetics with muscle depth

Twitch kinetics tended to become faster with increasing depth at 0.65 *BL* in the tuna (Fig. 2). If twitch kinetics become slower in an anterior to posterior direction (Fig. 2), as many studies have now shown, then depth and position along the body will interact in a complex way to determine twitch kinetics, produced by the complex three-dimensional myotomal structure (Alexander, 1969). Changes in kinetics due to sampling from different myotomes are unlikely to be more than a small component of the observed changes with depth. Jayne and Lauder (1995) have shown in largemouth bass that the propagation of muscle activity is by the sequential activation of myotomes, but that not all of a particular myotome is necessarily active: different zones within the fast fibre population may be activated independently. We know too little about any particular fish to propose a mechanism for how this is achieved or to give it functional significance, but regional variations in mechanical properties must be very important to an understanding of swimming, and require further study.

Temperature sensitivity of twitch kinetics

Temperature has been shown previously to have a large effect on muscle function in vertebrates (e.g. Bennett, 1984). In the tuna and bonito, both activation and relaxation times were temperature-dependent, and sensitivity was greatest at low temperatures. The muscle of the two species showed a similar temperature sensitivity, with temperature coefficients within the range reported for muscles of other ectothermic animals (reviewed by e.g. Johnston and Altringham, 1989; Rome, 1990). Regional endothermy in the tuna does not appear to have led to major adaptations in muscle kinetics.

Muscle power output and temperature

Maximum power outputs are comparable to values reported for the muscles of other ectotherms at similar temperatures and operating frequencies (for a summary, see James *et al.* 1995, their Fig. 8). This is in agreement with observations on the metabolic properties of yellowfin tuna slow-twitch muscle: citrate synthase activities measured at 20 °C were not significantly different between yellowfin tunas and the Eastern Pacific bonito *S. chiliensis* (Dickson, 1996). The effects of temperature on slow muscle citrate synthase activity in tunas and bonitos have also been shown to have a similar Q_{10} (1.91 for tuna, 1.98 for bonito from 10 to 20 °C). Power output in all muscle preparations was highly temperature-dependent. A counter-current heat exchanger which could maintain a 10 °C temperature differential would typically double the maximum muscle power output and the frequency at which it was obtained (f_{opt}). A similar Q_{10} has been reported for scup slow muscle power output (derived using the work loop technique) (Rome and Swank, 1992). Notably, there is a trend towards increasing temperature sensitivity with increasing depth into the body of the tuna. If the deep muscle has undergone some adaptation to the stable, elevated temperatures, then we might expect to see not only this greater temperature-dependence, but also a more marked difference at the lowest temperatures, and this is indeed the case: the highest temperature coefficients for power output were in the deep, slow muscle of tuna at 15–20 °C. Evidence for an adaptation to a higher operating temperature is seen the ability of deep tuna muscle to function at 30 °C, developing almost 40 % more power than at 25 °C. Slow muscle from bonito showed impaired performance at 30 °C and was to some degree irreversibly damaged. Do these differences reflect a functional adaptation of the deep slow muscle of the tuna for endothermic operation? The geographical distribution of yellowfin tuna takes them into slightly warmer waters than the Eastern Pacific bonito. Yellowfin collected from the same area as the tunas used in this study (the most northern part of their range) have been followed using acoustic telemetry and were found to spend most of their time between the top of the thermocline at 17.5 °C and surface waters of 20 °C (Block *et al.* 1997). The tuna frequently dive for short periods (1–5 min) into the cool waters beneath the thermocline. In warmer regions such as Hawaii, the yellowfin tuna are found between the top of the thermocline and the surface and experience temperatures of 19–28 °C (Holland *et al.* 1992). Surface water temperature where the bonito is thought to occur most often is within the range 16–23 °C. *S. chiliensis* is uncommon north of Point Conception, but has been caught as far north as Alaska, although it is unclear whether these northern occurrences are associated with El Nino events (Yoshida, 1980). Measurements on the superficial fibres of the tuna at 30 °C would have helped to confirm these hypotheses but, for logistical reasons and owing to the limited supply of fish, this was unfortunately not done.

Muscle properties and swimming performance

The frequency for maximum power output, f_{opt}, of slow muscle was higher than the tailbeat frequency of undisturbed cruising tuna, and this, together with the high intrinsic power

output of the large slow muscle mass, suggests that cruising fish have a substantial slow muscle power reserve. This may be sufficient to power significantly higher sustainable swimming speeds, presumably at lower energetic cost than if the intrinsically less efficient fast fibres were recruited. During feeding, the brief, rapid swimming bursts observed (8–12 Hz tailbeat frequency) were presumably driven by fast fibres, but between these bursts tuna swam with a tailbeat frequency of approximately 3 Hz when searching for food, well within the range of slow fibre recruitment (see below). The smaller bonito cruised with a similar tailbeat frequency, but their greater stride length gave them a higher length-specific swimming speed.

From oxygen consumption measurements, Dewar and Graham (1994*a*) calculated that, at 24 °C, a 51 cm (2.2 kg) yellowfin tuna, swimming at 2 *BL* s^{-1} (at a tailbeat frequency of approximately 3.2 Hz, Dewar and Graham, 1994*b*), consumed 0.67 W. Assuming a metabolic efficiency of 50 %, and a mechanical muscle efficiency of 50 %, then this would yield 0.17 W of mechanical power [see recent measurements on fish (Curtin and Woledge, 1993) and mammalian (Barclay, 1994) slow muscle under work loop conditions]. Slow muscle wet mass for yellowfin tuna is 6.5 % of body mass (Graham *et al.* 1983): 0.143 kg in a 2.2 kg fish. From the present study, this mass of slow muscle could produce 30–40 % of maximum power at 3 Hz and 24 °C, or 0.5–0.7 W. Thus, only 50–65 % of the slow muscle would be needed to power swimming at 2 *BL* s^{-1}, and at this swimming speed the slow muscle is working well below its f_{opt} (Figs 4, 5). By recruiting more of the slow muscle, at higher tailbeat frequencies, significantly higher swimming speeds should be possible using only slow muscle. The fish used in the present study were larger than those used by Dewar and Graham (1994*a*,*b*) (mean lengths 0.67 and 0.48–0.53 m respectively: a difference in mass of more than twofold). At a given length-specific speed, tailbeat frequency in the smaller fish is approximately 40 % higher, and this is probably reflected in faster muscle kinetics and a shift to a higher f_{opt} (e.g. Altringham and Johnston, 1990*b*; Anderson and Johnston, 1992), which would perhaps increase the power reserve of slow muscle still further. Electromyographic studies, to determine the swimming speed at which the different fibre types are recruited, would help validate these calculations.

The above discussion assumes that the slow fibres operate *in vivo* under conditions which yield maximum power output, and that *in vivo* strain is ±5 % l_0. Neither of these assumptions can be verified directly as yet, but they are consistent with many published studies on other fish species, as discussed above.

Swimming speeds

One hypothesis for heat retention in the slow muscles of tunas is that warming of the locomotory muscles permits increases in maximum sustained and burst swimming speeds, thus aiding in the search for prey in the patchy oceanic environment. Testing this is difficult because of the problems of measuring swimming speeds of free-swimming tunas. Although direct telemetry of swimming speed has not been accomplished on any tuna species, improved acoustic tracking, with regular global positions *via* satellite to a ship, provides a reasonable means of assessing average swimming speeds. Recent data on small tunas indicate mean swimming speeds for cruising ranging from 0.5 to 1.0 *BL* s^{-1} and maximum sustained speeds of up to 3.5 *BL* s^{-1} for over an hour (Block *et al.* 1997). Telemetry studies on blue marlin (Block *et al.* 1992), which lack central or lateral heat exchangers, indicate sustained speeds similar to the slower speeds observed for the yellowfin tuna, but the higher continuous speeds were not observed. It remains possible that the observed differences are due to the warming of the slow-twitch muscles. Tunas in captivity have displayed remarkable bursts of speed that are estimated to range up to 8 *BL* s^{-1} (B. A. Block, unpublished observation), and comparisons with ectothermic taxa such as bonito should be possible.

Regional endothermy in tuna

The entire *Thunnus* clade is hypothesized to have radiated from a pantropical distribution to a more temperate and subpolar niche (Collette, 1978; Sharp and Pirages, 1978). Under this scenario, warming of the slow-twitch muscles would have evolved in a warm tropical ocean. Recent studies suggest inconsistencies between molecular and morphological phylogenies. Morphologists have separated tunas into a warm-water clade consisting of of the yellowfin tuna (*T. albacares*), blackfin tuna (*T. tonggol*) and longtail tuna (*T. atlanticus*), which possess both central and lateral heat exchangers in the slow muscle. The cold-water clade includes the bigeye tuna (*T. obesus*), albacore (*T. alalunga*), northern bluefin (*T. thynnus*) and southern bluefin (*T. maccoyii*), which have either lost or reduced the central heat exchanger (Gibbs and Collette, 1967; Collette, 1978). The changes in vascular retia among the two subgroups of tunas are paralleled by a shift in their latitudinal distribution patterns (Graham, 1975; Sharp, 1978). The yellowfin, blackfin and longtail tunas occur in subtropical and tropical waters, primarily in warmer waters above the thermocline (Carey and Olson, 1982; Holland *et al.* 1990; Block *et al.* 1997), whereas the bluefins, albacore and big-eye tunas have extended their range to cooler waters at higher latitudes or below the thermocline (Carey and Teal, 1969; Laurs *et al.* 1978; Block *et al.* 1997). The thermal excess for yellowfin tuna (2.2–6 kg) ranges from 1.4 to 4 °C (Dizon and Brill, 1979; Dewar *et al.* 1994), but in northern bluefin (220 kg) has been reported to be up to 21 °C (Carey and Lawson, 1973).

The major distinction between morphological and molecular phylogenetic analyses is that genetic studies indicate that the cold-water tunas (albacore, bluefins, big-eye) are earlier offshoots of the *Thunnus* radiation than the warm-water tunas (Sharp and Pirage, 1978; Block *et al.* 1993; Finnerty and Block, 1995; Chow and Kishino, 1995; Bremer *et al.* 1997). These data imply that the most recent common ancestor of *Thunnus* evolved endothermy in cold seas. Albacore, big-eye and bluefin have a wider thermal niche (7–25 °C) relative to the warm tropical tunas. From the results presented here, it is

clear that the evolution of mechanisms for retaining metabolic heat in slow muscles would have enabled these species to improve their muscle power output and contraction frequency when foraging or migrating in cooler waters. We have shown here that the retention of these mechanisms in the slow muscle of the yellowfin tuna, which occurs in waters that range from 17.5 to 28 °C, would also provide an increase in muscle performance.

This work was supported by grants from the Royal Society and the Wain Fund of the BBSRC to J.D.A. and NSF IBN9507499 to B.A.B. We are grateful to the staff of the Monterey Bay Aquarium (MBA) for their assistance, with special thanks to Chuck Farwell for his enthusiastic support. We thank Captain Tedd Dunn and the crew of the F/V *Shogun* for their help in collecting the tuna and bonito. J.D.A. and family thank all those people at Hopkins and the MBA who gave help and hospitality.

References

ALEXANDER, R. McN. (1969) Orientation of muscle fibres in the myomeres of fishes. *J. mar. biol. Ass. U.K.* **49**, 263–290.

ALEYEV, Y. G. (1977) *Nekton*. The Hague: Dr W. Junk.

ALTRINGHAM, J. D. AND JOHNSTON, I. A. (1990*a*). Modelling muscle power output in a swimming fish. *J. exp. Biol.* **148**, 395–402.

ALTRINGHAM, J. D. AND JOHNSTON, I. A. (1990*b*). Scaling effects in muscle function: power output of isolated fish muscle fibres performing oscillatory work. *J. exp. Biol.* **151**, 453–467.

ANDERSON, M. E. AND JOHNSTON, I. A. (1992). Scaling of power output in fast muscle fibres of the Atlantic cod during cyclical contractions. *J. exp. Biol.* **170**, 143–154.

BARCLAY, C. J. (1994). Efficiency of fast- and slow-twitch muscles of the mouse performing cyclic contractions. *J. exp. Biol.* **193**, 65–78.

BENNETT, A. F. (1984). Thermal dependence of muscle function. *Am. J. Physiol.* **247**, R217–R229.

BLOCK, B. A., BOOTH, D. A. AND CAREY, F. G. (1992). Direct measurement of swimming speeds and depth of blue marlin. *J. exp. Biol.* **166**, 267–284.

BLOCK, B. A. AND FINNERTY, J. R. (1994). Endothermy in fishes: a phylogenetic analysis of constraints, predispositions and selection pressures. *Env. Biol. Fish.* **40**, 283–302.

BLOCK, B. A., FINNERTY, J. R., STEWART, A. F. R. AND KIDD, J. (1993). Evolution of endothermy in fish: mapping physiological traits on a molecular phylogeny. *Science* **260**, 210–214.

BLOCK, B. A., KEEN, J. E., CASTILLO, B., DEWAR, H., FREUND, E. V., MARCINEK, D. J., BRILL, R. W. AND FARWELL, C. (1997). Environmental preferences of yellowfin tuna (*Thunnus albacares*) at the northern extent of their range. *Mar. Biol.* (in press).

BONE, Q. AND CHUBB, A. D. (1983). The retial system of the locomotor muscles in the thresher shark. *J. mar. biol. Ass. U.K.* **63**, 239–241.

BREMER, J. R. A., NASERI, I. AND ELY, B. (1997). Orthodox and unorthodox phylogenetic relationships among tunas revealed by the nucleotide sequence analysis of the mitochondrial DNA control region. *J. Fish Biol.* **50**, 540–554.

BRILL, R. W. (1987). On the standard metabolic rate of tropical tunas, including the effect of body size and acute temperature change. *Fishery Bull. Fish. Wildl. Serv. U.S.* **85**, 25–35.

BRILL, R. W. (1996). Selective advantages conferred by the high performance physiology of tunas, billfishes and dolphin fish. *Comp. Biochem. Physiol.* **113**A, 3–15.

CAREY, F. G. (1981). Warm fish. In *A Companion to Animal Physiology* (ed. C. R. Taylor, K. Johansen and L. Bolis), pp. 216–233. Cambridge: Cambridge University Press.

CAREY, F. G. (1990). Further observations on the biology of the swordfish. In *Planning the Future of Billfishes* (ed. R. H. Stroud), pp. 103–122. Savannah: Nat. Coal. Mar. Cons.

CAREY, F. G. AND LAWSON, K. D. (1973). Temperature regulation in free-swimming bluefin tuna. *Comp. Biochem. Physiol.* **44**A, 375–392.

CAREY, F. G. AND OLSON, R. J. (1982). Sonic tracking experiments with tunas. *Coll. Vol. Sci. Pap. Int. Comm. Cons. Atlan. Tunas* **17**, 458–466.

CAREY, F. G. AND SCHAROLD, J. V. (1991). Movements of blue sharks in course and depth. *Mar. Biol.* **106**, 329–342.

CAREY, F. G. AND TEAL, J. M. (1966). Heat conservation in tuna fish muscle. *Proc. natn. Acad. Sci. U.S.A.* **56**, 1464–1469.

CAREY, F. G. AND TEAL, J. M. (1969). Regulation of body temperature in bluefin tuna. *Comp. Biochem. Physiol.* **28**, 205–213.

CAREY, F. G., TEAL, J. M., KANWISHER, J. W., LAWSON, K. D. AND BECKETT, J. S. (1971). Warm-bodied fish. *Am. Zool.* **11**, 135–143.

CHOW, S. AND KISHINO, H. (1995). Molecular evidence for MtDNA transfer between large tuna species. *J. molec. Evol.* **41**, 741–748.

COLLETTE, B. B. (1978). Adaptations and systematics of the mackerels and tunas. In *Physiological Ecology of Tunas* (ed. G. D. Sharp and A. E. Dizon), pp. 7–40. New York: Academic Press.

CURTIN, N. A. AND WOLEDGE, R. C. (1993). Efficiency of energy conversion during sinusoidal movement of red muscle fibres from the dogfish, *Scyliorhinus canicula*. *J. exp. Biol.* **185**, 195–206.

DEWAR, H. AND GRAHAM, J. B. (1994*a*). Studies of tropical tuna swimming performance in a large water tunnel. I. Energetics. *J. exp. Biol.* **192**, 13–31.

DEWAR, H. AND GRAHAM, J. B. (1994*b*). Studies of tropical tuna swimming performance in a large water tunnel. III. Kinematics. *J. exp. Biol.* **192**, 45–59.

DEWAR, H., GRAHAM, J. B. AND BRILL, R. W. (1994). Studies of tropical tuna swimming performance in a large water tunnel. II. Thermoregulation. *J. exp. Biol.* **192**, 33–44.

DICKSON, K. A. (1996). Locomotor muscle of high performance fishes: what do comparisons of tunas with ectothermic sister taxa reveal? *Comp. Biochem. Physiol.* **113**A, 39–49.

DIZON, A. E. AND BRILL, R. W. (1979). Thermoregulation in yellowfin tuna, *Thunnus albacares*. *Physiol. Zool.* **52**, 581–593.

FINNERTY, J. R. AND BLOCK, B. A. (1995). Evolution of cytochrome b in the Scombroidei (Teleostei): molecular insights into billfish (Istiophoridae) and Xiphiidae) relationships. *Fishery Bull. Fish. Wildl. Serv. U.S.* **93**, 78–96.

GIBBS, R. H. AND COLLETTE, B. B. (1967). Comparative anatomy and systematics of the tunas, genus *Thunnus*. *Fishery Bull. Fish. Wildl. Serv. U.S.* **66**, 65–130.

GRAHAM, J. B. (1975). Heat exchange in the yellowfin tuna, *Thunnus albacares* and skipjack tuna, *Katsuwonus pelamis* and the adaptive significance of elevated body temperatures in scombrid fishes. *Fishery Bull. Fish. Wildl. Serv. U.S.* **73**, 219–229.

GRAHAM, J. B. AND DICKSON, K. A. (1981). Physiological thermoregulation in the albacore *Thunnus alalunga*. *Physiol. Zool.* **54**, 470–486.

GRAHAM, J. B., KOEHRN, F. J. AND DICKSON, K. A. (1983). Distribution and relative proportions of red muscle in scombrid fishes: consequences of body size and relationships to locomotion and endothermy. *Can. J. Zool*. **61**, 2087–2096.

HERTEL, H. (1966). *Structure, Form and Movement*. New York: Reinhold.

HESS, F. AND VIDELER, J. J. (1984). Fast continuous swimming of saithe (*Pollachius virens*): a dynamic analysis of bending moments and swimming power. *J. exp. Biol*. **109**, 229–251.

HOLLAND, K. N., BRILL, R. W. AND CHANG, R. K. C. (1990). Horizontal and vertical movements of yellowfin and bigeye tuna associated with fish aggregating devices. *Fishery Bull. Fish. Wildl. Serv. U.S.* **88**, 493–507.

HOLLAND, K. N., BRILL, R. W., CHANG, R. K. C., SIBERT, J. R. AND FOURNIER, D. A. (1992). Physiological and behavioural thermoregulation in bigeye tuna (*Thunnus obesus*). *Nature* **358**, 410–412.

JAMES, R. S., ALTRINGHAM, J. D. AND GOLDSPINK, D. F. (1995). The mechanical properties of fast and slow skeletal muscles of the mouse in relation to their locomotory function. *J. exp. Biol*. **198**, 491–502.

JAYNE, B. C. AND LAUDER, G. V. (1995). Are muscle fibres within fish myotomes activated synchronously? Patterns of recruitment within deep myomeric musculature during swimming in largemouth bass. *J. exp. Biol*. **198**, 805–815.

JOHNSTON, I. A. AND ALTRINGHAM, J. D. (1989). Muscular energetics and environment in ectotherms. In *Energy Transformations in Cells and Organisms* (ed. W. Wieser and E. Gnaiger), pp. 71–80. Stuttgart: Thieme Verlag.

JOSEPHSON, R. K. (1985). Mechanical power output from striated muscle during cyclic contractions. *J. exp. Biol.* **114**, 493–512.

LAURS, R. M., YUEN, H. S. H. AND JOHNSON, J. H. (1978). Small-scale movements of albacore, *Thunnus alalunga*, in relation to ocean features as indicated by ultrasonic tracking and oceanographic sampling. *Fishery Bull. Fish. Wildl. Serv. U.S.* **80**, 347–355.

ROME, L. C. (1990). Influence of temperature on muscle recruitment and muscle function *in vivo*. *Am. J. Physiol*. **259**, R210–R222.

ROME, L. C. AND SWANK, D. (1992). The influence of temperature on power output of scup red muscle during cyclical length changes. *J. exp. Biol.* **171**, 261–281.

ROME, L. C., SWANK, D. AND CORDA, D. (1993). How fish power swimming. *Science* **261**, 340–343.

SHARP, G. D. (1978). Behavioural and physiological properties of tuna and their effects on vulnerability to fishing gear. In *The Physiological Ecology of Tunas* (ed. G. D. Sharp and A. E. Dizon), pp. 397–449. New York: Academic Press.

SHARP, G. D. AND PIRAGES, S. W. (1978). The distribution of red and white swimming muscles, their biochemistry and the biochemical phylogeny of selected scombroid fishes. In *The Physiological Ecology of Tunas* (ed. G. D. Sharp and A. E. Dizon), pp. 41–78. New York: Academic Press.

VAN LEEUWEN, J. L., LANKHEET, M. J. M., AKSTER, H. A. AND OSSE, J. W. M. (1990). Function of red axial muscles of carp (*Cyprinus carpio* L.): recruitment and normalised power output during swimming in different modes. *J. Zool., Lond*. **220**, 123–145.

WALTERS, V. (1962). Body form and swimming performance in the scombroid fishes. *Am. Zool*. **2**, 143–149.

WARDLE, C. S., VIDELER, J. J. AND ALTRINGHAM, J. D. (1995). Tuning in to fish swimming waves: body form, swimming mode and muscle function. *J. exp. Biol.* **198**, 1629–1636.

WEIHS, D. (1989). Design features and mechanics of axial locomotion in fish. *Am. Zool.* **29**, 151–160.

YOSHIDA, H. O. (1980). Synopsis of biological data on bonitos of the genus *Sarda*. *NOAA Technical Report NMFS Circular* **432**, 1–50.

We thank W. van Staaden, D. Wright and L. Wright for logistical support, A. Gray and P. Brock of MTN Inc. for the use of their tower, the KwaZulu-Natal Parks Board for collecting permits, R. Huber and O. Larsen for commenting on the manuscript, and two anonymous referees for constructive suggestions. A. Pabst produced some of the micrographs. Funding was provided by Austrian Science Foundation grant P09523-BIO.

References

ALEXANDER, A. J. (1992). The bladder grasshopper: a 'nu-nu' of mystery and intrigue. *Afr. Wildlife* **46**, 261–262.

ALEXANDER, A. J. AND VAN STAADEN, M. J. (1989). Alternative sexual tactics in male bladder grasshoppers (Orthoptera, Pneumoridae). In *Alternative Life-History Styles of Animals* (ed. M. N. Bruton), pp. 261–277. Dordrecht: Kluwer Academic Publishers.

ARAK, A. AND EIRIKSSON, T. (1992). Choice of singing sites by male bushcrickets (*Tettigonia viridissima*) in relation to signal propagation. *Behav. Ecol. Sociobiol*. **30**, 365–372.

ARAK, A., EIRIKSSON, T. AND RADESÄTER, T. (1990). The adaptive significance of acoustic spacing in male bushcrickets *Tettigonia viridissima*: a perturbation experiment. *Behav. Ecol. Sociobiol*. **26**, 1–7.

BAILEY, W. J., CUNNINGHAM, R. C., LEBEL, L. AND WEATHERILT, C. (1990). Song power, spectral distribution and female phonotaxis in the bushcricket *Requena verticalis* (Tettigoniidae, Orthoptera): active female choice or passive attraction. *Anim. Behav*. **40**, 33–42.

BAILEY, W. J. AND YEOH, P. B. (1988). Female phonotaxis and frequency discrimination in the bushcricket *Requena verticalis*. *Physiol. Ent.* **13**, 363–372.

BENNET-CLARK, H. C. (1987). The tuned singing burrow of mole crickets. *J. exp. Biol.* **128**, 383–409.

BENNET-CLARK, H. C. (1994). The world's noisiest insects – cicada song as a model of the biophysics of animal sound production. *Verh. dt. zool. Ges*. **87**, 165–176.

BRENOWITZ, E. A. (1982). The active space of red-winged blackbird song. *J. comp. Physiol.* A **147**, 511–522.

CANARD-CORUNA, S., LEWY, S., VERMOREL, J. AND PARMENTIER, G. (1990). Long range sound propagation near the ground. *Noise Cntrl. Eng*. **34**, 111–119.

DIRSH, V. M. (1965). Revision of the Family Pneumoridae (Orthoptera: Acridoidea). *Bull. B. M. (N. H.) Ent*. **15**, 325–396.

EMBLETON, T. F. W. (1996). Tutorial on sound propagation outdoors. *J. acoust. Soc. Am*. **100**, 31–48.

ENDLER, J. A. (1992). Signals, signal conditions and the direction of evolution. *Am. Nat*. **139**, 125–153.

FIELD, L. H. (1978). The stridulatory apparatus of New Zealand wetas in the genus *Hemideina* (Insecta: Orthoptera: Stenopelmatidae). *J. R. Soc. New Zeal.* **8**, 359–375.

FORREST, T. G. (1983). Calling songs and mate choice in mole crickets. In *Orthopteran Mating Systems: Sexual Competition in a Diverse Group of Insects* (ed. D. T. Gwynne and G. K. Morris), pp. 185–304. Boulder, CO: Westview Press.

FORREST, T. G. AND GREEN, D. M. (1991). Sexual selection and female choice in mole crickets (Scapteriscus: Gryllotalpidae): Modelling the effects of intensity and male spacing. *Bioacoustics* **3**, 93–109.

GARSTANG, M., LAROM, D., RASPET, R. AND LINDEQUE, M. (1995). Atmospheric controls on elephant communication. *J. exp. Biol*. **198**, 939–951.

GOGALA, M. AND RIEDE, K. (1995). Time sharing of song activity by cicadas in Temengor Forest Reserve, Hulu Perak and Sabah, Malaysia. *Malaysian Nature J*. **48**, 297–305.

GREENFIELD, M. D. (1988). Interspecific acoustic interactions among katydids (*Neoconocephalus*): inhibition-induced shifts in diel periodicity. *Anim. Behav*. **36**, 684–695.

GUILFORD, T. AND DAWKINS, M. S. (1991). Receiver psychology and the evolution of animal signals. *Anim. Behav*. **42**, 1–14.

HARRIS, C. M. (1966). Absorption of sound in air *versus* humidity and temperature. *J. acoust. Soc. Am*. **40**, 148–159.

LAROM, D., GARSTANG, M., PAYNE, K., RASPERT, R. AND LINDEQUE, M. (1997). The influence of surface atmospheric conditions on the range and area reached by animal vocalizations. *J. exp. Biol*. **200**, 421–431.

LATIMER, W. AND SIPPEL, M. (1987). Acoustic cues for female choice and male competition in *Tettigonia cantans*. *Anim. Behav*. **35**, 887–910.

LAWRENCE, B. D. AND SIMMONS, J. A. (1982). Measurements of atmospheric attenuation at ultrasonic frequencies and the significance for echolocation by bats. *J. acoust. Soc. Am*. **71**, 585–590.

LEWIN, A., MOHR, F. AND SELBACH, H. (1990). Heterodyn-Interferometer zur Vibrationsanalyse. *Techn Messen* **57**, 335–345.

LEWIS, R. T. (1891). On the stridulating organs of *Cystocaelia immaculata*. *J. Quekett Micr. Cl*. **4**, 243–245.

MICHELSEN, A. (1978). Sound reception in different environments. In *Sensory Ecology* (ed. M. A. Ali), pp. 345–373. New York: Plenum.

MOORE, S. W., LEWIS, E. R., NARINS, P. M. AND LOPEZ, P. T. (1989). The call-timing algorithm of the white-lipped frog, *Leptodactylus albilabris*. *J. comp. Physiol.* A **164**, 309–319.

MORTON, E. S. (1975). Ecological sources of selection on avian sounds. *Am. Nat*. **108**, 17–34.

NARINS, P. (1995). Frog communication. *Scient. Am*. **273**, 62–67.

PARTRIDGE, L., HOFFMANN, A. AND JONES, J. S. (1987). Male size and mating success in *Drosophila melanogaster* and *D. pseudoobscura* under field conditions. *Anim. Behav*. **35**, 468–476.

PAUL, R. C. AND WALKER, T. J. (1979). Arboreal singing in a burrowing cricket, *Anurogryllus arboreus*. *J. comp. Physiol.* A **132**, 217–233.

PÉRINGUEY, L. (1916). Descriptions of new and little-known Orthoptera in the collection of the South African Museum, Part 1. *Ann. S. Afr. Mus*. **15**, 401–413.

PIERCY, J. E., EMBLETON, T. F. W. AND SUTHERLAND, L. C. (1977). Review of noise propagation in the atmosphere. *J. acoust. Soc. Am*. **61**, 1402–1418.

PRESTON-WHYTE, R. A. AND TYSON, P. D. (1988). *The Atmosphere and Weather of Southern Africa*. Cape Town: Oxford University Press.

PROZESKY-SCHULZE, L., PROZESKY, O. P. M., ANDERSON, F. AND VAN DER MERWE, G. J. J. (1975). Use of a self-made sound baffle by a tree cricket. *Nature* **255**, 142–143.

RICHARDS, D. G. AND WILEY, R. H. (1980). Reverberations and amplitude fluctuations in the propagation of sound in a forest: implications for animal communication. *Am. Nat.* **115**, 381–399.

ROBERTSON, J. S., JACOBSON, M. J., SIEGMANN, W. L. AND SANTANDREA, J. P. (1989). Acoustical effects of a large ridge on low-frequency sound propagation in stationary and moving atmospheres. *RPI Math. Rep*. **181**, 6–11.

RÖMER, H. (1997). The sensory ecology of acoustic communication in insects. In *Comparative Hearing: Insects* (ed. R. R. Hoy, A. N.

Popper and R. R. Fay). *Springer Handbook of Auditory Research* (in press).

RÖMER, H., BAILEY, W. J. AND DADOUR, I. (1989). Insect hearing in the field. III. Masking by noise. *J. comp. Physiol.* A **164**, 609–620.

RÖMER, H. AND VAN STAADEN, M. J. (1996). The evolution of hearing organs in grasshoppers: an insect with five pairs of ears and a hearing distance of 1 km. In *Proceedings of the 24th Göttingen Neurobiology Conference* (ed. N. Elsner and H.-U. Schnitzler), p. 54. Stuttgart, New York: Thieme-Verlag.

RYAN, M. J. AND KEDDY-HECTOR, A. (1992). Directional pattern of female mate choice and the role of sensory biases. *Am. Nat.* **139**, S4–S35.

SHUVALOV, V. F. AND POPOV, A. V. (1973). Significance of some of the parameters of the calling songs of male crickets *Gryllus bimaculatus* for phonotaxis of females (in Russian). *J. evol. Biochem. Physiol.* **9**, 177–182.

THORNHILL, R. (1979). Male and female sexual selection and the evolution of mating systems in insects. In *Sexual Selection and Reproductive Competition in Insects* (ed. M. S. Blum and N. A. Blum), pp. 81–121. New York: Academic Press.

THORSON, J., WEBER, T. AND HUBER, F. (1982). Auditory behaviour of the cricket. II. Simplicity of calling song recognition in *Gryllus* and anomalous phonotaxis at abnormal carrier frequencies. *J. comp. Physiol.* A **146**, 361–376.

THUNBURG, C. P. (1775). Pneumore, et nytt genus ibland insecterne, uptäckt och beskrifvit. *K. svenska VetenskAkad. Handl.* **36**, 254–260.

VAN SON, G. (1958). Locust mystery solved. *Afr. Wildlife* **12**, 26–27.

WASER, P. M. AND WASER, M. S. (1977). Experimental studies of primate vocalizations: specializations for long-distance propagation. *Z. Tierpsychol.* **43**, 239–263.

WILEY, R. H. (1994). Errors, exaggeration and deception in animal communication. In *Behavioral Mechanisms in Ecology* (ed. L. A. Real), pp. 157–189. Chicago: University of Chicago Press.

WILEY, R. H. AND RICHARDS, D. G. (1978). Physical constraints on acoustic communication in the atmosphere: Implications for the evolution of animal vocalizations. *Behav. Ecol. Sociobiol.* **3**, 69–94.

WILEY, R. H. AND RICHARDS, D. G. (1982). Adaptations for acoustic communication in birds: Sound transmission and signal detection. In *Acoustic Communication in Birds* (ed. D. E. Kroodsma, E. H. Miller and H. Quellet), pp. 131–181. New York: Academic Press.

YOUNG, D. AND HILL, K. G. (1977). Structure and function of the auditory system of the cicada, *Cystosoma saundersii*. *J. comp. Physiol.* A **117**, 23–45.

The Journal of Experimental Biology 200, 2629–2639 (1997)
Printed in Great Britain © The Company of Biologists Limited 1997
JEB1126

VENTILATION AND GAS EXCHANGE IN LIZARDS DURING TREADMILL EXERCISE

TOBIAS WANG*,[1], DAVID R. CARRIER[2] AND JAMES W. HICKS[1]

[1]*Department of Ecology and Evolutionary Biology, University of California at Irvine, Irvine, CA 92717, USA* and [2]*Department of Biology, University of Utah, Salt Lake City, UT 84112, USA*

Accepted 5 August 1997

Summary

The extent to which lizards ventilate their lungs during locomotion is controversial. Direct measurements of airflow across the nostrils suggest a progressive reduction in tidal volume and minute ventilation with increased running speed, while other studies have demonstrated that arterial P_{O_2} remains constant during exercise. To resolve these conflicting findings, we measured minute ventilation and gas exchange rate in five specimens of *Varanus exanthematicus* and five specimens of *Iguana iguana* during treadmill locomotion at speeds between 0.14 and 1.11 m s^{-1} at 35 °C. These speeds are much lower than maximal running speeds, but are greater than the maximal aerobic speed. In both species, the ventilatory pattern during locomotion was highly irregular, indicating an interference between locomotion and lung ventilation. In *Varanus exanthematicus*, treadmill locomotion elicited a six- to eightfold increase in minute ventilation from a pre-exercise level of 102 ml kg^{-1} min^{-1}, whereas the rate of oxygen uptake increased approximately threefold (from 3.9 to 12.6 ml kg^{-1} min^{-1}). After exercise, both minute ventilation and gas exchange rate decreased immediately. Because minute ventilation increased more than did oxygen consumption, an increase in lung P_{O_2} during exercise is predicted and, thus, *Varanus exanthematicus* appears effectively to ventilate its lungs to match the increased metabolic rate during locomotion at moderate speed. In *Iguana iguana*, both minute ventilation and gas exchange rate increased above resting values during locomotion at 0.28 m s^{-1}, but both decreased with further increases in locomotor speed. Furthermore, following exercise, both minute ventilation and oxygen uptake rate increased significantly. *Iguana iguana*, therefore, appears to be unable to match the increased oxygen demand with adequate ventilation at moderate and higher speeds.

Key words: reptile, lizards, *Varanus exanthematicus*, *Iguana iguana*, exercise, locomotion, ventilation, breathing pattern, gas exchange, cardiovascular.

Introduction

In most vertebrates, ventilation increases during physical activity to meet the increased metabolic demands of the working muscles. In the lizards *Varanus exanthematicus* and *Iguana iguana*, measurements of arterial blood gases and pulmonary gas exchange rate indicate that ventilation adequately maintains arterial blood gas composition during treadmill exercise at speeds greater than their maximal aerobic speed (Mitchell *et al.* 1981*a*,*b*; Bennett, 1994). In a subsequent study, Carrier (1987*a*) measured inspired airflow across the nostrils in four species of lizards (*Iguana iguana*, *Ctenosaura similis*, *Varanus exanthematicus* and *Varanus salvator*) during rest, activity and recovery. At speeds greater than walking speed, all four species displayed a progressive decrease in tidal volume, resulting in a decrease in total ventilation in spite of an increased breathing frequency. On the basis of these findings and the musculoskeletal anatomy of lizards, Carrier (1987*a*,*b*) suggested that lizards are mechanically constrained from breathing during rapid locomotion because the hypaxial muscles contribute to both ventilatory and locomotor movements. This interpretation was subsequently supported by electromyographic recordings from the hypaxial muscles during walking and ventilation in *Iguana iguana* (Carrier, 1989, 1990). The disparity between the studies by Mitchell *et al.* (1981*a*,*b*) and Carrier (1987*a*,*b*) is not easily explained since ineffective pulmonary ventilation during locomotion must result in predictable changes in the composition of arterial blood gases. However, because lizards often employ intermittent locomotion, even on treadmills, it is possible that blood gas composition is maintained by ventilating the lungs during brief pauses between locomotor activity. The possible inability of lizards to ventilate their lungs effectively during exercise is in sharp contrast to the pattern observed in birds and mammals and has important implications concerning the evolution of sustained locomotion in tetrapods (e.g. Carrier,

*Present address: Center of Respiratory Adaptation, Institute of Biology, University of Odense, Campusvej 55, DK-5230 Odense, Denmark (e-mail: wang@biology.ou.dk).

1987*b*; Bramble and Jenkins, 1989; Bennett, 1994; Ruben, 1995).

Given the conflicting results of these studies, we re-examined ventilatory responses to exercise in *Varanus exanthematicus* and *Iguana iguana*. Ventilation and gas exchange were measured directly, both at rest and at speeds that were in excess of maximum aerobic capacity.

Materials and methods

Experimental animals

Five savannah monitors (*Varanus exanthematicus* Bosc) with body masses ranging from 260 to 660 g were purchased from a licensed supplier in Florida, USA, and transported by air to Irvine, CA, USA. In addition, five green iguanas (*Iguana iguana* L.) weighing 330–1900 g were obtained from local pet stores. All lizards were housed in large terraria with free access to water and a thermal gradient and were maintained on a light:dark cycle of 12 h:12 h.

Measurement of ventilation and gas exchange rate

In all experiments, the ventilatory airflows across the nostrils were measured using pneumotachography. To provide a gas-tight connection between the nostrils and the pneumotachograph, thin-walled Tygon tubing was inserted into each nostril of unanaesthetised animals and then merged and glued to the head using epoxy. In the smallest iguanas, the nostrils were too small for this arrangement, and a small plastic mask was glued over the nostrils instead. The pneumotachograph (8421, series 0-5 LPM, H. Rudolph, Inc., MO, USA), connected to a differential pressure transducer (Validyne MP 45-1-871), was attached to the tubing leaving the nostrils or mask. The pneumotachograph was calibrated by inserting a syringe where the tubing or mask was connected during the experiments and manually simulating breaths. All calibration procedures produced very tight correlations between injected gas volumes and the integrated flow signal ($r^2 \geqslant 0.98$) and were reproducible before and after the experiments. To provide an independent verification of our pneumotachograph recordings, we also collected the exhaled gases in a Mylar bag during many of the trials on the varanids. The volume of the exhaled gas in the Mylar bag was subsequently determined by withdrawing the gas into an airtight glass syringe. To collect exhaled gases, a miniature T-shaped two-way non-rebreathing valve (series 2384, H. Rudolph, Inc., MO, USA) was inserted between the tubes leaving the nostrils and the pneumotachograph (which, in turn, was connected to the Mylar bag). The inhalation and exhalation ports of this valve each contain a diaphragm creating a unidirectional airflow between inhaled air and the Mylar bag; thus, only exhaled airflow could be measured in this experimental design. There was excellent agreement between the direct determination of the exhaled gas and that determined by pneumotachography: a linear regression yielded $V_m=0.999V_p$ ($r^2=0.98$; $N=52$), where V_m is the volume of exhaled gas in the Mylar bag and V_p is the volume of exhaled gas calculated from pneumotachography.

Gas exchange rate was measured differently in the two species of lizards. In preliminary experiments, we verified that the two experimental designs yielded similar values for O_2 uptake and CO_2 excretion rates. For the varanids, gas exchange rate was determined from minute ventilation (as measured by pneumotachography) and exhaled gas composition in the gas collected in the Mylar bags. Exhaled gas composition was analysed using Applied Electrochemistry O_2 and CO_2 analysers (S-3A and CD-3A, respectively) connected in series. From these measurements, $\dot{V}_{O_2}$ and $\dot{V}_{CO_2}$ were calculated as $(F_{IO_2}-F_{EO_2})V$ and $(F_{ECO_2}-F_{ICO_2})V$, respectively, where V is the volume of exhaled gas, F_I designates the inspired gas fraction and F_E designates the expired gas fraction. All $\dot{V}_{O_2}$ and $\dot{V}_{CO_2}$ measurements were corrected to STPD. For *Iguana iguana*, gas exchange rate was determined as described by Wang and Warburton (1995). Briefly, the tubing leaving the nostrils was connected to a T-piece attached at both ends to gas-tight Tygon tubing. One end fed into the gas analysers (described above), connected in series, whereas the other served as a reservoir. An Applied Electrochemistry flow pump, connected in series with the gas analysers, maintained a constant gas flow from the T-piece and the gas analysers. The pneumotachograph was inserted into the reservoir tubing and measured a decrease in the airflow rate during exhalation and an increase in the airflow rate during inhalation. In this system, the signal from the differential pressure transducer preceded that of the gas analysers by approximately 2 s. $\dot{V}_{O_2}$ and $\dot{V}_{CO_2}$ were determined as the area below the baseline signal for each gas observed during a breath-hold; the relationship between this area and gas exchange rate was determined by simulating exhalations with known gas compositions and volumes.

Measurement of systemic blood flow and heart rate

After completing all measurements on the ventilatory responses to treadmill exercise, four varanids were instrumented using a blood-flow probe (2R, Transonic System, Inc., Ithaca, NY, USA) for determination of systemic blood flow and heart rates. Shortly before surgery, lizards were placed in a bucket with a cloth soaked in Halothane to induce light anaesthesia to allow intubation. After intubation, the lizards were artificially ventilated (8–15 breaths min^{-1} and a tidal volume of 10–20 ml kg^{-1}) using an SAR-830 CWE Inc. ventilator (Ardmore, PA, USA) and a gas mixture consisting of 30 % O_2, 3 % CO_2 (balance N_2) prepared by a gas-mixing flow meter (GF-3, Cameron Instruments, TX, USA). This gas mixture passed through a Halothane vaporizer (Dräger, Lubeck, Germany) initially set at 3–4 % and subsequently reduced to 0.5–1 % throughout the surgery. To implant the flow probe, a 2–3 cm incision was made on the ventral side caudal to the sternum. Because we felt it was imperative to minimize damage to the rectus abdominus muscle, the flow probe was inserted on the most easily accessible vessel. This differed among animals, and flow probes were, therefore, implanted around either the left aortic arch or a branch of the right aortic arch. After placement of the flow probe, the incision was closed with intermittent sutures and cyanacrylate tissue glue (Nexaband; S/C-TriPoint Medical, Raleigh, NC, USA). Artificial ventilation without Halothane was continued until the lizard regained

consciousness and started breathing on its own. It was then placed in a small container maintained at 30–35 °C and allowed to recover for at least 48 h.

Flow probes were connected to a dual-channel blood flow meter (T201, Transonic System, Inc.) for simultaneous measurement of both mean blood flow rate and instantaneous blood flow velocity, which was used for on-line determination of heart rate. Because we were not able to place flow probes around all the systemic outflow vessels, our measurements underestimate systemic blood flow rate and blood flow measurements are therefore expressed as relative values compared with rest.

Monitoring of the locomotor cycle

The locomotor cycle was monitored using a photocell apparatus that recorded lateral bending of the trunk. The apparatus consisted of a photocell and a light-emitting diode (LED) situated at opposite ends of a 10 cm piece of flexible tubing attached to the dorsal midline of the lizards using strips of Velcro. The photocell formed one arm of a Wheatstone bridge. As the lizard walked and ran on the treadmill, lateral bending of the trunk bent the tube and changed the amount of light from the LED illuminating the photocell, providing an analogue record of the locomotor cycle. In addition, all experiments were video-taped using a VHS video system (60 images s^{-1}), which enabled subsequent analysis of exercise performance.

Experimental protocols

In both species, ventilation and gas exchange rate were determined simultaneously (as described above) before, during and after exercise using a similar experimental protocol. At least 24 h prior to experimentation, lizards were equipped with masks or tubing inserted in the nostrils and allowed to acclimate to the experimental temperature (35 °C). A few hours before treadmill exercise, the lizard was placed on the treadmill and left undisturbed with the mask or tubing connected to the experimental apparatus. Immediately before running, pre-exercise ventilation and gas exchange rates were measured over a 10–20 min period. Although the lizards quickly relaxed when placed on the treadmill, these pre-exercise values do not represent true resting values. To minimize fatigue, each lizard was exercised on two consecutive days. For the varanids, the exercise regime commenced with a walking speed of 0.14 m s^{-1}, followed by 0.28, 0.42 and 0.56 m s^{-1} (in that order) on the first day, whereas the exercise regime consisted of 0.28 and 0.83 m s^{-1} on the second day. For the iguanas, the first day consisted of 0.28, 0.56 and 0.83 m s^{-1} (in that order), whereas the exercise regime consisted of 0.28 and 1.11 m s^{-1} on the second day. In both species, the maximum speed used represents the highest speed at which the lizards were able to match the belt speed for at least 2 min. At the lower locomotor speeds, the belt speed was kept constant for approximately 5 min. In each trial, the belt speed of the treadmill was slowly increased to the desired level and kept constant for at least 5 min or until the animal was no longer able to match the belt speed. In both species, gas exchange and minute ventilation were measured during the last 2–3 min of each exercise trial. Following exercise, gas exchange rates and minute ventilation were measured for 3–4 min immediately following exercise (however, owing to the low ventilation following the lowest speeds in *Varanus exanthematicus*, it was necessary to sample for up to 7 min to collect sufficient gas for precise determination of gas exchange). This period immediately following exercise is referrred to as the recovery period. After each exercise trial, the lizard was allowed to recover further until the ventilatory pattern resembled that recorded during the pre-exercise period. In general, the period required for this criterion to be fulfilled increased with increasing running speed and lasted for between 15 and 60 min.

The iguanas were not able to perform sustained exercise. Therefore, to determine whether the pronounced increase in ventilation immediately following exercise (see Fig. 3A,B) resulted from a time-dependent change in the ventilatory response to exercise or to the cessation of locomotion proper, an additional experimental protocol was employed. In these experiments, iguanas were exercised repeatedly at 0.56, 0.83 or 1.11 m s^{-1} in exercise bouts lasting 30 s followed by a 2 min recovery period. This exercise regime was repeated six or seven times, or until the lizard displayed significant signs of fatigue and was no longer able to match the belt speed. It was assumed that this protocol resulted in an elevated metabolic rate during the period of recovery and allowed comparison of minute ventilation during exercise and immediately prior to and immediately preceding exercise.

Data collection, analysis and statistics

All signals from the differential pressure transducer, the blood flow meter and the photocell for measurement of lateral bending were collected on a computer at 50 Hz using Acknowledge data-acquisition system software (Biopac System, Goleta, CA, USA). All subsequent data analysis was performed using Acknowledge data-analysis software (version 3.0).

The effects of running speed on all parameters studied were assessed using a one-way analysis of variance (ANOVA) for repeated measures. Differences among means were distinguished using a Student–Newman–Keuls analysis. A fiducial limit for significance of $P<0.05$ was chosen, and all results are presented as mean ±1 S.E.M.

Results

Critique of treadmill exercise

In this study, lizards were forced to walk and run on a treadmill, which is a very unnatural situation. In most lizards, the typical locomotor pattern consists of either slow walking or sprints of high speed and short duration. Nevertheless, the varanids performed consistently well at the lower speeds and were able to match the belt speed for longer than 10 min. In contrast, the iguanas performed poorly, and half of the animals purchased could not match the belt speed of the treadmill for any sustained period. Furthermore, these individuals exhibited behavioural traits such as defensive posturing and ‘tail thrashing’ and, consequently, we do not report the data

obtained on these animals. The data reported were obtained from five subjects of each species that performed consistently well. Within each species, the responses to exercise were consistent and, therefore, we feel that our data represent the cardiopulmonary response to increased metabolic rate during locomotion in these species.

Physiological variables were determined for lizards ambulating at speeds up to a maximum of 0.83 m s^{-1} for varanids and up to 1.11 m s^{-1} for iguanas. These speeds are well above the maximum aerobic speeds of both species (0.33–0.54 m s^{-1} for *Varanus exanthematicus* and 0.14 m s^{-1} for *Iguana iguana*; Gleeson *et al.* 1980; see also Fig. 3), but are considerably lower than the maximum running speeds of both species (2.0 m s^{-1} for *Varanus exanthematicus*, and 4.5 m s^{-1} for *Iguana iguana*; Carrier, 1987*a*). In the present study, 0.83 m s^{-1} and 1.11 m s^{-1}, respectively, were the highest speeds that the lizards were able to maintain on the treadmill. The previous studies by Gleeson *et al.* (1980) and Mitchell *et al.* (1981*a*,*b*) reported physiological measurements only at speeds up to 0.28 and 0.54 m s^{-1} for *Iguana iguana* and *Varanus exanthematicus*, respectively.

Breathing pattern during and following locomotion

In all specimens of both species, the breathing pattern was altered during locomotion (Fig. 1). While the breathing pattern at rest in *Varanus exanthematicus* consisted of evenly spaced single breaths commencing with expiration followed by inhalation, the ventilatory airflows during locomotion were characterized by frequent and abrupt changes (Fig. 1A–C). The maximum airflow rate increased, whereas the inspiratory and expiratory times decreased relative to pre-exercise values. Following exercise, tidal volume immediately increased above pre-exercise values and the breathing pattern returned to distinct, evenly spaced breaths. In *Iguana iguana*, ventilation was typically continuous before exercise, which probably indicates that these animals were not in a resting state. At the onset of locomotion, the breathing pattern was characterized by a high-frequency ventilatory oscillation of low-volume inspiratory and expiratory flows, interrupted by larger breaths of high and erratic rates of airflow (Fig. 1D–F). The changes in tidal volume during and following exercise are presented in Fig. 2 for both species. In this analysis, only expiratory airflows that were separated by substantial inspiratory airflows are reported. Thus, many of the

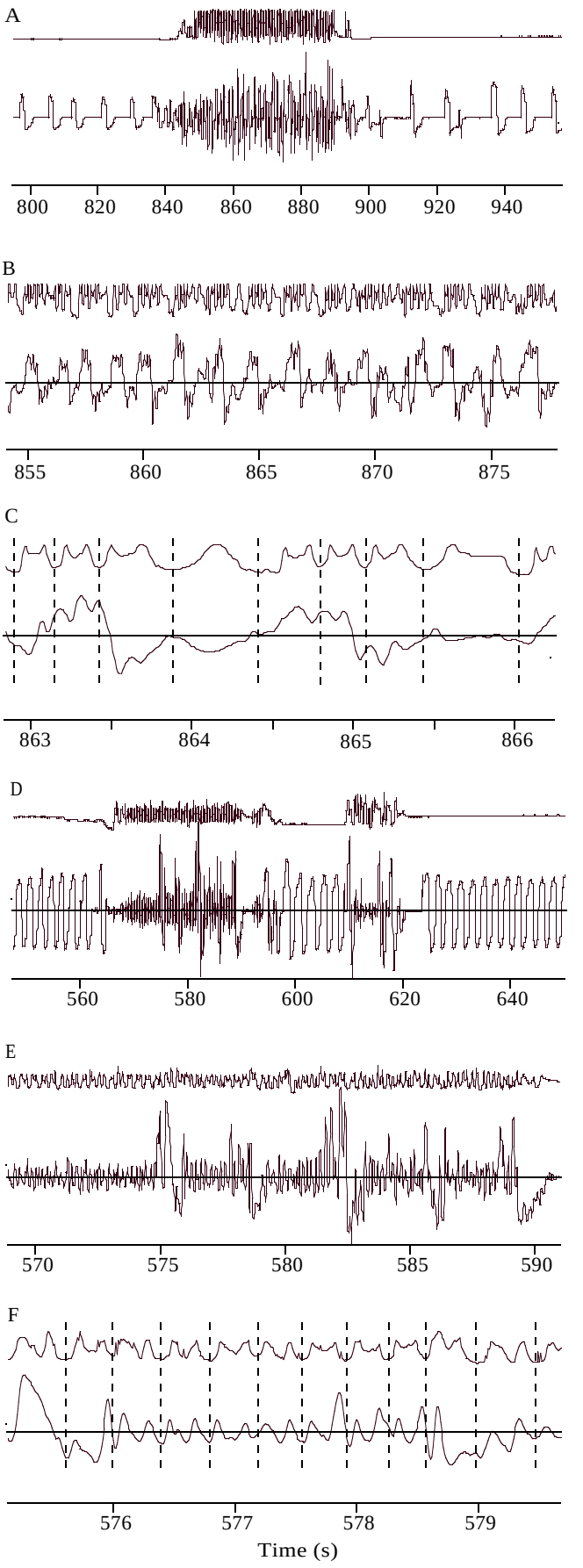

Fig. 1. Sample recordings of ventilatory airflow rates in *Varanus exanthematicus* and *Iguana iguana* running on a treadmill at 0.83 m s^{-1}. In each example, the upper trace is a recording of lateral bending of the trunk. A flat trace indicates that the lizard was stationary. Once the treadmill was turned on and the lizard began to move, each wave cycle on the trace represented one locomotor cycle. In each example, the lower trace is a pneumotachograph recording of ventilatory airflow rates at the nares. Expiratory flow occurred when the trace was above baseline. (A) A 30 s bout of running in *V. exanthematicus* illustrating ventilation before, during and after locomotion. (B,C) Enlarged segments of the running portion of trial A. (D) A 30 s bout of running in *I. iguana* illustrating ventilation before, during and after locomotion. (E,F) Enlarged segments of the running portion of trial D.

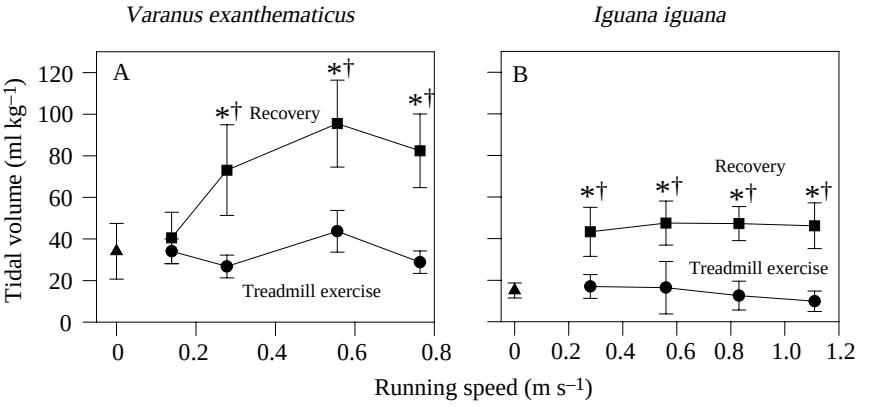

Fig. 2. Expiratory tidal volume during (●) and following (■) treadmill exercise at different locomotor speeds in *Varanus exanthematicus* (A) and *Iguana iguana* (B). Values are means ± 1 S.E.M. (*N*=5). Mean values that are significantly different from pre-exercise levels (▲) are marked with an asterisk. Mean values during recovery that are significantly different from those for exercise at the same speed are marked with a dagger.

small breaths (which presumably do not contribute to gas exchange) are not included. In both species, tidal volume during exercise was not significantly different from that during rest, but increased two- to fourfold immediately following exercise.

Ventilation and gas exchange before, during and following locomotion

The data for minute ventilation and gas exchange rate in both species are presented in Fig. 3 and Tables 1 and 2. In *Varanus exanthematicus*, minute ventilation increased from a pre-exercise value of 102±23 ml kg^{-1} min^{-1} to a maximum of 771±91 ml kg^{-1} min^{-1} at 0.56 m s^{-1} (Fig. 3A). At speeds between 0.14 and 0.56 m s^{-1}, minute ventilation increased significantly during the recovery period. The rate of oxygen uptake ($\dot{V}_{O_2}$) increased from a pre-exercise level of 3.9±0.7 ml kg^{-1} min^{-1} to a maximum of 12.6±2.2 ml kg^{-1} min^{-1} at 0.56 m s^{-1} and

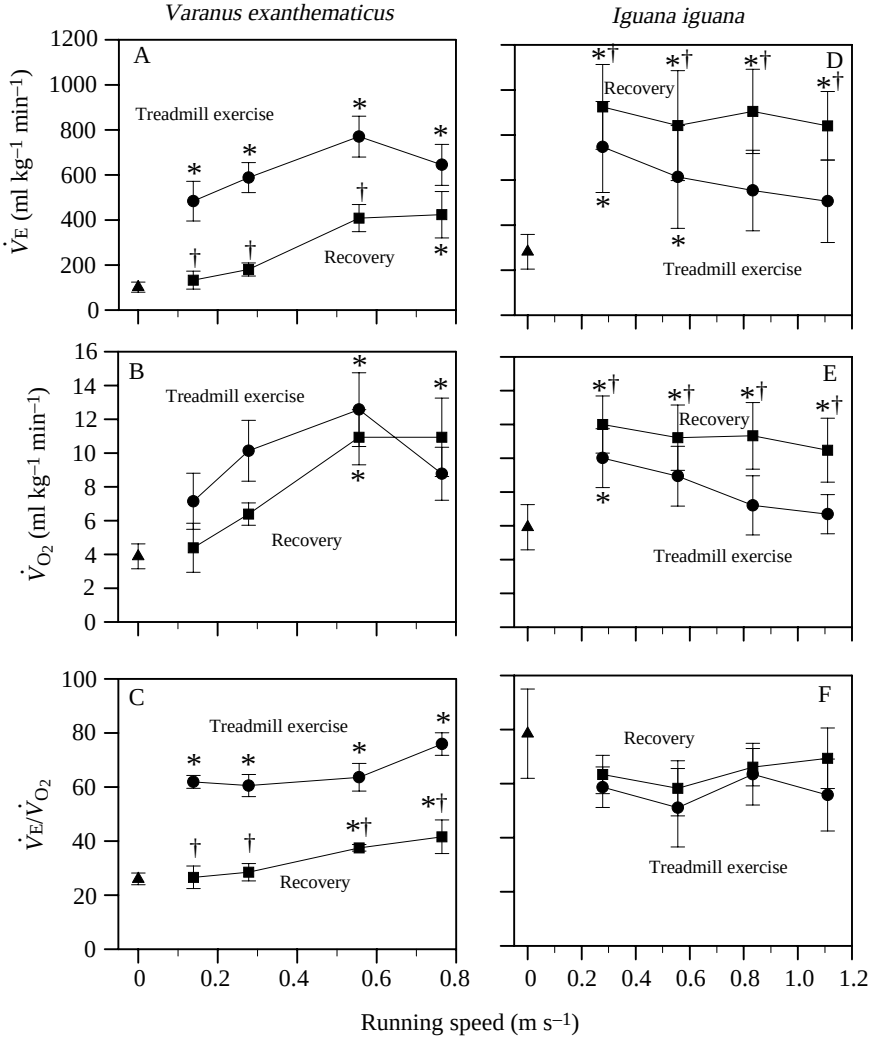

Fig. 3. The ventilatory and respiratory responses to exercise in *Varanus exanthematicus* and *Iguana iguana*. Minute ventilation ($\dot{V}_E$), oxygen uptake rate ($\dot{V}_{O_2}$) and air convection requirements ($\dot{V}_E/\dot{V}_{O_2}$) during treadmill locomotion (●) and during the immediate recovery period (■) in *Varanus exanthematicus* (A–C) and *Iguana iguana* (D–F). Values are means ± 1 S.E.M. (*N*=5). Mean values that are significantly different from pre-exercise levels (▲) are marked with an asterisk. Mean values during recovery that are significantly different from those for exercise at the same speed are marked with a dagger.

Table 1. *The respiratory gas exchange ratio during locomotion and immediately following exercise in* Varanus exanthematicus *and* Iguana iguana

Varanus exanthematicus			*Iguana iguana*		
	RER			RER	
Speed ($m\,s^{-1}$)	Locomotion	Recovery	Speed ($m\,s^{-1}$)	Locomotion	Recovery
Pre-exercise	0.77±0.07		Pre-exercise	0.70±0.08	
0.14	0.93±0.02	0.82±0.15	0.28	0.95±0.10	1.45±0.13*,†
0.28	0.85±0.04	0.78±0.08	0.56	0.78±0.08	1.27±0.08*,†
0.56	1.04±0.06*	1.23±0.05*	0.83	0.68±0.14	1.19±0.12*,†
0.76	1.01±0.11	1.12±0.06*	1.11	0.72±0.04	1.29±0.08*,†

*Significantly different from the pre-exercise value; †significantly different from the exercise value at the same speed.
The respiratory exchange ratio, RER, is calculated as $\dot{V}_{O_2}/\dot{V}_{CO_2}$.

decreased, although not significantly, with a further increase in speed (Fig. 3B). At lower speeds, $\dot{V}_{O_2}$ during recovery was lower than during exercise, but this difference disappeared at higher speeds (Fig. 3B). The rate of elimination of CO_2 ($\dot{V}_{CO_2}$) followed the same pattern as $\dot{V}_{O_2}$, although the changes in the recovery period were more pronounced (data not shown). The respiratory gas exchange ratio (RER; $\dot{V}_{CO_2}/\dot{V}_{O_2}$) increased from 0.77±0.07 to 1.04±0.06 with increased speed up to $0.56\,m\,s^{-1}$, reaching values as high as 1.23±0.05 following exercise (Table 1). At all speeds, minute ventilation increased relatively more than did $\dot{V}_{O_2}$ or $\dot{V}_{CO_2}$, resulting in increased air convection requirements ($\dot{V}_E/\dot{V}_{O_2}$ or $\dot{V}_E/\dot{V}_{CO_2}$; Fig. 3C; Table 2). During recovery, air convection requirement quickly decreased and $\dot{V}_E/\dot{V}_{O_2}$ was significantly higher than pre-exercise values only after the fastest running speeds. However, $\dot{V}_E/\dot{V}_{CO_2}$ during recovery did not differ significantly from the pre-exercise level of 35.2±3.1 (Table 2).

In *Iguana iguana*, minute ventilation increased significantly during exercise from a pre-exercise level of $282±77\,ml\,kg^{-1}\,min^{-1}$ to a maximum of $747±202\,ml\,kg^{-1}\,min^{-1}$ at $0.28\,m\,s^{-1}$ (Fig. 3D). Comparison of the minute ventilation at each locomotor speed (pre-exercise not included) using a one-way ANOVA for repeated measures revealed a statistically significant reduction in minute ventilation with increased running speed. In contrast to the varanids, minute ventilation increased significantly relative to pre-exercise levels immediately following locomotion and reached levels as high as $925±188\,ml\,kg^{-1}\,min^{-1}$. Similarly, $\dot{V}_{O_2}$ increased from a pre-exercise level of $5.92±1.34\,ml\,kg^{-1}\,min^{-1}$ to a maximum of $10.01±1.74\,ml\,kg^{-1}\,min^{-1}$ at $0.28\,m\,s^{-1}$ and was significantly increased relative to pre-exercise levels during recovery from all locomotor speeds, reaching a maximum value of $12.02±1.69\,ml\,kg^{-1}\,min^{-1}$ (Fig. 3E). Furthermore, at the two highest locomotor speeds, both minute ventilation and $\dot{V}_{O_2}$ were significantly lower ($506±183\,ml\,kg^{-1}\,min^{-1}$ and $6.69±1.16\,ml\,kg^{-1}\,min^{-1}$, respectively), than the levels measured at $0.28\,m\,s^{-1}$. There were no systematic changes in minute ventilation relative to $\dot{V}_{O_2}$ and $\dot{V}_{CO_2}$ (Fig. 3D; Table 2), whereas RER increased significantly during the recovery period and reached maximum values as high as 1.45±0.13 from a pre-exercise value of 0.70±0.08 (Table 2).

The changes in heart rate and systemic blood flow rate during exercise in *Varanus exanthematicus* are presented in Table 3. Heart rate increased significantly from a pre-exercise level of $45.5±3.6\,beats\,min^{-1}$ to a maximum of $99.4±5.7\,beats\,min^{-1}$ at the highest speed, which was mirrored by a simultaneous significant increase in relative systemic blood flow rate.

Table 2. *Minute ventilation relative to ventilatory CO_2 production during locomotion and immediately following exercise in* Varanus exanthematicus *and* Iguana iguana

Varanus exanthematicus			*Iguana iguana*		
	$\dot{V}_E/\dot{V}_{CO_2}$			$\dot{V}_E/\dot{V}_{CO_2}$	
Speed ($m\,s^{-1}$)	Locomotion	Recovery	Speed ($m\,s^{-1}$)	Locomotion	Recovery
Pre-exercise	35.2±3.1		Pre-exercise	78.5±16.4	
0.14	61.9±2.4*	33.2±1.7†	0.28	78.1±12.1	55.0±8.1
0.28	60.5±4.1*	38.5±5.6†	0.56	76.7±13.5	54.8±6.2
0.56	63.6±5.1*	30.6±1.9†	0.83	134.7±31.1*	69.5±7.4
0.76	75.9±4.2*	37.1±5.3†	1.11	90.6±15.2	64.0±7.5

*Significantly different from the pre-exercise value; †significantly different from the exercise value at the same speed.
Minute ventilation, $\dot{V}_E$, and ventilatory CO_2 production ($\dot{V}_{CO_2}$) are measured in $ml\,kg^{-1}\,min^{-1}$.

Ventilation during and after repeated bouts of exercise

The ventilatory responses to exercising iguanas repeatedly in bouts of 30 s followed by 120 s of recovery are presented in Fig. 4. During this protocol, minute ventilation invariably decreased during exercise compared with the preceding recovery period, indicating that the increase in ventilation following exercise can be ascribed to the cessation of locomotion *per se*, rather than being the result of time-dependent changes in the ventilatory response to exercise.

Discussion

Previous studies on *Iguana iguana* and *Varanus exanthematicus* demonstrated that arterial blood gas composition is maintained during treadmill exercise (Mitchell *et al.* 1981*a*,*b*), indicating that minute ventilation increases in proportion to metabolic rate. In contrast, a later study on the same species (Carrier, 1987*a*) showed a progressive decline in minute ventilation as speed increased above slow walking. Given this disparity, the primary purpose of the present study was to obtain direct measurements of minute ventilation and ventilatory patterns during locomotion in these lizards. Our data show that both *Varanus exanthematicus* and *Iguana iguana* are capable of ventilating their lungs during a locomotor stride (Fig. 1). However, in both species, the ventilatory pattern was influenced by locomotion, and in

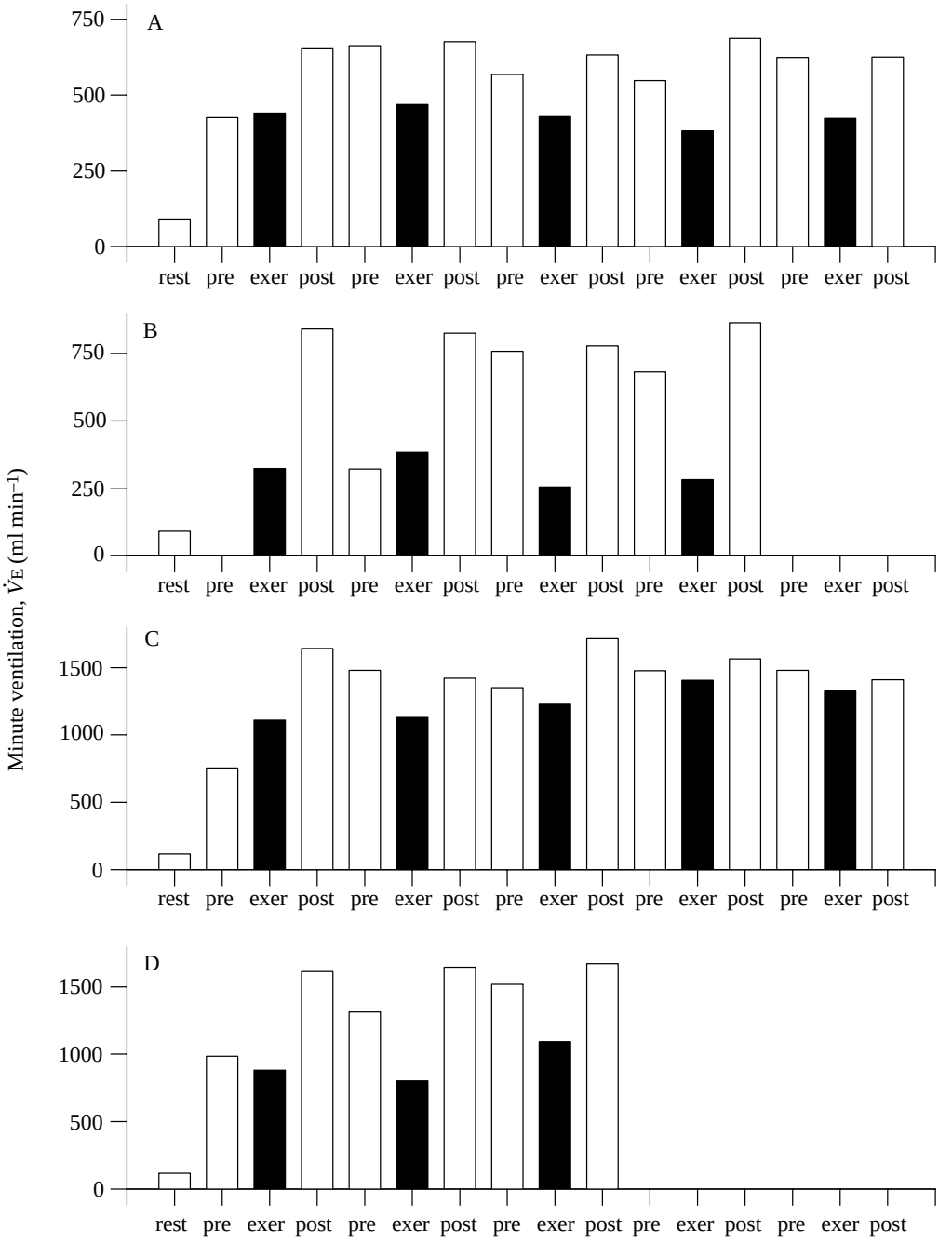

Fig. 4. Minute ventilation in two specimens of *Iguana iguana* during experiments in which the lizards repeatedly walked for 30 s and then rested for 2 min. In each histogram, 'rest' represents resting minute ventilation. The minute ventilation recorded during the 30 s period immediately prior to exercise (exer) is labelled 'pre' and the minute ventilation recorded immediately after the exercise is labelled 'post'. Trials are shown for a 0.33 kg lizard walking at 0.56 m s^{-1} (A) and 0.83 m s^{-1} (B), and for a 1.90 kg lizard walking at 0.56 m s^{-1} (C) and 1.11 m s^{-1} (D)

Iguana iguana there was a progressive decrease in minute ventilation with increased running speed (Fig. 3D).

Breathing patterns during exercise

The breathing pattern in both species was altered during exercise and was characterized by breaths of higher flow velocities and shorter duration than both before and after exercise (Fig. 1). This is in accordance with the findings of Carrier (1987*b*), but is in sharp contrast to earlier studies on ventilation during forced activity in restrained lizards and snakes, which report large increases in tidal volume and small changes in breathing frequency during activity (Wilson, 1971; Dm'iel, 1972; Bennett, 1973; Cragg, 1978). These differences are most probably explained by the differences in experimental design. In the earlier studies, the animals were physically restrained and activity was induced by pinching the legs or through electrical shocks, whereas the lizards in the present study ran freely on a treadmill. In humans, increases in tidal volume account for most of the exercise hyperpnoea that occurs at moderate levels of exercise, while increases in breathing frequency become more important during more severe or prolonged exercise (e.g. Hanson *et al.* 1982). In mammalian quadrupeds, the increased level of ventilation during exercise results primarily from an increase in breathing frequency, whereas changes in tidal volume are more variable; for example, in dogs, tidal volume decreases during exercise (Flandrois *et al.* 1971), whereas tidal volume increases slightly in ponies, goats and calves (Bisgard *et al.* 1978, 1982; Smith *et al.* 1983; Kuhlmann *et al.* 1985).

Immediately following cessation of locomotion, the breathing pattern in both species was characterized by large tidal volumes (Figs 1, 2). In *Varanus exanthematicus*, breathing frequency decreased following exercise, leading to a decrease in minute ventilation (Fig. 3). In contrast, ventilation following exercise in *Iguana iguana* was virtually continuous which, in concert with the increased tidal volume, resulted in a large increase in minute ventilation (Figs 1–3). Consistent with this observation, *Iguana iguana* exhibited an increased minute ventilation following locomotion in the experiments employing short bouts of repeated exercise (Fig. 4). These findings suggest that the observed changes in the breathing pattern are correlated with the cessation of exercise rather than resulting from time-dependent changes in the ventilatory response to exercise. Changes in breathing pattern following exercise have been reported only rarely for mammals. In dogs, tidal volume increases modestly following exercise, but returns to pre-exercise levels within minutes (Flandrois *et al.* 1971).

The effects of exercise on minute ventilation and gas exchange rates

The present study shows that minute ventilation and gas exchange rates increased during locomotion in both species, but that the response to exercise differed between *Varanus exanthematicus* and *Iguana iguana* (Fig. 3; Tables 1, 2). In *Varanus exanthematicus*, minute ventilation increased significantly above pre-exercise levels at all locomotor speeds and decreased immediately following exercise (Fig. 3A,B). A similar pattern was seen for $\dot{V}_{O_2}$ and $\dot{V}_{CO_2}$. In *Iguana iguana*, minute ventilation, $\dot{V}_{O_2}$ and $\dot{V}_{CO_2}$ increased significantly above the pre-exercise levels at the slowest locomotor speeds, but decreased with further increases in running speed (Fig. 3D,E).

Previous studies on the ventilatory responses to exercise in these two species used different techniques from those employed here. Mitchell *et al.* (1981*b*; see also Mitchell *et al.* 1981*a*; Gleeson *et al.* 1980) measured arterial blood gas composition and gas exchange rates at treadmill speeds up to 0.28 and 0.56 m s^{-1} for *Iguana iguana* and *Varanus exanthematicus*, respectively. On the basis of arterial P_{CO_2} and pulmonary gas exchange rates, the effective minute ventilation of the lungs ($\dot{V}_{eff}$) and lung P_{O_2} were calculated using well-established equations for gas exchange in mammals (e.g. Otis, 1964). In these studies, arterial P_{CO_2} decreased during exercise in both species, suggesting that $\dot{V}_{eff}$ relative to $\dot{V}_{O_2}$ ($\dot{V}_{eff}/\dot{V}_{O_2}$) was increased.

The use of arterial P_{CO_2} to calculate $\dot{V}_{eff}$ relies on the assumption that arterial P_{CO_2} is identical to lung P_{CO_2} and that only ventilatory changes affect arterial P_{CO_2}. This, in turn, assumes no cardiac or pulmonary shunt and that the lung functions as a perfect gas exchanger (i.e. no ventilation–perfusion inhomogeneity and no diffusion limitation). However, factors that influence arterial P_{CO_2}, independently of minute ventilation, will alter this estimation. For example, if arterial P_{CO_2} is higher than lung P_{CO_2}, $\dot{V}_{eff}$ will be underestimated. Alternatively, improved lung function (e.g. less ventilation–perfusion inhomogeneity) or a reduction in the cardiac right-to-left shunt decrease arterial P_{CO_2} at constant minute ventilation relative to $\dot{V}_{CO_2}$. Therefore, if the cardiac shunt is reduced and/or lung function improved during exercise compared with rest, it is possible that the calculations of Mitchell *et al.* (1981*a*,*b*) will overestimate the relative increase in minute ventilation. Unfortunately, very little is known about changes in cardiac shunt and lung function during exercise in reptiles and, consequently, it is difficult to evaluate the magnitude of these possible errors. In *Varanus exanthematicus* walking at low speed (0.28 m s^{-1}), left atrial P_{O_2} increases during exercise, in spite of an increased ventilation–perfusion inhomogeneity (Hopkins *et al.* 1995), which supports the existence of an exercise hyperpnoea. Finally, using measurements of blood gas composition to calculate minute ventilation may not provide a good time resolution; because lizards often run intermittently (even on treadmills), it is conceivable that they maintain a constant blood gas composition by ventilating their lungs during brief pauses in locomotor activity (Carrier, 1987*a*). Presumably, this potential problem would be most pronounced at higher locomotor speeds.

Carrier (1987*a*) reported a substantial reduction in minute ventilation of both *Varanus exanthematicus* and *Iguana iguana* at running speeds that are equivalent to those of our study. It is possible that the discrepancy in the results from the present study is due to the different techniques employed. Carrier (1987*a*) assessed inspiratory airflow rates using the rate of heat loss from heated thermistors implanted over one nostril. This system was difficult to calibrate over a wide range of airflow rates and, because maximum airflow rates were predicted to occur

following locomotion, Carrier (1987*a*) calibrated the recording system using the airflows observed during recovery from exercise. However, the present study shows that the maximum flow rates occur during locomotion and that the difference in flow rate between exercise and recovery is more pronounced for *Varanus exanthematicus* than for *Iguana iguana* (Fig. 1). Consequently, an error in the calibration of the flow probe in Carrier's (1987*a*) study may have resulted in underestimated minute ventilation during exercise in *Varanus exanthematicus*.

In spite of differences in experimental design, there is reasonable agreement between our results and those from previous studies. For *Varanus exanthematicus*, Mitchell *et al.* (1981*b*) calculated a $\dot{V}_{eff}$ of approximately 60 ml kg^{-1} min^{-1} at rest and a $\dot{V}_{eff}/\dot{V}_{O_2}$ of 18. During exercise, $\dot{V}_{eff}/\dot{V}_{O_2}$ increased to approximately 40, corresponding to a $\dot{V}_{eff}$ of approximately 800 ml kg^{-1} min^{-1} (Fig. 1 in Mitchell *et al.* 1981*b*). Our determination of total minute ventilation (i.e. effective minute ventilation *and* dead-space minute ventilation) is comparable at rest (102 ml kg^{-1} min^{-1}), while the maximum level during exercise is slightly lower (771 ml kg^{-1} min^{-1}) than in this previous report. Carrier (1987*a*) reported a minute ventilation of 110 ml kg^{-1} min^{-1} at rest and 304 ml kg^{-1} min^{-1} during locomotion at 0.8 m s^{-1} in *Varanus exanthematicus*, which is likely to be an underestimation for the reasons given above. Mitchell *et al.* (1981*b*) determined that $\dot{V}_{O_2}$ increased progressively with increasing locomotor speed from a resting value of 3.2 ml O_2 kg^{-1} min^{-1} to a maximum value of almost 20 ml O_2 kg^{-1} min^{-1} at 0.3–0.4 m s^{-1} in *Varanus exanthematicus*. The maximum $\dot{V}_{O_2}$ in our study was lower (12.6 ml kg^{-1} min^{-1}), whereas the pre-exercise level (3.9 ml kg^{-1} min^{-1}) was slightly higher. For *Iguana iguana*, the pre-exercise $\dot{V}_{O_2}$ determined in the present study (5.9 ml kg^{-1} min^{-1}) is almost twice as high as the resting value of 3.0 ml kg^{-1} min^{-1} reported by Mitchell *et al.* (1981). This difference probably reflects the fact that the iguanas in the present study were not completely undisturbed and that our pre-exercise condition did not resemble true resting conditions. This explanation is also supported by the high pre-exercise minute ventilation and $\dot{V}_E/\dot{V}_{O_2}$ in the present study (Fig. 3F) compared with the previous studies. For *Iguana iguana*, Mitchell *et al.* (1981*b*) reported that $\dot{V}_{O_2}$ increased to 13.8 ml kg^{-1} min^{-1} at 0.14 m s^{-1} and calculated $\dot{V}_{eff}$ to be approximately 800 ml kg^{-1} min^{-1} at this speed, while Carrier (1987*a*) reported a minute ventilation of approximately 900 ml kg^{-1} min^{-1} at 0.1–0.2 m s^{-1}. These values are similar to the minute ventilation and gas exchange rates at 0.28 m s^{-1} in the present study (Fig. 3D,E). As in our study (Fig. 3D), Carrier (1987*a*) also observed a progressive decrease in minute ventilation when locomotor speed was increased above 0.2 m s^{-1}; Mitchell *et al.* (1981*a*,*b*) did not study the physiological responses to speeds higher than 0.28 m s^{-1}.

In *Iguana iguana*, both experimental protocols show that minute ventilation increased significantly after exercise (Figs 3D, 4) and that this hyperpnoea during recovery from exercise was associated with a significant increase in $\dot{V}_{O_2}$ (Fig. 3E,F). In *Varanus exanthematicus*, minute ventilation decreased following exercise (Fig. 3A), and only after the fastest running speeds did $\dot{V}_{O_2}$ remain high during recovery (Fig. 3B). Carrier (1987*a*) reported large increases in minute ventilation following locomotion in both species, but did not measure $\dot{V}_{O_2}$ or $\dot{V}_{CO_2}$. In the absence of blood and lung gas composition measurements, it is difficult to interpret increased V£.$_{O_2}$ following exercise in *Iguana iguana*. In *Iguana iguana*, systemic blood flow appears to increase following exercise (Farmer *et al.* 1996), which may increase the convective transport of O_2 and thus $\dot{V}_{O_2}$, but this possibility must be verified experimentally. Furthermore, if effective ventilation ($V_T - V_{DS} \times f$, where V_T is tidal volume, V_{DS} is dead space volume and f is breathing frequency) is decreased during locomotion, lung and blood O_2 content would decline, and if these O_2 stores are replenished following locomotion, $\dot{V}_{O_2}$ (measured across the nostrils) would increase transiently during the recovery period. In this scenario, arterial P_{O_2} would be expected to decrease during exercise; this is not supported by direct measurements of blood gas composition (Mitchell *et al.* 1980*a*,*b*).

In summary, in *Varanus exanthematicus*, it appears that minute ventilation increases during exercise sufficiently to meet $\dot{V}_{O_2}$ during locomotion at speeds up to 0.8 m s^{-1}. This is indicated by the large increase in minute ventilation relative to $\dot{V}_{O_2}$ (Fig. 3A–C), also found by Mitchell *et al.* (1981*a*,*b*), and the decrease in $\dot{V}_{O_2}$ immediately following exercise. In *Iguana iguana*, however, the present study and that of Carrier (1987*a*) indicate that minute ventilation decreases progressively as locomotor speed is increased above 0.28 m s^{-1} and that this decrease is associated with a decrease in $\dot{V}_{O_2}$. Furthermore, as tidal volume tended to decrease with increased locomotor speed (although the decrease was not statistically significant), it is possible that effective ventilation decreased at the highest locomotor speeds in spite of the increase in $\dot{V}_E/\dot{V}_{O_2}$ (Fig. 3D). This interpretation is supported by the increased $\dot{V}_{O_2}$ and minute ventilation following exercise, which may indicate a reduction in lung and blood O_2 content during exercise.

The observation that minute ventilation and $\dot{V}_{O_2}$ decrease in *Iguana iguana* as the speed of locomotion increases does not necessarily imply that these lizards are mechanically incapable of ventilating their lungs while running. It is possible, for example, that muscular exercise is associated with changes in the control of ventilation, such that exercise exerts an inhibitory action on the central motor output to the muscles responsible for ventilation. In this case, the proximal explanation for the reduction in ventilation would not be a mechanical limitation *per se*, but rather a result of the central integration of afferent input. It may, however, be argued that such changes in ventilatory control would only be of adaptive value (and presumably then selected for) if breathing during locomotion were energetically inefficient or if ventilatory efforts were to reduce locomotor performance (e.g. by affecting acceleration or maximum running speed).

The hypothesis of mechanical interference between locomotion and pulmonary ventilation

Given that lizards use their hypaxial muscles for both locomotion and ventilation (Carrier, 1989*a*,*b*, 1990), it is

plausible that the observed changes in breathing pattern result from interference between the locomotor and ventilatory functions. In the group of bony fishes from which tetrapods evolved, the hypaxial muscles did not contribute to lung ventilation (Liem, 1985), but were probably associated with lateral bending of the trunk and provided torsional stability during swimming. In salamanders, the obliquely oriented hypaxial muscles (the external oblique, internal oblique and transversalis muscles) are active during terrestrial walking in a manner that indicates that they stabilize the trunk against the long axis (Carrier, 1993). A similar pattern of activity during walking has been observed in the hypaxial muscles of *Iguana iguana* (Carrier, 1990). Recent observations suggest that the obliquely oriented hypaxial muscles of lizards are responsible for the lateral bending of the trunk during locomotion (Ritter, 1995, 1996). Finally, in trotting dogs, the locomotor action of the interosseous intercostal muscles has been found to predominate over their ventilatory action (Carrier, 1996). Therefore, it seems reasonable to suggest that locomotion may place limits on ventilatory function in lizards. The erratic nature of the breathing pattern observed during locomotion in both species in this study and the reduction in minute ventilation with increased running speed observed in *Iguana iguana* are consistent with mechanical interference between locomotor and ventilatory function as originally proposed by Carrier (1987*a*,*b*, 1989, 1990).

The findings for *Varanus exanthematicus* clearly conflict with the hypothesis of an ancestral conflict between ventilation and locomotion. Among lizards, varanids are thought to be a highly derived lineage, whereas iguanids are phylogenetically among the most basal of extant lizards (Estes *et al.* 1988). Given this phylogeny, the most parsimonious explanation is that the ability of *Varanus exanthematicus* to breathe effectively during locomotion is due to a modification of the ancestral condition to facilitate simultaneous running and breathing. In varanids, there is a pronounced anatomical distinction between the first few thoracic ribs and intercostal muscles and the ribs and intercostal muscle throughout the rest of the trunk (D. R. Carrier, unpublished observations). Visual observations indicate that the cranial ribs move during ventilation and that there may be a cranial-to-caudal division of labour in the intercostal musculoskeletal system of varanids that is not present in iguanids. Furthermore, the lizard *Uromastyx microlipes* can ventilate its lungs using a buccal pressure force pump (Al-Ghamdi *et al.* 1995), and it has recently been reported that *Varanus exanthematicus* can use contractions of the buccal cavity to inflate the lungs following exercise (Brainerd and Owerkowicz, 1996). Although the actual contribution of this mechanism during exercise remains to be determined, these gular movements may participate in lung ventilation.

Does ventilation limit $\dot{V}_{O_2}$ during exercise?

Carrier (1987*b*) suggested that limited minute ventilation, particularly at high running speeds, limits $\dot{V}_{O_2}$ and, therefore, renders lizards incapable of sustained locomotion. This argument assumes that minute ventilation limits oxygen transport during exercise and implies that an increased minute ventilation could sustain a higher $\dot{V}_{O_2}$. At a given systemic cardiac output and a fixed cardiac right-to-left shunt, minute ventilation limits systemic oxygen delivery ($\dot{Q}_{sys}\times[O_2]_a$, where $\dot{Q}_{sys}$ is the systemic blood flow and $[O_2]_a$ is the oxygen content of systemic arterial blood) if lung P_{O_2} falls to an extent where pulmonary venous blood is no longer saturated. The lung P_{O_2} at which the haemoglobin oxygen-saturation of pulmonary venous blood is compromised depends on both blood oxygen-affinity and the P_{O_2} difference between lung gas and blood leaving the lungs. This P_{O_2} difference is generally larger in reptiles than in mammals (1–3 kPa *versus* 0.5–13 kPa) and results from a combination of intrapulmonary shunts, diffusion limitation and ventilation–perfusion inhomogeneity (reviewed by Powell, 1994). In *Varanus exanthematicus*, minute ventilation increased proportionally more than did gas exchange rates during exercise, as demonstrated by the large changes in air convection requirement for both O_2 and CO_2 (Fig. 3C; Mitchell *et al.* 1981*b*). The resulting increase in lung P_{O_2} may help to overcome diffusion limitations or the inability to increase diffusion capacity during exercise (Mitchell *et al.* 1981*b*; Hopkins *et al.* 1995). Finally, in *Varanus exanthematicus* walking at low speed (0.28 m s^{-1}), Hopkins *et al.* (1995) reported an increase in left atrial P_{O_2} during exercise, in spite of an increased ventilation–perfusion inhomogeneity which, in combination with the increase in ventilation, does not support the suggestion that lung P_{O_2} limits gas exchange during exercise in this species.

A vigorous analysis of O_2 transport limitations during exercise must determine O_2 transfer rates between the inhaled gas, the lungs, pulmonary capillary blood, systemic blood O_2 transport and O_2 diffusion between systemic capillary blood and mitochondria. To complicate matters further, in reptiles, the time constant for attaining steady state during progressive exercise may be exceedingly long, and a transient reduction in transfer rate at one step in the O_2 transport cascade is therefore not necessarily indicative of an O_2 transport limitation. There are no studies that have measured all of the O_2 transfer components in a single species of reptile. Nevertheless, a previous study on *Iguana iguana* and *Varanus exanthematicus* concluded that sustained aerobic activity was limited not by minute ventilation, but rather by the circulatory

Table 3. *Heart rate and relative changes in systemic blood flow rate ($\dot{Q}_{sys}$) during locomotion in* Varanus exanthematicus

Speed (m s^{-1})	Heart rate, f_H (beats min^{-1})	Relative change in $\dot{Q}_{sys}$
0	45.5±3.6	1.0±0.0
0.14	76.1±6.4*	2.0±0.4*
0.28	92.5±6.9*	2.5±0.7*
0.56	98.2±7.8*	2.7±0.6*
0.76	99.4±5.7*	2.8±0.6*

*Significantly different from the pre-exercise value.

system (Gleeson *et al*. 1980; Bennett, 1994). This conclusion was based on the relative hyperventilation and the attainment of maximal cardiac output and arterial–venous oxygen differences at maximal aerobic speeds. The relative changes in systemic blood flow and heart rate shown in Table 3 for *Varanus exanthematicus* are consistent with this interpretation. In contrast, the reduced gas exchange observed in *Iguana iguana* at the higher locomotor speeds may be a consequence of an altered breathing pattern during locomotion. Additional studies are required to quantify the various transport steps before conclusions regarding physiological limitations can be seriously addressed.

This study was supported by NSF grant IBN-9218936 to J.W.H. and NSF grant IBN 9306466 to D.R.C. T.W. was in receipt of a postdoctoral fellowship from the Carlsberg Foundation (Denmark). We are extremely grateful to Dr C. Farmer for assisting during the *Iguana* experiments and we thank Dr A. F. Bennett for lending equipment (NSF grant IBN-9420155) and providing laboratory space to perform this study. In addition, we thank Dr W. K. Milsom, Dr G. S. Mitchell and the anonymous referees for helpful comments on an earlier version of this manuscript.

References

AL-GHAMDI, M. S., JONES, J. F. X. AND TAYLOR, E. W. (1995). Central control of respiration and the heart in the anesthetized agamid lizard, *Uromastyx microlipes*. *J. Physiol., Lond.* **483**, 6P.

BENNETT, A. F. (1973). Ventilation in two species of lizards during rest and activity. *Comp. Biochem. Physiol*. **46**A, 653–671.

BENNETT, A. F. (1994). Exercise performance in reptiles. *Adv. vet. Sci. comp. Med*. **38**A, 113–138.

BISGARD, G. E., FORSTER, H. V., BYRNES, B., STANEK, K., KLEIN, J. AND MANOHAR, M. (1978). Cerebrospinal fluid acid–base balance during muscular exercise. *J. appl. Physiol*. **45**, 94–101.

BISGARD, G. E., FORSTER, H. V., MESINA, J. AND SARAZIN, R. G. (1982). Role of the carotid body in hyperpnea of moderate exercise in goats. *J. appl. Physiol*. **52**, 1216–1222.

BRAINERD, E. L. AND OWERKOWICZ, T. (1996). Role of the gular pump in lung ventilation during recovery from exercise in *Varanus exanthematicus*. *Am. Zool*. **36**, 88A.

BRAMBLE, D. M. AND JENKINS, F. A. (1989). Structural and functional integration across the reptile–mammal boundary: the locomotor system. In *Complex Organismal Functions: Integration and Evolution in Vertebrates* (ed. D. B. Wake and G. Roth), pp. 133–146. New York: John Wiley & Sons Ltd.

CARRIER, D. R. (1987*a*). Lung ventilation during walking and running in four species of lizards. *Exp. Biol*. **47**, 33–42.

CARRIER, D. R. (1987*b*). The evolution of locomotor stamina in tetrapods: circumventing a mechanical constraint. *Paleobiology* **13**, 326–341.

CARRIER, D. R. (1989). Ventilatory action of the hypaxial muscles of the lizard *Iguana iguana*: a function of a slow muscle. *J. exp. Biol.* **143**, 435–457.

CARRIER, D. R. (1990). Activity of the hypaxial muscles during walking in the lizard *Iguana iguana*. *J. exp. Biol*. **152**, 453–470.

CARRIER, D. R. (1993). Action of the hypaxial muscles during walking and swimming in the salamander, *Dicamptodon ensatus*. *J. exp. Biol*. **180**, 75–83.

CARRIER, D. R. (1996). Function of the intercostal muscles in trotting dogs: ventilation or locomotion? *J. exp. Biol*. **199**, 1455–1465.

CRAGG, P. A. (1978). Ventilatory patterns and variables in rest and activity in the lizard, *Lacerta*. *Comp. Biochem. Physiol*. **60**A, 399–410.

DM'IEL, R. (1972). Effect of activity and temperature on metabolism and water loss in snakes. *Am. J. Physiol*. **223**, 510–516.

ESTES, R., QUEIROZ, K. AND DE ANDGAUTHIER, J. (1988). Phylogenetic relationships within Squamata. In *Phylogenetic Relationships of the Lizard Families* (ed. R. Estes and G. Pregill), pp. 119–281. Stanford, CA: Stanford University Press.

FARMER, C., CARRIER, D. R. AND HICKS, J. W. (1996). Effect of the respiratory pump on venous return during exercise in iguanas. *Physiologist* **39**, A10,3.

FLANDROIS, R., LACOUR, J. R. AND OSMAN, H. (1971). Control of breathing in the exercising dog. *Respir. Physiol*. **13**, 361–371.

GLEESON, T. T., MITCHELL, G. S. AND BENNETT, A. F. (1980). Cardiovascular responses to graded activity in the lizards *Varanus* and *Iguana*. *Am. J. Physiol*. **239**, R174–R179.

HANSON, P., CLAREMONT, A., DEMPSEY, J. AND REDDAN, W. (1982). Determinants and consequences of ventilatory responses to competitive endurance running. *J. appl. Physiol*. **52**, 615–623.

HOPKINS, S. R., HICKS, J. W., COOPER, T. K. AND POWELL, F. L. (1995). Ventilation and pulmonary gas exchange during exercise in the Savannah monitor lizard (*Varanus exanthematicus*). *J. exp. Biol*. **198**, 1783–1789.

KUHLMANN, W. D., HODGSON, D. S. AND FEDDE, M. R. (1985). Respiratory, cardiovascular and metabolic adjustments to exercise in the Hereford calf. *J. appl. Physiol*. **58**, 1273–1280.

LIEM, K. F. (1985). Ventilation. In *Functional Vertebrate Morphology* (ed. M. Hildebrand, D. M. Bramble, K. F. Liem and D. B. Wake), pp. 185–209. Cambridge, MA: Harvard University Press.

MITCHELL, G. S., GLEESON, T. T. AND BENNETT, A. F. (1981*a*). Ventilation and acid–base balance during graded activity in lizards. *Am. J. Physiol*. **240**, R29–R37.

MITCHELL, G. S., GLEESON, T. T. AND BENNETT, A. F. (1981*b*). Pulmonary oxygen transport during activity in lizards. *Respir. Physiol*. **43**, 365–375.

OTIS, A. B. (1964). Quantitative relationships in steady-state gas exchange. In *Handbook of Physiology*, section 3, vol. 1 (ed. W. O. Fenn and H. Rahn), pp. 681–698. Washington, DC: American Physiological Society.

POWELL, F. L. (1994). Respiratory gas exchange during exercise. *Adv. vet. Sci. comp. Med*. **38**A, 253–285.

RITTER, D. (1995). Epaxial muscle function during locomotion in a lizard (*Varanus salvator*) and the proposal of a key innovation in the vertebrate axial musculoskeletal system. *J. exp. Biol*. **198**, 2477–2490.

RITTER, D. (1996). Role of the axial muscles in the locomotion of lizards. *J. exp. Biol*. **199**, 2499–2510.

RUBEN, J. (1995). The evolution of endothermy in mammals and birds: From physiology to fossils. *A. Rev. Physiol*. **57**, 69–95.

SMITH, C. A., MITCHELL, G. S., JAMESON, L. C., MUSCH, T. I. AND DEMPSEY, J. A. (1983). Ventilatory response of goats to treadmill exercise: grade effects. *Respir. Physiol*. **54**, 331–341.

WANG, T. AND WARBURTON, S. J. (1995). Breathing pattern and cost of breathing in American alligators. *Respir. Physiol*. **102**, 29–37.

WILSON, K. J. (1971). The relationships of activity, energy, metabolism and body temperature in four species of lizards. PhD thesis, Monash University, Clayton.